USGS science for a changing world

CGS CALIFORNIA GEOLOGICAL SURVEY

The SAFRR Tsunami Scenario—Physical Damage in California

Open-File Report 2013–1170–E
California Geological Survey Special Report 229

U.S. Department of the Interior
U.S. Geological Survey

COVER: Tsunami damage to port buildings in Seward Alaska, March 1964. This tsunami caused severe damage in communities around the Pacific Rim, including Alaska, Hawaii, Washington, Oregon, and California. (Photograph: Karl V. Steinbrugge Collection, National Information Service for Earthquake Engineering, University of California, Berkeley. Photo credit: Mildred E. Kirkpatrick, courtesy of the National Information Service for Earthquake Engineering, EERC, University of California, Berkeley.

The SAFRR (Science Application for Risk Reduction) Tsunami Scenario

Stephanie Ross and Lucile Jones, Editors

The SAFRR Tsunami Scenario—Physical Damage in California

By Keith Porter, William Byers, David Dykstra, Amy Lim, Patrick Lynett, Jamie Ratliff, Charles Scawthorn, Anne Wein, and Rick Wilson

Open-File Report 2013–1170–E

California Geological Survey Special Report 229

U.S. Department of the Interior
U.S. Geological Survey

U.S. Department of the Interior
SALLY JEWELL, Secretary

U.S. Geological Survey
Suzette M. Kimball, Acting Director

U.S. Geological Survey, Reston, Virginia: 2013
For product and ordering information:
World Wide Web: http://www.usgs.gov/pubprod
Telephone: 1-888-ASK-USGS

For more information on the USGS—the Federal source for science about the Earth,
its natural and living resources, natural hazards, and the environment:
World Wide Web: http://www.usgs.gov
Telephone: 1-888-ASK-USGS

Suggested citation:
Porter, K., Byers, W., Dykstra, D., Lim, A., Lynett, P., Ratliff, J., Scawthorn, C., Wein, A., and Wilson, R., 2013, The SAFRR tsunami scenario—Physical damage in California, chap. E *in* Ross, S.L., and Jones, L.M., eds., The SAFRR (Science Application for Risk Reduction) Tsunami Scenario: U.S. Geological Survey Open-File Report 2013–1170, 168 p., http://pubs.usgs.gov/of/2013/1170/e/.

STATE OF CALIFORNIA
EDMUND G. BROWN JR.
GOVERNOR

THE NATURAL RESOURCES AGENCY
JOHN LAIRD
SECRETARY FOR RESOURCES

DEPARTMENT OF CONSERVATION
MARK NECHODOM
DIRECTOR

CALIFORNIA GEOLOGICAL SURVEY
JOHN G. PARRISH, Ph.D.
STATE GEOLOGIST

Contents

Figures

Tables

The SAFRR Tsunami Scenario—Physical Damage in California

By Keith Porter,[1] William Byers,[2] David Dykstra,[3] Amy Lim,[3] Patrick Lynett,[4] Jamie Ratliff,[5] Charles Scawthorn,[6] Anne Wein,[5] and Rick Wilson[7]

Introduction—Chapter Objectives

By Keith Porter

This chapter attempts to depict a single realistic outcome of the SAFRR (Science Application for Risk Reduction) tsunami scenario in terms of physical damage to and recovery of various aspects of the built environment in California. As described elsewhere in this report, the tsunami is generated by a hypothetical magnitude 9.1 earthquake seaward of the Alaska Peninsula on the Semidi Sector of the Alaska–Aleutian Subduction Zone, 495 miles southwest of Anchorage, at 11:50 a.m. Pacific Daylight Time (PDT) on Thursday March 27, 2014, and arriving at the California coast between 4:00 and 5:40 p.m. (depending on location) the same day. Although other tsunamis could have locally greater impact, this source represents a substantial threat to the state as a whole.

One purpose of this chapter is to help operators and users of coastal assets throughout California to develop emergency plans to respond to a real tsunami. Another is to identify ways that operators or owners of these assets can think through options for reducing damage before a future tsunami. A third is to inform the economic analyses for the SAFRR tsunami scenario. And a fourth is to identify research needs to better understand the possible consequences of a tsunami on these assets. The asset classes considered here include the following:

- Piers, cargo, buildings, and other assets at the Ports of Los Angeles and Long Beach
- Large vessels in the Ports of Los Angeles and Long Beach
- Marinas and small craft
- Coastal buildings
- Roads and roadway bridges
- Rail, railway bridges, and rolling stock
- Agriculture

[1]University of Colorado at Boulder and SPA Risk LLC.
[2]Private consultant.
[3]Moffatt and Nichol Engineers.
[4]University of Southern California.
[5]U.S. Geological Survey.
[6]SPA Risk LLC.
[7]California Geological Survey.

- Fire following tsunami

Each asset class is examined in a subsection of this chapter. In each subsection, we generally attempt to offer a historical review of damage. We characterize and quantify the assets exposed to loss and describe the modes of damage that have been observed in past tsunamis or are otherwise deemed likely to occur in the SAFRR tsunami scenario. Where practical, we offer a mathematical model of the damageability of assets exposed to loss. Then, applying the damageability model and the velocity, wave amplitude, and inundation models discussed in other SAFRR chapters we offer a single realistic depiction of damage. Other outcomes are of course possible for this hypothetical event. Where practical we estimate repair costs and estimate the duration required to restore the assets to their pre-tsunami condition. We identify opportunities to enhance the resiliency of the assets, either through making them less vulnerable to damage or able to recover more quickly in spite of the damage.

Finally, we identify uncertainties in the modeling where research would improve our understanding of the underlying mechanisms of damage and loss or otherwise improve our ability to estimate the future impacts of tsunamis and inform risk-management decisions for tsunamis. However, it is certain that the kinds of damages discussed here have occurred in past tsunamis, even in developed nations, and in a sufficiently large event, will occur in California. Our uncertainties can operate in either direction, either leading to an overestimate of damage or an underestimate. Therefore, losses in an actual future tsunami could be greater than depicted here. Furthermore this evaluation is not intended to be an exhaustive depiction of what could happen in this or similar tsunamis. Other impacts could occur that are not presented here.

Damage and Restoration of the Ports of Los Angeles and Long Beach

By David Dkystra, Amy Lim, and Keith Porter

Introduction

Background

The purpose of this section is to provide a detailed estimate of tsunami impacts in the Ports of Los Angeles and Long Beach (POLA/POLB) and a more general assessment of potential damage to other ports and harbors along the California coast. The detailed assessment of impacts to POLA/POLB is an engineering evaluation of the impacts to vessels and port structures, along with the resulting supply-chain impacts.

For the purposes of estimating the impacts to POLA/POLB, it is assumed that vessel traffic and cargo inventories are as indicated in the Google Earth image dated March 7, 2011. The engineering evaluation presented in this section includes an estimate of physical impacts to the ports, damage costs, repair activities, other restoration activities, and resilience strategies. The impacts to shipping and infrastructure are based on conditions illustrated in the March 7, 2011, Google Earth image.

Historical Tsunami Events at the Ports of Los Angeles and Long Beach

Prior to evaluating potential tsunami damage to POLA/POLB from the SAFRR scenario, it is useful to review the impacts associated with historical tsunamis. Although these historical

events are not necessarily equivalent to the SAFRR scenario, they do help inform the process of evaluating the potential damage from the proposed scenario based on engineers' experiences during the events. Over the years, there have been measurements of significant water level fluctuations in the ports related to distant tsunamis from sources located in Alaska and Chile. Although tsunamis were generated from other sources, such as the 2004 Sumatra earthquake and 2011 Tohoku earthquake, these events did not generate significant water level fluctuations in POLA/POLB. The significant historical events include the following:

- 1922 Chilean tsunami
- 1946 Aleutian tsunami
- 1960 Chilean tsunami
- 1964 Alaskan tsunami
- 2010 Chilean tsunami

These events and their associated seismic moments are summarized in table 1.The basic data for these tsunamis in Southern California are available from Wilson (1971), Raichlen (1972), Berkman and Symons (1964), and Spaeth and Berkman (1967). Note that because of the magnitude, proximity, and directionality of the tsunami scenario, effects in the Ports of Los Angeles and Long Beach from this tsunami would be greater than in these past events.

An example of the tide gage records (marigrams) during the 1960 and 1964 events is presented in figure 1. The initial wave heights, as measured from peak to trough, reached as high as approximately 4.5 feet (ft) for the 1960 and 1964 tsunamis, as shown. It should be noted that the configuration of the harbor has changed over the years compared with what exists today in both ports, but the tsunami response has remained consistent over time and over varying locations within the Ports (Moffatt and Nichol, 2007).

It is significant to note that tsunamis generated by distant seismic sources other than those listed above for Alaska and Chile do not produce inland inundation in southern California during the 20th Century. The most recent major 2011 Tohoku earthquake and tsunami in Japan produced measured water level fluctuations on the order of 1 to 2 ft. The 2004 Sumatra earthquake and tsunami produced wave heights on the order of inches in POLA/POLB. There was no reported damage to any port facilities in either of these events.

On the basis of discussions with engineers from POLA/POLB and review of available literature, the only historical tsunamis to generate significant damage were the 1960 Chilean and 1964 Alaskan tsunamis. A Los Angeles Times articles at of 1960 suggests approximately $1 million worth of damage and two deaths. The damage was limited to a small craft harbor area along the Cerritos Channel where strong currents damaged boats, floating docks, and guide piles. There was no impact to port facilities or infrastructure during the 1960 Chilean tsunami or any of the other tsunamis. During the 1964 Alaska tsunami, 100 boats were unmoored and six were sunk (Lander and others, 1993). During the most recent tsunami from the 2010 Chilean tsunami, port operations and vessel navigation were halted as a result of the advanced tsunami warning. Strong currents were observed by the port pilots in some of the constricted channels. The currents persisted for several days, making navigation somewhat more difficult.

It should be noted that the port facilities at Los Angeles and Long Beach are extensively engineered and continually upgraded to conform to the latest codes, including increased seismic considerations. The facilities are also being continuously modified to provide efficient handling of cargo, increasing vessel traffic, and increasing vessel sizes. The improvements include the breakwaters, jetties, shoreline revetments, channel protections, and wharves. These continued improvements contribute toward minimizing risk of damage during tsunami events.

Table 1. Historical seismic events with tsunamis in the Ports of Los Angeles and Long Beach.
[M_w, moment magnitude]

Source	Date	Magnitude M_W
Chile	November 10, 1922	8.5
Aleutian Trench	April 1, 1946	8.1
Chile	May 23, 1960	9.5
Alaska	March 28, 1964	9.2
Chile	February 27, 2010	8.8

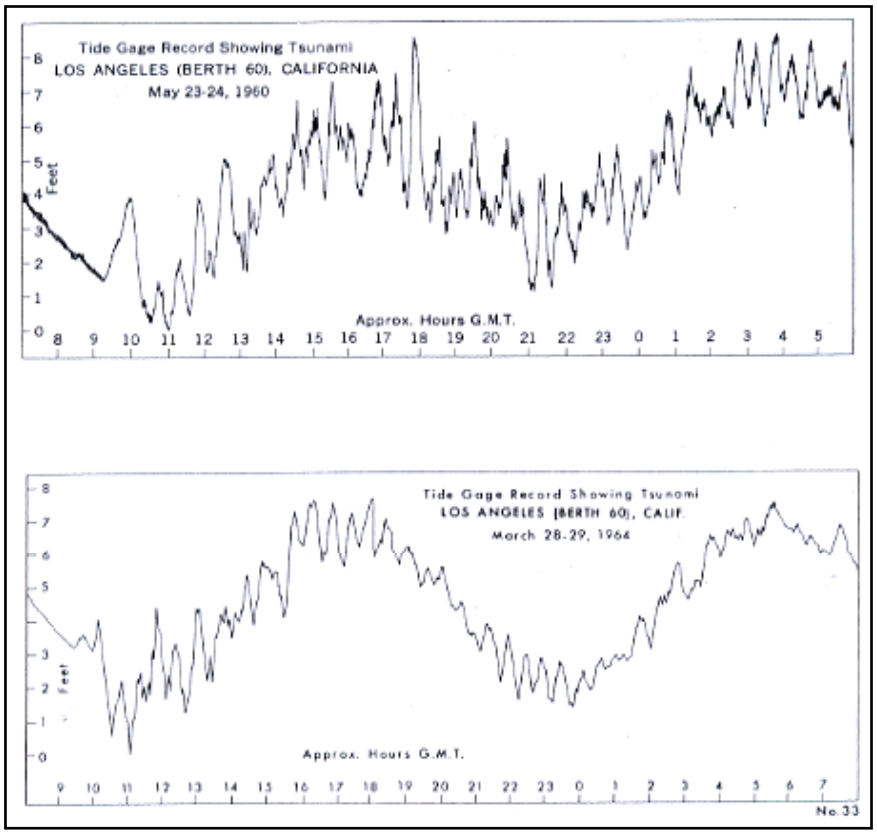

Figure 1. Tide gage records at Port of Los Angeles Berth 60 for the 1960 Chilean Tsunami and the 1964 Alaskan Tsunami (image from U.S. Coast and Geodetic Survey).

Damage and Restoration of Similar Ports During Tsunamis

Over the past decade, there have been three devastating tsunamis around the world: the 2004 Sumatra tsunami, the 2010 Chilean tsunami, and the 2011 Tohoku, Japan tsunami. Following each of these tsunamis, many reconnaissance teams representing the engineering community were sent to review the damage at impacted sites and to learn about port design implications (American Society of Civil Engineers (ASCE), Coasts, Oceans, Ports, and Rivers Institute, (COPRI), 2005, 2010, and ASCE, Technical Council on Lifeline Earthquake Engineering (TCLEE), 2011). In addition, there is a PIANC (World Association for Waterborne Transport Infrastructure) Working Group 53 preparing a report on tsunami disasters in ports (PIANC, 2009). The reports from these reconnaissance teams and PIANC participants have provided a wealth of information on possible port damage mechanisms. In addition, several Moffatt and Nichol (M&N) personnel have participated in these reconnaissance teams and have

provided personal observations. The discussion in this section summarizes some of the damage mechanisms that have occurred in port facilities around the world during these most recent tsunami events. Not all these damage mechanisms are necessarily applicable to the ports.

The three most recent tsunami events created the most damage near the coastline immediately adjacent to the seismic source. There was very little advance warning other than ground shaking during the earthquakes. The lack of warning time increased the vulnerability of nearby ports since there was little time to prepare or evacuate. Although southern California is a seismically active zone, the faults are predominantly strike slip faults, which are much less likely to generate major tsunamis compared to the subduction zone faults of the most recent extreme tsunamis. Earthquakes on these faults could still generate submarine landslides that could cause a large local tsunami with minimal warning time, but these events have a low occurrence probability. Thus, locally generated major tsunamis in southern California with the associated minimal warning time are unlikely.

It was also noted by the reconnaissance teams that port facilities that were well engineered generally fared better than older, or less well-maintained, ports. This was particularly evident in Chile and Japan where tsunami events are relatively common and building codes are geared toward minimizing both the seismic damage and resultant tsunami damage. For the case of both the Chile 2010 and the Tohoku, Japan tsunamis, it was noted that the bulk of the damage was related to the extreme tsunamis rather than failures from the seismic event. This suggests that most of the observed damage to the port facilities following these events was the result of the tsunamis.

Damage To and Caused by Vessels

The first class of port damage is related to vessels within the port, both navigating and moored vessels. The most commonly observed, and a dramatic phenomenon, is the displacement of vessels onto land by the rising water level and flooding. This requires substantial inundation exceeding the vessel draft. Examples of this type of damage are illustrated in figures 2 and 3. The Sumatra tsunami of 2004 deposited a dredge on a Sri Lankan wharf, damaging port buildings and other infrastructure (fig. 2). The vessel MV *Glovis Mercury* was deposited on a wharf in Sendai, shown in figure 3, damaging a crane and a port building. Removal of these vessels and repair to the facilities is typically on the order of a few months. Because of the shallow inundation depth and limited flooded area throughout POLA/POLB for the identified scenario, this damage mechanism is unlikely in the ports with the possible exception of small craft and floating debris.

Figure 2. Photograph of Sri Lanka Port of Galle dredge grounded on wharf by a 5.3-meter tsunami wave during the 2004 Sumatra tsunami (photograph from American Society of Civil Engineers, Coasts, Oceans, Ports, and Rivers Institute, 2005).

Figure 3. Photograph of *MV Glovis Mercury* displaced on top of wharf and damaged crane at Sendai Port, Japan, during 2011 Tohoku tsunami (photograph by Keith Porter).

The strong currents associated with tsunami propagation through port areas makes navigation extremely difficult and can result in vessels striking breakwaters and other port structures. If the vessels are damaged and sink within main shipping channels or harbor entrances, all vessel traffic will be halted until the channel is cleared. This type of vulnerability is illustrated in figures 4 and 5. Clearing the channel would normally be on the order of weeks, depending on the availability of equipment to remove the vessels. Repair of wharves or similar structures will take longer. If the damage is to a breakwater or jetty, the damage may not be immediately necessary for maintaining operations. Headland and others (2006) conducted vessel-maneuvering simulations for POLA/POLB during a hypothetical tsunami event. Their conclusions suggested difficult, but manageable maneuvering through Angel's Gate during the peak currents of the hypothetical event.

Strong currents can also have the potential to damage the mooring components for the vessels within the harbor due to excessive current drag on the vessels. This results in broken mooring lines, wharf bollards, or, in more extreme cases, broken mooring dolphins. Once the vessel is essentially freely floating within the harbor, there is a danger of striking port facilities. This type of damage is illustrated in figures 6 through 8. These examples are for the Port of Chennai, India as a result of the 2004 Sumatra tsunami. Despite the evident damage, the port was operating at significant capacity within days of the tsunami, because it is a fairly modern port. Vessels were rerouted to other undamaged berths and cleanup operations were optimized to restore minimally damaged facilities and reduce down time. Older, less well-engineered port facilities were reported to take significantly longer to return to capacity following the Chile 2010 tsunami.

In addition to current loads on moored vessels, there is evidence that vessels moving vertically due to the tsunami water level fluctuations can cause lines to part if the lines are not properly tended during the tsunami (Headland and others 2006). As the vessels rise with the water level, the lines become taut and potentially part.

Water level fluctuations within ports can persist for days following the initial arrival of the tsunami with consequent unpredictable high currents. The persistence of these erratic currents is of concern because there may be the possibility of harbor resonance with the tsunami wave and possible impacts to port operations sensitive to currents, such as container wharves where excessive vessel motion may produce hazardous conditions during crane placement of containers (PIANC, 2009).

Figure 4. Photograph of Port of Colombo, Sri Lanka—A ship lost control in this entrance during the 2004 Sumatra Tsunami (photograph from American Society of Civil Engineers, Coasts, Oceans, Ports, and Rivers Institute, 2005).

Figure 5. Photograph of broken back of coal carrier in navigation channel at Port of Shinchi, Japan, during the 2011 Tohoku tsunami (photograph by Keith Porter).

Figure 6. Photograph of Port of Chennai, India—Vessel hitting shore crane during the 2004 Sumatra Tsunami (photograph by Martin Eskijian).

Figure 7. Photograph of Port of Chennai, India—two mooring dolphins missing after the 2004 Sumatra Tsunami (photograph by Martin Eskijian).

Figure 8. Photograph of hoppers destroyed by out of control vessel in Port of Chennai, India, during the 2004 Sumatra Tsunami (photograph by Martin Eskijian).

Shoaling and Scour Caused by Currents

The second class of damage is direct damage to port facilities and infrastructure from tsunami flooding. There is the potential for scour or shoaling due to substantial sediment movement during the tsunami. Sediment transport during the tsunami scenario, possibly resulting in scour or shoaling, was not simulated, but impacts can be significant. During the 2004 Sumatra tsunami, the Port of Galle in Sri Lanka experienced 2 meters (m) of shoaling within the harbor, which impacted vessel navigation within the port. A bathymetric survey would be required following the tsunami to identify this damage, which may not be immediately apparent. Either other viable channels would have to be identified or the port would be limited in operations. This could possibly be accommodated by restricting the draft of vessels accessing the port. The shoal material would have to be dredged prior to restoring normal port operations, which could take on the order of a few months depending on the availability of dredges.

The scour resulting from the high current speeds could also result in scour around the base of rock armored slopes or breakwater and impact the stability of these types of structures. Damage to the actual slope armor is illustrated in figure 9 during the Chile tsunami of 2010. This damage actually occurred on the lee side of the breakwater where the tsunami overtopped the breakwater. The armor units were displaced down slope toward the toe of the breakwater. These displaced armor units could impact navigation if they are within the navigation channel. Another example of a damaged armor revetment is illustrated in figure 10, where a seawall and adjacent road were damaged from the overtopping during the Chile tsunami of 2010. Typically, damaged breakwaters or armored revetments would not impact port operations following the tsunami because they would remain fairly functional.

Figure 9. Photograph of breakwater damaged in Chile 2010 Tsunami (photograph from American Society of Civil Engineers, Coasts, Oceans, Ports, and Rivers Institute, 2005).

Figure 10. Photograph of seawall and road damaged in Chile Tsunami of 2010 (photograph from American Society of Civil Engineers, Coasts, Oceans, Ports, and Rivers Institute, 2005).

Deformation of Wharves, Cranes, and Cargo

Tsunami damage to container wharves has also been observed at several ports. Displacement of the pile-supported wharf area relative to the backfilled land area is illustrated in figure 11*A*. The actual mechanism for this displacement is unclear, but it could be related to scour around the supporting piles, damage to the piles themselves, or excessive hydrostatic vertical load during the tsunami. It is possible that the displacement in this particular case at Port Blair was caused by seismic failure because the earthquake ground motions here were substantial. Container crane rails have also been misaligned, as illustrated in figure 11*B*, due to flow over the decks or pile damage from scour. The utility trenches and crane power supply trenches have been damaged by filling in with mud and debris, as illustrated in figure 12.

There is a potential for empty containers to float off the container wharf if the inundation depth is great enough. These floating containers could cause damage to adjacent structures if currents are sufficiently high. In the case illustrated in figure 13 for the Port of Chennai, India, the flow depth was inadequate to displace the containers, as they were stacked sufficiently high. If full, it may be assumed that the contents of the bottom containers will be damaged beyond recovery. All impacts to containership facilities would likely take on the order of weeks to repair and restore operations. It should be noted that the cranes themselves were not damaged in Port Blair or the Port of Chennai, and were operational within days after the tsunami.

Container crane damage can occur if the motors are submerged during the tsunami. This damage potential is illustrated in figure 14. Container cranes can also be damaged by strong currents at the base, as illustrated in figure 15. These types of damage to the container cranes will take several months to repair and restore the container berths to operation. Break bulk cargo, such as steel, is less vulnerable to tsunami damage, as shown figure 16.

A *B*

Figure 11. Photographs of damage from 2004 Sumatra Tsunami in Port Blair, India. *A*, Differential settlement between pile supported wharf and backfill area in Port Blair, India. *B*, Container crane rail misalignment. (Photographs by Martin Eskijian).

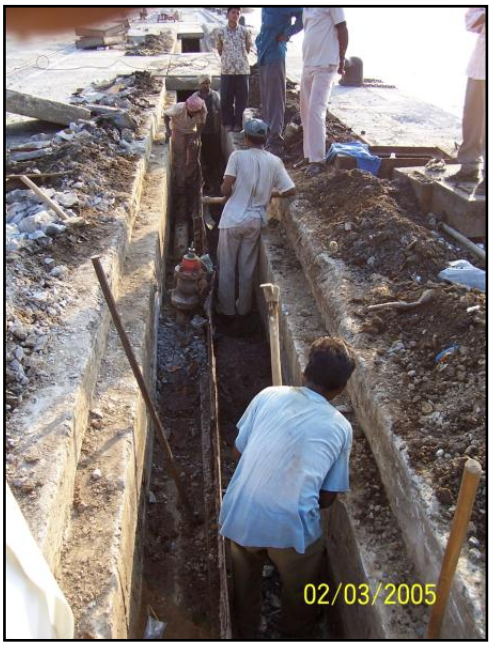

Figure 12. Photograph of utility and crane rail trench filled with debris and utilities damaged by the 2004 Sumatra Tsunami in Port Blair, India (photograph by Martin Eskijian).

Figure 13. Photograph of flooding of container wharf at Port of Chennai, India, in the 2004 Sumatra Tsunami (4.1-meter tsunami wave) (photograph by Martin Eskijian).

Figure 14. Photograph of damaged container crane motor in Port of Sendai, Japan, following the 2011 Tohoku tsunami (photograph by Keith Porter).

Figure 15. Photograph of container cranes collapsed due to tsunami current forces at Port of Shinchi, Japan, following the 2011 Tohoku tsunami (photograph by Keith Porter).

Figure 16. Photograph of undamaged steel at Port of Sendai, Japan, following the 2011 Tohoku tsunami (photograph by Keith Porter).

Warehouse Flooding and Current Loads

Port warehouses adjacent to the waterfront may be damaged due to the flooding and current loads on the structures, as illustrated in figure 17. Floating debris, other than ships, such as vehicles, containers, and other equipment and structures can cause damage to otherwise undamaged facilities. Where there is warehouse damage, there is the possibility of igniting electrical fires. Where sheet pile walls exist within the ports, there is the possibility of damage to the walls from hydrostatic pressure from flooding, seafloor scour at the toe, and wave forces. Pier decks can be removed from the tops of the supporting piles, as shown in figure 18. This is likely due to wave uplift in conjunction with the high current speeds striking the side of the decks. Deck uplift with removal or damage can be significant if the tsunami wave period is short enough. For the case of the Chile tsunami of 2010, illustrated in figure 18, both mechanisms may have contributed because the tsunami event was a near field event, which typically contains shorter period waves than distant tsunami sources. Repair of these types of damage could take several months to a year. Tsunamis can flood cargo storage areas, wetting or floating vehicles and containerized cargo, as illustrated in figure 19.

Damage to Liquid Bulk Terminals

Liquid bulk terminals may be susceptible to damage by rupturing pipelines. For example, as illustrated in figure 20, the Tohoku tsunami "caused multiple breaks of pipelines and many small hydrocarbon leakages from pipe connections which ignited. In two places, releases of heavy oil (4,400 and 3,900 m^3, respectively) were triggered due to connected pipe breaking by the tsunami." (Kraussman and Cruz, 2013). Figure 21 shows how tsunami scour can undermine pipe supports. Tanks can be damaged by tsunami flows or debris, as shown in figure 22, and empty tanks can be floated away from their foundations, as illustrated in figure 23. These types of impacts could present significant environmental damage as the product is released into the flood waters and subsequently transported over a wide region.

California oil terminals are currently designed and maintained to the latest standards provided in Marine Oil Terminal Engineering and Maintenance Standards (MOTEMS) (California State Lands Commission, 2010) incorporated in the California Building Code. The MOTEMS requirements incorporate mechanisms for rapidly shutting down oil pipelines to minimize the risk of an oil spill during a seismic event. A similar approach would be used during a tsunami event.

Current practice within most ports of the world and specifically California is to construct a containment dike or wall around tank farms and pipelines. These containment dikes are designed to retain any leakage within the designated area, but could also easily be designed to be of sufficient height to reduce or eliminate tsunami overtopping. The tank farms within the ports are all contained within dikes or walls, which would reduce or eliminate the potential for floating tanks and damaging pipelines.

Damage to Port Rail Facilities

Many modern ports include trains for transporting goods from the port facilities. There is the potential for train rails to be damaged similarly to container crane rails. Where rail bridges are included, there is the potential for the rail decks to be removed similarly to open piers, as illustrated in figure 24. Where rail links are crucial to port operations, this type of damage could

result in significant downtime to the port following the tsunami because damage repair would likely be on the order of a few months. Rail is addressed more broadly elsewhere in this chapter.

Figure 17. Photograph of Sri Lankan Port of Galle warehouse damage during 2004 Sumatra Tsunami (photograph from American Society of Civil Engineers, Coasts, Oceans, Ports, and Rivers Institute, 2005).

Figure 18. Photograph of pier deck removed in Chile Tsunami of 2010 (photograph from American Society of Civil Engineers, Coasts, Oceans, Ports, and Rivers Institute, 2010).

A *B*

Figure 19. Photographs of damage by the 2011 Tohoku, Japan, tsunami. *A*, Cars floated into a building by the 2011 Tohoku tsunami (photograph by Keith Porter). *B*, Cargo containers in Kashima after the 2011 Tohoku tsunami (photograph from Wikimedia Commons).

Figure 20. Photograph of a fire at the Cosmo Oil Refinery in Ichihara after the 2011 Tohoku, Japan, tsunami (photograph from Wikimedia Commons).

Figure 21. Photograph of pipes whose supports seem to have been undermined by tsunami scour in Ishinomaki, Japan, after the 2011 Tohoku tsunami (photograph by Keith Porter).

Figure 22. Photograph of tsunami-damaged tanks in Ishinomaki, Japan, after the Tohoku 2011 tsunami (photograph by Keith Porter).

Figure 23. Photograph of tank floated off its foundation during the 2011 Tohoku, Japan, tsunami (photograph by Keith Porter).

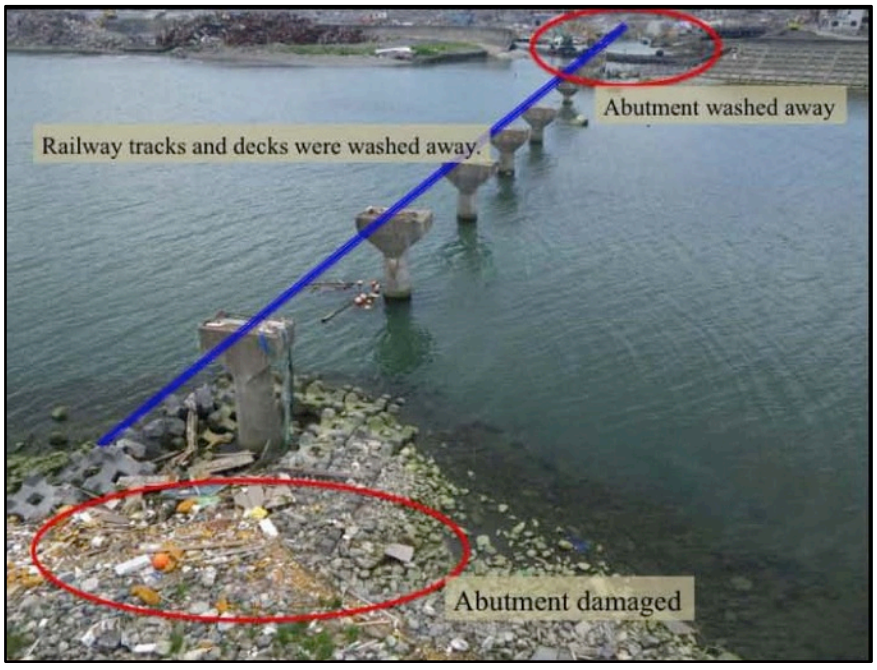

Figure 24. Photograph of railroad-bridge deck removed during the 2011 Tohoku, Japan, tsunami (photograph from American Society of Civil Engineers, Technical Council on Lifeline Earthquake Engineering, 2011).

Substation Damage

Other potential damage to the ports is flooding of power substations, thus shutting down all port facilities. This damage is extremely significant in that custom-built transformers can take more than six months to replace. The likelihood of substation damage or impacts to port operations can be reduced by placement of the substations inland away from areas of expected inundation or construction of containment dikes or walls to reduce the risk of flooding.

Substation damage also makes evacuation more difficult and hazardous. There was a case in the Chile tsunami of 2010 where the power was lost while a container crane was placing a container in the hull of the vessel. The container ship attempted to leave port to protect the vessel and destroyed the crane in the process (COPRI, 2010). The scenario suggests that the seismic event was responsible for the power loss because it was still possible for the vessel to successfully navigate. A more robust design of the power system for seismic sources may have eliminated this problem.

Tsunami Hazard Assessment Models

Generalized tsunami hazard assessment models are currently very limited for use in the United States. The Federal Emergency Management Agency (FEMA), in conjunction with the National Institute of Building Sciences has developed a model for estimating losses from natural disasters. The primary purpose of the model, Hazards U.S.-Multihazard (HAZUS-MH), is to provide a methodology and software application to develop earthquake, flood, and hurricane losses at a regional scale. These loss estimates would be used primarily by local, State, and regional officials to plan and stimulate efforts to reduce risks from disasters and to prepare for emergency response and recovery.

Although the HAZUS model proves to be a valuable source for loss estimation, the hazards estimation database is rather generic and not necessarily up to date. M&N has applied the model for a tsunami hazards assessment for POLA/POLB in a previous effort, but the damage assessment provided in this current SAFRR scenario is more accurate due to the use of a ‘snapshot’ assessment on specific terminals and vessels on a particular day.

Tsunami Messages Related to the Ports of Los Angeles and Long Beach

In this scenario, a tsunami watch is issued for Coastal California shortly after the earthquake (11:54 a.m. on March 27, 2014), with a forecast start of the tsunami at San Pedro (and thus the Ports of Los Angeles and Long Beach) at 5:37 p.m. the same day. The watch is issued by the National Oceanic and Atmospheric Administration’s (NOAA) National Weather Service (NWS) West Coast/Alaska Tsunami Warning Center in Palmer, Alaska. A tsunami watch means the warning center does not yet know the expected impact in the area addressed, and advises the reader to stay alert for further instructions.

The watch is replaced at 2:05 p.m. on March 27, 2014, by a tsunami warning for the coastal areas of California from Alamitos Bay, 20 miles southeast of Los Angeles Oregon-California border (which includes the Ports of Los Angeles and Long Beach). For areas under tsunami warning, NOAA informs the reader that “Widespread dangerous coastal flooding accompanied by powerful currents is possible and may continue for many hours after tsunami arrival” and that “the first wave may not be the largest.” The reader in a warning area is advised to “move inland to higher ground,” not to “go to the coast to observe the tsunami” nor to “return to the coast until local emergency officials indicate it is safe to do so.” In the 2:05 p.m. tsunami

message, NOAA advises the reader that the forecast start of the tsunami at San Pedro is 5:35 p.m. with amplitudes of 1.6 ft ± 0.5 ft (0.5m ± 0.15 m) at San Pedro. In particular, this amplitude would be at NOAA National Data Buoy Center station 46222, at coordinates 33.618°N. 118.317°W., about 6.4 nautical miles (11.8 kilometers, km) southeast of San Pedro harbor where the water is 457 m deep. Amplitudes would be greater in the harbor. Because NOAA's tsunami messages provide amplitudes in U.S. units, we quote these and provide SI unit in parentheses.

Thus it is 3.5 hours before the tsunami's arrival that NOAA first warns the Ports of Los Angeles and Long Beach that a tsunami with powerful currents and widespread dangerous coastal flooding is coming in 3.5 hours. Note that as further tsunami messages arrive, the forecast tsunami arrival time does not change significantly, but forecast amplitude at San Pedro does increase, as follows.

- 3:01 p.m.: estimated amplitude increased to 1.7 ft ± 0.5 ft (0.52 m ± 0.15 m)
- 4:01 p.m.: estimated amplitude increased to 1.8 ft ± 0.5 ft (0.55 m ± 0.15 m)
- 5:02 p.m.: estimated amplitude increased to 2.0 ft ± 0.6 ft (0.61 m ± 0.18 m)
- 6:02 p.m.: estimated amplitude increased to 2.2 ft ± 0.6 ft (0.67 m ± 0.18 m), with an amplitude of 1.2 ft (0.37 m) already observed at the San Pedro buoy.
- 7:01 p.m.: estimated amplitude increased to 2.3 ft ± 0.7 ft (0.70 m ± 0.21 m, 1.2 ft or 0.37 m observed)
- 8:01 p.m.: estimated amplitude increased to 2.4 ft ± 0.7 ft (0.73 m ± 0.21 m, 2.8 ft or 0.85m already observed)
- 9:01 p.m. the forecast amplitude has not changed but 3.1 ft (0.94 m) has been observed.
- At 5:04 p.m. on Friday March 28, 2014, 29 hours after the earthquake, the warning for San Pedro is changed to an advisory
- At 9:01 a.m. on Saturday March 29, 2014 (45 hours after the earthquake), the advisory is cancelled for the stretch of the California coast from a point 15 miles southeast of Santa Barbara to the California-Mexico border, which includes the Ports of Los Angeles and Long Beach.

Tsunami Inundation Maps and Duration

The tsunami propagation modeling indicates that the first wave produces the maximum wave amplitude and associated maximum currents. The maximum drawdown and significant waves will have passed by 6:00 p.m. PDT, a little over an hour after initial arrival, but as shown in figures 25 and 26, significant wave activity continues for several hours after the arrival of the first wave. As the tsunami reflects around the Pacific Ocean, higher than normal current speeds and less severe water level fluctuations in POLA/POLB are predicted to occur over the following several days. The base water depth at time of the tsunami's arrival is taken as 20 centimeters (cm) above mean high water (denoted here by MHW+20).

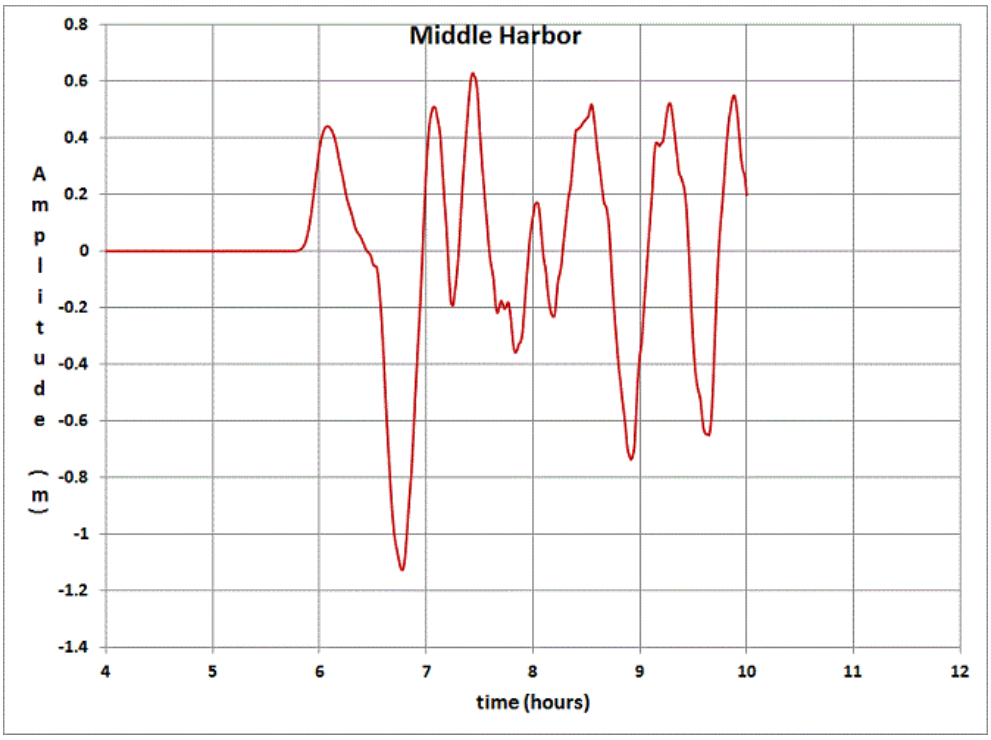

Figure 25. San Pedro Harbor, California, Middle Harbor marigram for the SAFRR tsunami scenario.

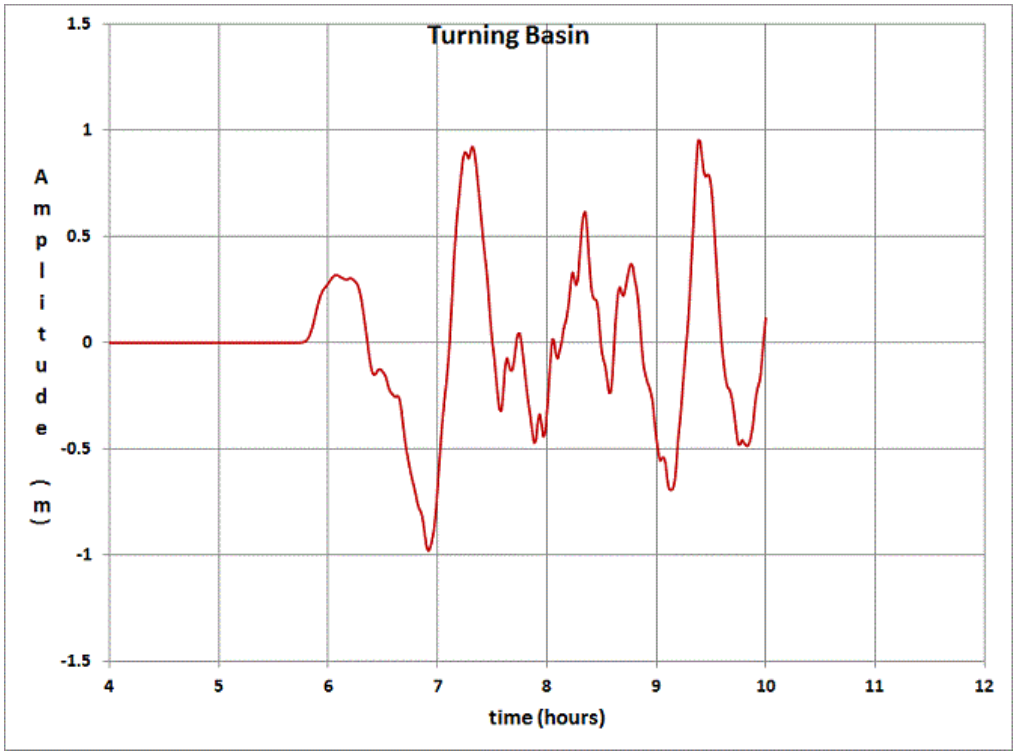

Figure 26. San Pedro Harbor, California, Turning Basin marigram for the SAFRR tsunami scenario.

Basin-wide hydrodynamic modeling was conducted for the selected SAFRR tsunami source seaward of the Alaska Peninsula on the Semidi Sector of the Alaska–Aleutian subduction zone. Higher resolution and high-order modeling was conducted for selected ports and harbors including the Ports of Los Angeles and Long Beach. The hydrodynamic modeling resolution for inundation in the ports was 10 m. The limit of inundation (referred to here as the inundation line) was based on 2009–2011 topography from LIDAR DEM with 1-m resolution.

The DEM used for the basis of the hydrodynamic modeling and creation of the inundation limits did not include some of the additional landfills and other modifications to the ports since the development of the DEM. Therefore, recent aerial photography (circa 2011) was used to check and update the inundation maps to reflect the newer landfills. These landfill areas included the Cabrillo Marina shoreline reconfiguration, Port of Long Beach Pier G, Middle Harbor, and Pier T dry dock landfills, and the Port of Los Angeles landfill in the dry dock area adjacent to the U.S. Coast Guard station. Two areas in the Port of Long Beach near Pier G and Piers E/F, where landfill work is currently ongoing, were not altered. The resolution of the DEM was insufficient to resolve containment dikes and containment walls surrounding tank farms. If these structures are adequately designed to withstand tsunami loads and depths, no inundation would occur there. In addition, maximum current speeds through the channel constrictions leading to basins where landfills are being constructed would be expected to be reduced, because the tsunami prism within the basins is reduced. Figure 25 depicts the resultant inundation limits for San Pedro Harbor.

Figure 26 represents the maximum tsunami-generated current velocities. Maximum current speeds reach as high as 8 knots through Angel's Gate and Queens Gate and some of the channel constrictions leading to specific basin areas such as Southeast Basin and West Basin in the Port of Long Beach. Maximum current speeds along the sides of the channels where vessels are moored are generally 2 to 3 knots.

Distribution of Assets

The Ports of Los Angeles and Long Beach make up two of the busiest ports on the west coast. Together, they are the number-one container port in the United States. In 2011, the ports accounted for approximately 10 percent of the U.S. total volume of foreign waterborne cargo and 22 percent of the U.S. total foreign value of cargo, as shown in figure 27. In the event of a tsunami, neighboring ports along the west coast that may serve as alternative vessel loading/unloading locations include the Port of Seattle, the Port of Tacoma, the Vancouver-Prince Rupert ports in Canada, and possibly some ports in Mexico. Other closer alternate ports along the Pacific coast are expected to experience some damage and operational downtime during the tsunami scenario. These include Port Hueneme, the Port of San Diego, the Port of Oakland, and the Port of San Francisco.

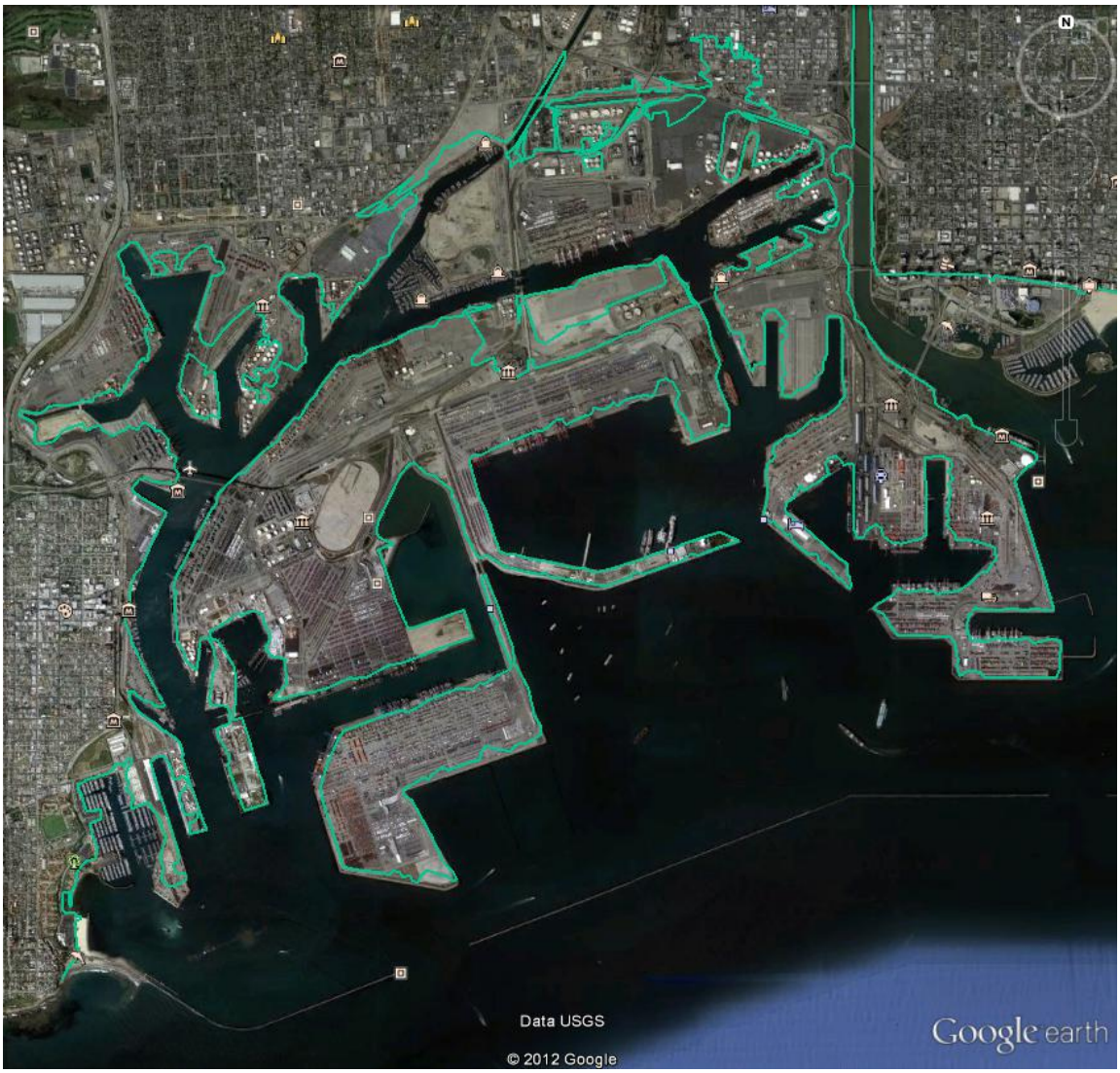

Figure 27. Inundation map during the SAFRR tsunami for the Ports of Long Beach and Los Angeles. Green line, maximum run-up. (Base map from Google Earth.)

Displacement of maritime activities

The following section summarizes the major cargo present at POLA/POLB during the tsunami scenario. The location and travel direction of vessels in the harbor during the tsunami were taken from the satellite imagery and Maritime Exchange information on March 7, 2011 (figure 25). These particular vessels are listed under 'Vessel Name' in table 2. Quantities of cargo exposed to the tsunami were estimated from the 2011 annual throughput values. Throughput values for March 27, 2014, are assumed to take on the same throughput values of a typical day in 2014.

Containerized

Containerized cargo includes any type of cargo moving within standard shipping containers. Such containers primarily contain finished goods such as clothing, toys, and furniture. Liquids and other unique cargoes may be shipped in specialized containers. Figure 28 highlights the main container terminals at the Port of Long Beach and distribution of cargo types can be seen in figure 29. Projected annual and average daily throughput values for each terminal are presented in table 2. Column indicating "Projected throughout on March 27, 2014," is assumed to be the same value at the location at 11:50 a.m. March 27, 2014. Vessel names are given at each location to provide some tangible detail on the day of the tsunami. At locations where no vessel name is listed, assume no particular vessel is present.

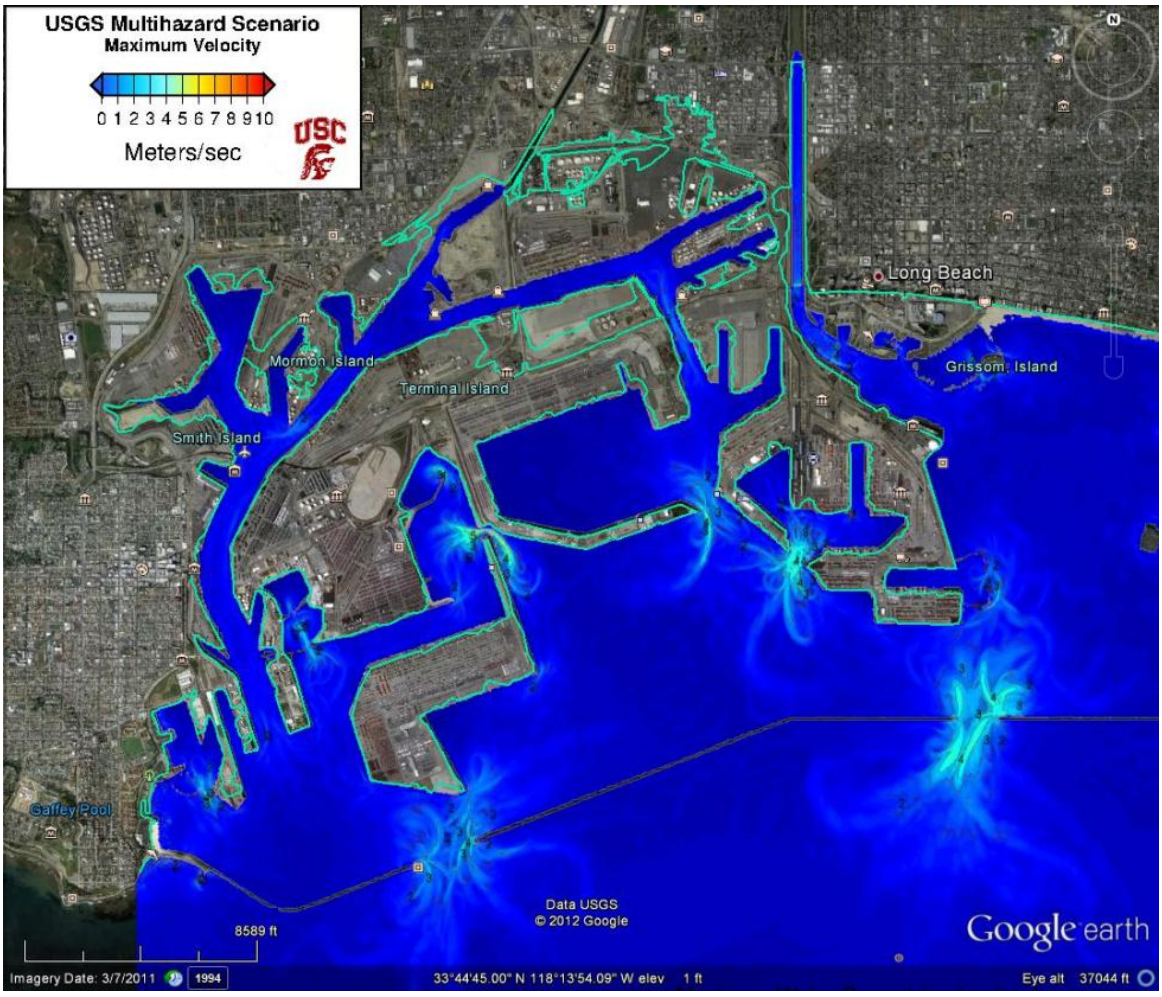

Figure 28. Map of maximum velocity for the Ports of Long Beach and Los Angeles during the SAFRR tsunami. Green line, maximum run-up. (Base map from Google Earth.)

U.S. WATERBORNE FOREIGN TRADE 2011
RANKING OF U.S. CUSTOMS DISTRICTS BY VALUE OF CARGO
Millions of U.S. Dollars

EXPORTS			IMPORTS			TOTAL TRADE		
Rank	Customs District	Dollars	Rank	Customs District	Dollars	Rank	Customs District	Dollars
1	Houston-Galveston, TX	$108,943	1	Los Angeles, CA	$302,134	1	Los Angeles, CA	$381,712
2	Los Angeles, CA	$79,578	2	New York City, NY	$150,244	2	Houston-Galveston, TX	$242,508
3	New York City, NY	$57,799	3	Houston-Galveston, TX	$133,564	3	New York City, NY	$208,043
4	New Orleans, LA	$57,015	4	New Orleans, LA	$96,346	4	New Orleans, LA	$153,361
5	Savannah, GA	$34,378	5	Seattle, WA	$62,772	5	Seattle, WA	$87,794
6	Miami, FL	$26,577	6	Savannah, GA	$51,346	6	Savannah, GA	$85,723
7	Seattle, WA	$25,023	7	San Francisco, CA	$46,598	7	San Francisco, CA	$69,209
8	Norfolk, VA	$24,132	8	Philadelphia, PA	$46,218	8	Charleston, SC	$58,893
9	San Francisco, CA	$22,611	9	Charleston, SC	$36,660	9	Norfolk, VA	$54,990
10	Charleston, SC	$22,234	10	Port Arthur, TX	$33,604	10	Philadelphia, PA	$54,321
11	Baltimore, MD	$20,634	11	Norfolk, VA	$30,858	11	Baltimore, MD	$51,391
12	Tampa, FL	$16,191	12	Baltimore, MD	$30,757	12	Miami, FL	$50,066
13	Columbia-Snake, OR	$12,990	13	Miami, FL	$23,489	13	Port Arthur, TX	$44,370
14	Port Arthur, TX	$10,766	14	Mobile, AL	$22,372	14	Tampa, FL	$32,590
15	Mobile, AL	$9,075	15	Tampa, FL	$16,399	15	Mobile, AL	$31,446
16	Philadelphia, PA	$8,102	16	U.S. Virgin Islands	$12,150	16	Columbia-Snake	$22,334
17	Wilmington, NC	$4,126	17	Boston, MA	$10,957	17	U.S. Virgin Islands	$14,432
18	Anchorage, AK	$4,080	18	Columbia-Snake	$9,343	18	Boston, MA	$13,113
19	San Juan, PR	$3,396	19	San Juan, PR	$9,201	19	San Juan, PR	$12,597
20	Detroit, MI	$3,339	20	Providence, RI	$6,620	20	Wilmington, NC	$10,426
21	U.S. Virgin Islands	$2,281	21	Wilmington, NC	$6,300	21	Providence, RI	$6,984
22	Boston, MA	$2,156	22	Honolulu, HI	$5,239	22	Honolulu, HI	$5,525
23	Ogdensburg, NY	$1,098	23	San Diego, CA	$5,146	23	San Diego, CA	$5,252
24	Cleveland, OH	$781	24	Portland, ME	$3,791	24	Anchorage, AK	$4,902
25	Buffalo, NY	$717	25	Chicago, IL	$1,440	25	Detroit, MI	$4,640
26	Portland, ME	$686	26	Detroit, MI	$1,300	26	Portland, ME	$4,476
27	Mineapolis, MN	440.58	27	Cleveland, OH	$1,231	27	Cleveland, OH	$2,012
28	Providence, RI	$365	28	Laredo, TX	$945	28	Chicago, IL	$1,666
29	Laredo, TX	343	29	Anchorage, AK	$823	29	Laredo, TX	$1,288
30	Honolulu, HI	$286	30	Duluth, MN	$650	30	Ogdensburg, NY	$1,106
31	Chicago, IL	$226	31	Mineapolis, MN	$225	31	Buffalo, NY	$904
32	Milwaukee, WI	$207	32	Buffalo, NY	$187	32	Duluth, MN	$832
33	Duluth, MN	$181	33	Milwaukee, WI	$172	33	Mineapolis, MN	$666
34	San Diego, CA	$107	34	Ogdensburg, NY	$9	34	Milwaukee, WI	$379
35	Washington, DC	$3	35	Washington, DC	$6	35	Washington, DC	$9
	Total	$570,286		Total	$1,159,096		Total	$1,729,382

Source: U.S. Census Bureau, U.S. Merchandise Trade, Selected Highlights (Report FT 920)

Figure 29. Ranking of U.S. customs districts by value of cargo (data from U.S. Census Bureau, 2013).

Figure 30. Map of Port of Long Beach containerized terminals (image courtesy Port of Long Beach).

Table 2. Port of Long Beach container terminal throughput values.

[TEUs, twenty-foot equivalent units]

Location	2011 Throughput (TEUs)	2014 Projected Throughput (TEUs)*	Projected throughput on March 27, 2014 (TEUs)	Gantry Cranes	Acreage	Vessel Name
Pier T Berth T132-T140	1,358,000	1,561,700	4,290	14	385	Hanjin
Pier G: Berths G226-G236	743,000	854,450	2,347	17	246	CSAV LUMACO
Pier F: Berths F6-F10	671,000	771,650	2,120	7	102	OOCL TOKYO—Arrival 3:15 p.m.
Pier J: Berths J243-J247, J266, J270	1,613,000	1,854,950	5,096	7	256	POS HONGKONG, departing
Pier A: Berths A88-A96	1,340,000	1,541,000	4,234	10	200	SEA-LAND INREPID, arrived 4:15 a.m.
Pier C: Berths C60-C62	337,000	387,550	1,065	3	70	MAUNAMWILI, arrived 6:45 p.m.
Total	6,062,000	6,971,300	19,152	58	1,259	

*Projected 5-percent annual container growth rate.

Figure 31. Map of Port of Long Beach cargo types—dry bulk (image courtesy Port of Long Beach).

Dry Bulk

Dry bulk includes dry cargoes that are shipped in bulk and measured by weight or volume. Based on past dry bulk growth statistics, it is assumed 2014 throughput values are constant with 2011 throughput values, as presented in table 3.

Table 3. Port of Long Beach dry bulk summary.

[MTPH, metric tons per hour; --, no data]

Location	Material	Equipment/ Facilities	2011 Through-put value (metric tons)	Projected throughput on March 27, 2014 (metric tons)	Acreage	Vessel Name
Pier D—Berth D46	Gypsum	Elevated receiving hopper served by an elevated electric belt conveyor system.	111,000	305	9	--
Pier D-Berth D32	Cement	Silo capacity—50,000 tons. Unloads conveyer system direct to silos.			2	--
Pier F—Berth F211	Petroleum Coke, prilled sulfur	Receipt, storage, blending, and vessel loading of petroleum coke. Import/Export of prilled sulfur.	711,000	1954	7	--
Pier F-Berth F208	Cement	2 pneumatic ship unloaders with 800 MTPH and 180 MTPH capacity.			4	--
Pier F—Berth F210	Salt	Movable incline elevated electric belt conveyor system with receiving hopper extending from wharf to stockpile area. Packing g plant adjacent.			5	--
Pier G-Berths G212-G214	Petroleum coke, coal, potash, borax, sodium sulfate, soda ash, concentrates, and prilled sulfur.	2 electric traveling bulk ship loaders.	6,950,000	19,094	23	LEO ADVANCE, departing 3/8/11
Pier B-Berth B82	Gypsum	Adjustable, elevated receiving hopper served by an elevated electric belt conveyor system extending to 40,000 ton capacity storage building.	137,000	377	19	--
Total			7,909,000	21,730	69	

Liquid Bulk

Liquid forms of bulk cargo are measured by weight or volume. Commodities like crude oil, gasoline, and miscellaneous chemicals are common liquid bulk cargoes. Based on past liquid bulk growth statistics, it is assumed 2014 throughput values are constant with 2011 throughput values, as presented in table 4.

Table 4. Port of Long Beach liquid bulk summary.
[--. no data]

Location	Cargoes Served	Equipment/ Facilities	2011 Throughput values (metric tons)	Projected throughput on March 27, 2014 (metric tons)	Acreage	Vessel Name
Pier T-Berth T121	Crude oil and petroleum products	Four 16-in. diameter articulated crude unloading arms and one 8" dia. Particular bunker/diesel loading arm	17,916,000	49,220	6	--
Pier B—Berths B76-80	Petroleum products	Four 16-in. diameter articulated crude unloading arms and one 8" dia. Particular bunker/diesel loading arm			6	--
Pier B Berth B82,83	Gasoline, ethanol, gasoline blend stocks, diesel, biodiesel	Two 8-inch dock hoses connecting into two 10-inch dock lines capable of receiving up to 12,000 BBLS per hour	10,649,000	29,300	6	--
Pier B—Berth B84-B87	Crude oil, petroleum products, bunker fuel.	Discharge capacity: 32,000 BBLS, 24 in pipeline to storage and tank farm. Storage capacity—245,000 BBLS			11	--
Pier F—Berths F209-211	Petroleum products and bunker fuel	Storage capacity—425,000 BBLS. Pipeline system to handle ships, barges, trucks, railcars.	2,311,000	6,350	5	PENN 91, departing 3/9/11
Pier S Berth S101	Miscellaneous bulk liquid chemicals	Dedicated pump/piping system to transfer products to and from ships, barges, railcars and tank trucks. Storage cap. 15 million gallons.	2,030,000	5,580	10	--
Total:			31,826,000	90,450	44	

Break Bulk and Roll On-Roll Off

Large or heavy items such as steel, lumber, machinery, and food products moved on pallets are Break Bulk cargoes. Roll On-Roll Off cargoes are items that are driven on and off a vessel. Based on past break bulk growth statistics, it is assumed 2014 throughput values are constant with 2011 throughput values, as presented in table 5. Automobile terminal will assume a capacity of 80 percent.

Table 5. Port of Long Beach break bulk/roll on-off summary.
[n/a, not applicable; --. no data]

Location	Equipment/ Facilities	2011 Throughput Values	Projected throughput on March 27, 2014	Acreage	Vessel Name
Pier F Berths F204-F205	Steel products, plywood, and lumber.			21	--
Pier F— Berth F206, F207	Steel products, plywood, lumber, project cargoes, and large machinery.	440,000 metric tons	1,209 metric tons	22	--
Pier F Berth F201	Standby berth			600	--
Pier D, Berth D50-D54	Crescent Warehouse Company	n/a	n/a	13.3	--
Pier T, Berth T122	Lumber and Lumber products			17	
Pier T Berth T118	Recyclable metal and steel products.	904,000 metric tons	2,484 metric tons	16	PANAMAX SUCCESS, departing 3/8/11
Pier T-Berth T122	Lumber and lumber products.			18	--
Pier B Berth B82, B83	Automobiles, Office building, processing buildings, body shop and car wash	121,000 vehicles	2,000 vehicles	168	--
Total				875.3	

Port of Los Angeles

Containerized

Figure 30 highlights the main container terminals at the Port of Los Angeles. Projected annual and average daily throughput values for each terminal can be seen in table 6. Column indicating "Projected throughout on March 27, 2014," is assumed to be the same value at the location at 11:50 a.m. 27 March 2014. Vessel names are given at each location to provide some tangible detail on the day of the tsunami. At locations where no vessel name is listed, assume no particular vessel is present.

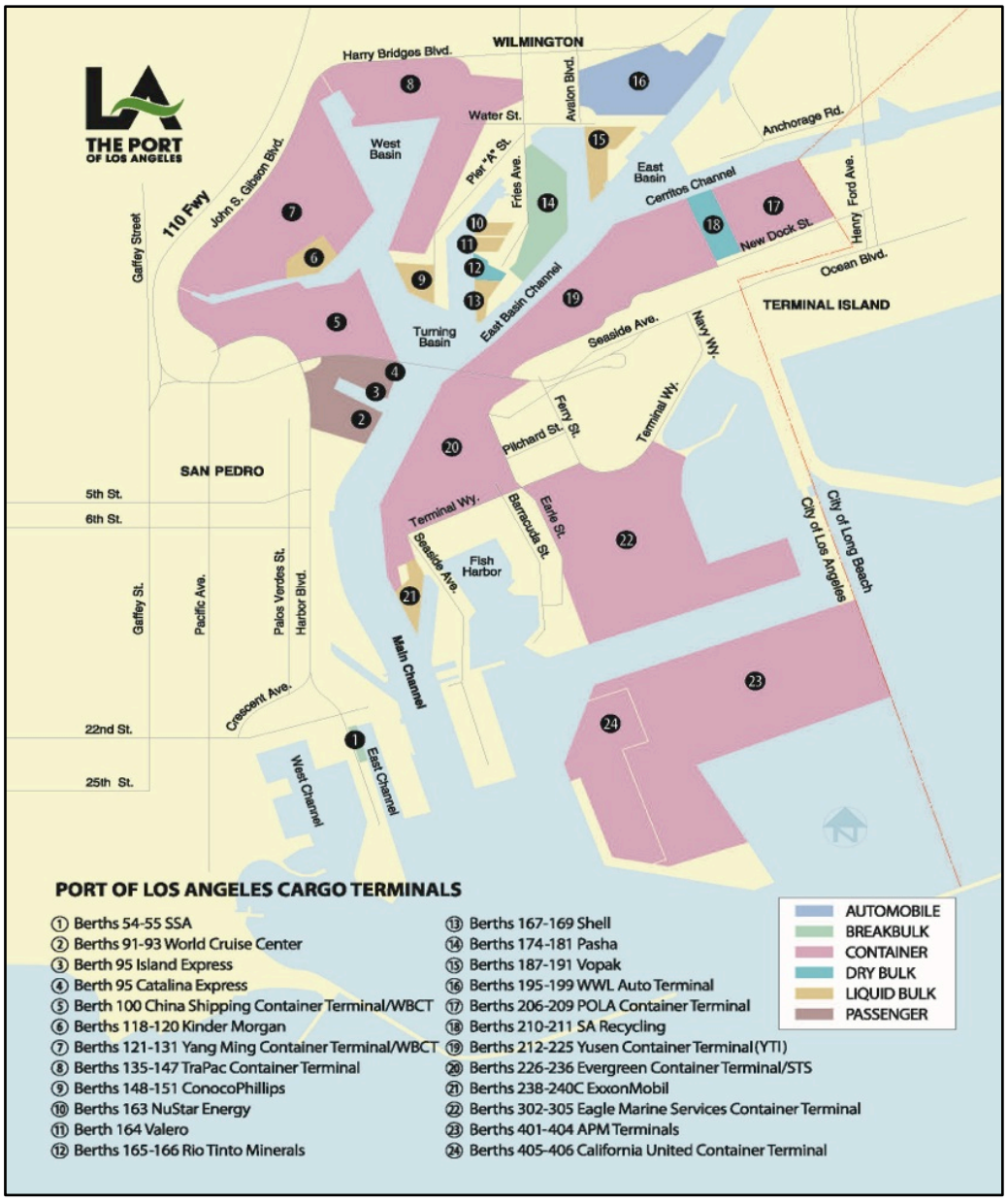

Figure 32. Port of Los Angeles facility map (image courtesy Port of Los Angeles).

Table 6. Port of Los Angeles container terminal throughput values.

[TEUs, twenty-foot equivalent units; --. no data]

Location	2011 Throughput (TEUs)	2014 Projected Throughput (TEUs)*	Projected throughput on March 27, 2014 (TEUs)	Gantry Cranes	Acreage	Vessel Name
Berths 100-102	401,000	461,150	1,270	8	91	--
Berths 121-131	820,000	943,000	2,590	5	186	126—YM PINE, departing 3/9/11
Berths 135-139	762,200	876,530	2,410	7	173	--
Berths 206-209	380,000	437,000	1,200	7	86	--
Berths 212-225	815,000	937,250	2,575	10	185	--
Berths 226-236	904,000	1,039,600	2,860	3	205	227-*EVER EAGLE*, departing 3/8/11
Berths 302-305	1,290,000	1,483,500	4,100	12	292	303- *MOL EFFICIENCY*, departing 3/8/11 304-APL Philippines, departing 3/9/11
Berths 401-404	2,133,500	2,453,525	6,470	14	484	401-*MAERSK WAKAYAMA*, departing 3/8 402- *MAERSK ALFIRK*, departing 3/8/11 403 404-*HORIZON HAWK*, departing 3/8/11
Berths 405-406	401,000	451,150	1,270	4	91	406—*HYUNDAI UNITY*, departing 3/8/11
Total	7,900,000	9,085,000	25,000	70	1793	

*Projected 5 percent annual container growth rate.

Dry Bulk

Based on past dry bulk growth statistics, it is assumed 2014 throughput values are constant with 2011 throughput values, as presented in table 7.

Table 7. Port of Los Angeles dry bulk summary.

[--. no data]

Location	Terminal features	2011 Throughput (metric tons)	2014 Projected Throughput (metric tons)	Projected throughput on March 27, 2014 (metric tons)	Acreage	Vessel Name
Berths 165-166	Industrial borates	306,570	306,570	843	7	--
Berths 210-211	Handles all grades of ferrous and non-ferrous scrap metals	1,169,340	1,169,340	3,212	26.7	--
Total		1,200,000	1,475,910	4,055	27.4	

Liquid Bulk

Based on past liquid bulk growth statistics, it is assumed 2014 throughput values are constant with 2011 throughput values, as presented in table 8.

Table 8. Port of Los Angeles liquid bulk summary.
[--. no data]

Location	Use:	2011 Throughput (metric tons)	2014 Projected Throughput (metric tons)	Projected throughput on March 27, 2014 (metric tons)	Acreage	Vessel Name
Berths 118-120	Receiving exporting petroleum products	980,866	980,866	2,695	12.4	--
Berths 148-151	Vessel unloading of partly or fully refined petroleum products	495,540	495,540	1,361	13.5	--
Berth 163	Marine oil	295,440	295,440	812	5.8	--
Berth 164	Fuels and lubricants	1,466,680	1,466,680	4,030	10.5	--
Berths 167-169	Fuels and lubricants	1,906,238	1,906,238	5,237	9.1	--
Berths 187-191	Liquid bulk chemical products	4,284,192	4,284,192	11,778	34.7	189- SUNSET BAY, depart 3/7/11 p.m.
Berths 238-240C	Fuels and lubricants	836,141	836,141	229	31.4	--
Total		10,265,097	10,265,097		117.4	

Automobile

From the satellite imagery, the automobile berth is estimated to be 80 percent full. Assuming 2011 vehicle storage is constant in 2014 (table 9), the number of vehicles present at the time of the tsunami can be projected.

Table 9. Port of Los Angeles automobile summary.

Location	Terminal features	Projected automobiles on March 27, 2014	Berth length	Acreage
Berths 195-199	Storage capacity up to 8,000 vehicles	6,400	2,250 feet	85

Break Bulk

Large or heavy items such as steel, lumber, machinery and food products moved on pallets are break-bulk cargoes. Based on past break bulk growth statistics, it is assumed 2014 throughput values are constant with 2011 throughput values, as presented in table 10.

Table 10. Port of Los Angeles break bulk summary.

[n/a, not applicable; --. no data]

Location	Terminal features	2011 Throughput (metric tons)	2014 Projected Throughput (metric tons)	Projected throughput on March 27, 2014 (metric tons)	Acreage	Vessel Name
Berths 49-53	Use: Break bulk steel	n/a	n/a	n/a	24	--
Berths 54-55	Imported meats, Chilean fruit, kiwis, apples	119,000	119,000	327	12	--
Berths 174-181	Steel	1,950,000	1,950,000	5,357	40	176-Pacific Flores, departing 3/8/11
Total		2,069,000	2,069,000	5,684	76	

Small Craft Basins

Within the Port of Los Angeles, there are a total of 16 marinas containing 3,795 recreational boat slips. There are 10 marinas located in Wilmington, five in San Pedro and one on Terminal Island, as summarized in table 11.

Table 11. Port of Los Angeles marinas and small craft slips.

Marina Name	Location	Slips
Al Larson's Marina	Berth 258	128
Cabrillo Beach Yacht Club	Berth 35	184
Cabrillo Way Marina	Berths 42-43	697
California Yacht Marina-Cabrillo Marina	Berth 29-33	885
California Yacht Marina	Berth 202	266
Cerritos Yacht Anchorage	Berth 205	90
Holiday Harbor-Fleitz Bros.	Berth 34	300
Holiday Harbor	Berth 201	169
Island Yacht Anchorage #1	Berth 205	22
Island Yacht Anchorage #2	Berth 200X	116
Leeward Bay Marina	Berth 201	190
Lighthouse Yacht Landing	Berth 205	70
Pacific Yacht Landing	Berth 203	178
San Pedro Marina	Berth 80	85
Yacht Centre-Newmarks	Berth 204	250
Yacht Haven Marina	Berth 202	165

Business-As-Usual Configuration

Modern container terminals are complex facilities designed to unload and load vessels and transfer containers to and from landside modes of transportation, that is, trucks and trains. Understanding how these facilities operate is important to understanding the potential changes or damages that may occur during and after a tsunami event.

Typical Container Terminal Operations

Terminal Components

In general, a modern container terminal (see figure 33) integrates a variety of physical components and operational processes. The physical components consist of:

- Dock structures or wharves with large, electric-powered gantry cranes;
- Container storage areas, known as the container yard;
- Entrance and exit gate complexes that include paperwork management facilities, physical screening facilities (for example, truck and chassis inspection areas, radiation monitors, and custom facilities), and truck queuing areas;
- Maintenance buildings for terminal equipment and chassis;
- Operations control buildings for marine and gate operations;
- An administration building;
- For terminals with intermodal capability, a rail yard and a rail operations control building; and
- Cargo handling equipment, including yard tractors, chassis for containers, light trucks and utility vehicles, and several types of mobile cranes and container handling equipment.

The operational processes include loading and unloading ships at the wharves, storing and handling containers in the container yard, managing in-terminal rail yard operations, dispatching containers to off-dock rail yards, and managing container delivery and pickup by trucks for local destinations.

Figure 33. Photograph of a modern container terminal (photograph from Wikimedia Commons).

Loading and Unloading of Vessels

Import containers arrive at and export containers depart from the terminals via container ships. Most container ships range from 700 to more than 1,100 feet in length and have cargo capacities from a few thousand to over 9,000 twenty-foot equivalent units (TEUs).

Once the vessel is tied at the wharf, the containers are loaded and unloaded by gantry cranes onto wheeled chassis. The cranes have steel wheels and are mounted on steel rails so they can move along the dock to serve multiple hatches and vessels. Each crane has a boom that is lowered over the vessel. The boom supports a container-lifting "spreader" with twist-locking corner devices that attach to the top corner castings of the containers to lift them. A crane operator rides in a cab above the spreader and controls the attachment and release functions. These cranes, which include specialized, highly computerized equipment that allows productive operations, can transfer 25 to 40 containers per hour. Typical modern gantry cranes stand approximately 150 feet high when the boom is outstretched and approximately 200 feet high when the boom is lifted, and mount on rails set 100 feet apart.

The number of cranes simultaneously servicing one ship can vary from one to five, or even more, depending on the size of the ship, the number of other vessels berthed at the terminal crane site, the availability of cranes, and the ship's scheduled port time. The amount of time a vessel spends at the berth varies with the amount of cargo to be unloaded and loaded and the number of cranes assigned to work the ship. Typical call durations range from 36 hours for small ships to five days for the largest vessels. Loading and unloading operations usually proceed around the clock.

Container Handling

After import containers are unloaded, they undergo security inspection. Each container is sealed with a metal ribbon attached to the doors, allowing a customs officer to ensure the contents of the container were not tampered with during voyage. Most containers are screened with an X-ray device, but every day some containers are inspected manually.

Once containers are off the vessel, they are taken to the container yard for temporary storage pending pickup by truck or train. Most of the export containers to be loaded are already stacked in the part of the container yard nearest the vessel berth and are transported to the crane via hostlers.

Gate Operations

Containers arrive at and depart from the terminal through the gate complex. The gate interchange is the legal exchange of possession of the container from the terminal to the trucking company, or vice versa.

Locally bound import containers are turned over to street-legal tractors (that is, semitrailer trucks) that arrive to pick up the cargo. The trucks arrive at the terminal either hauling export cargo or "bobtail" (that is, a tractor without a trailer) and, after presenting the appropriate paperwork, are directed to the container's location. For stacked cargo, the truck may need to pick up a chassis and then wait for a crane to load the container onto the chassis. For wheeled cargo, the truck can hitch up to the loaded chassis and proceed to the exit gate. Trucks hauling import cargo are processed out of the terminal at the exit gate, which involves passing through a radiation portal monitor, being inspected for road readiness, and clearing customs and brokerage paperwork.

Loaded export containers arriving from California, Arizona, Nevada, and some points farther east typically arrive at the gate on chassis pulled by trucks and are stacked or parked in the container yard to await their ship. Export cargo arriving from more distant locations typically arrive at the terminal via rail, either directly at the terminal's on-dock rail yard or at another local rail yard from which it is trucked to the terminal gate for receiving. Cargo containers are transferred from the rail cars to chassis or bomb carts using mobile cranes or RTGs and hauled by yard tractors to preplanned locations in the yard, where the containers are either lifted to grounded spots by another crane or parked on their chassis.

Truck Movement

Trucks fill the gap between the railcar and the shipper's loading dock, hauling containers between the warehouses, factories, or docks and the intermodal rail yards. Trucks are the vital first and last link in the goods movement chain. Short-haul trucking of marine cargo containers is known as drayage. Containers may be drayed between a marine terminal and an intermodal rail yard or between a marine terminal and a local distribution center, store, or transloading warehouse (see fig. 34).

Most of the population of the U.S. lives within 50 miles of the coast or of a major intermodal rail yard, and trucks excel at serving these markets because they can pick up a container and dray it to its destination the same day, with time remaining to return with a loaded or empty container (a movement not shown in fig. 34).

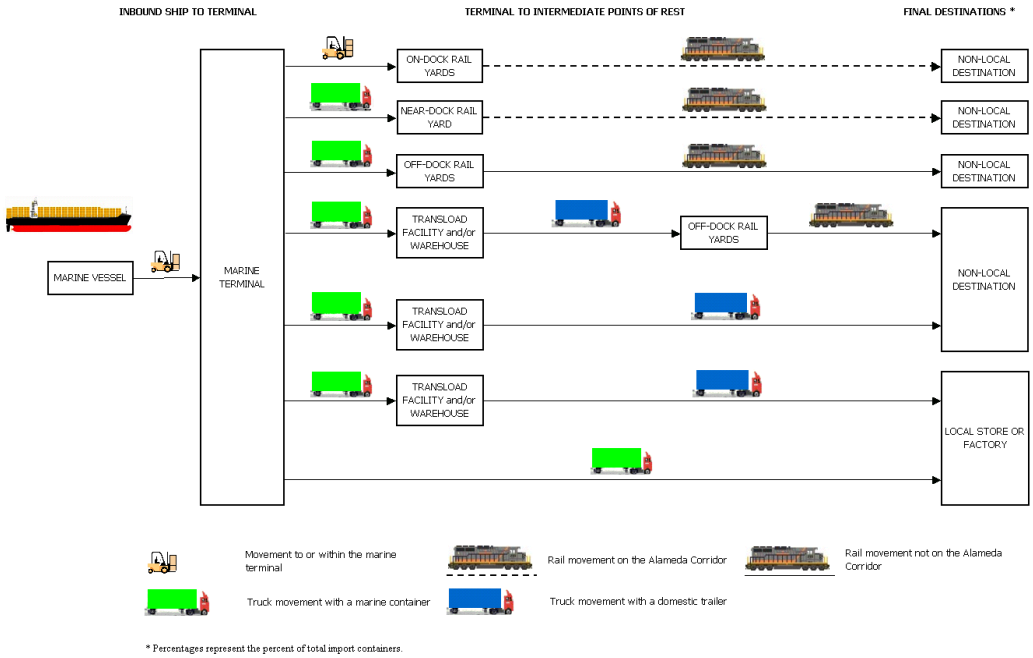

Figure 34. Diagram of San Pedro Bay loaded import container movement scenarios (image courtesy of Port of Long Beach).

Rail Movement

Five of the six container terminals at the Port of Long Beach are equipped with on-dock rail. On-dock rail allows containers to be loaded onto a train right at the terminal, minimizing travel time and costs. From a Port of Long Beach on-dock rail facility, a container can reach Chicago in about 72 hours. On average, about 60 trains depart from the on-dock rail facilities every week. The Port of Long Beach is served by two major trunk-line railroads: Union Pacific Railroad (UP) and BNSF Railway (BNSF), and a regional switching railroad, the Pacific Harbor Line (PHL).

Figure 35. Port of Long Beach rail map (image courtesy Port of Long Beach).

Physical Damage, Losses, and Logistics in the SAFRR Tsunami Scenario

Damage assessment has been quantified through careful analysis of each individual terminal at the time of the tsunami. A number of assumptions have been made in relation to damage assessment based on past tsunami experience and professional engineering judgment. With approximately four hours of warning time before the first wave arrives in the San Pedro Harbor, it has been estimated there will be at least 2 days in which port operations will come to a halt. The first day will consist of safely shutting down operations, beefing up moorings,

deploying tug boats, removing vessels where possible, and generally preparing for the tsunami arrival and evacuation of personnel. The second day is allocated for inspection of facilities prior to restoring operations. Not all terminals will be restored to full capacity based on observed damage. All loading and unloading equipment will be disengaged to prevent damage. The following sections summarize these damages.

Impacts on Maritime Activities

The majority of the impact on maritime activities can be attributed to the container terminals and dry bulk facilities. An important assumption to note is that the gantry crane motors are above water level during inundation, leaving minimal to no damage to cranes during the tsunami. It is possible crane power supply trenches will be flooded as well as some substations. However, discussions with design electrical engineers suggest that long-term damage to these facilities is not likely if they are properly shutdown prior to tsunami arrival. These facilities should be able to power up as soon as they are dried out from flooding.

The inundation levels for the tsunami scenario are insufficient to float any large vessels onto land so there will not be any damage related to this potential mechanism.

When assigning a dollar value to damages, refer to 2011 average value of damages in table 12. Values were retrieved from USA Trade Online (U.S. Census Bureau, 2012b). To obtain damage values in tables 13 through 22, "Value of Damage ($/TEU)" or "Value of Damage ($/Metric Ton)" from table 12 were multiplied by numbers in "Projected Throughput impacted on March 27, 2014." Import and exports are noted where available. For container traffic, this information is not readily available. It is suggested that the damage value to containers be distributed based on overall ratio of container imports to container exports.

Table 12. Assigning damage value to the Port of Long Beach and Port of Los Angeles.

[US$, U.S. dollars; kg, kilograms; TEUs, twenty-foot equivalent units]

Values	2009	2010	2011
Sum of Containerized Vessel Value (US$)	$228,372,241,028	$277,098,700,554	$309,743,852,223
Sum of Containerized Vessel SWT (kg)	56,871,671,800	65,776,161,955	68,793,600,118
Sum of TEUs (from kg)	7,393,931	8,660,123	8,959,111
Value of Damage ($/per TEU)	30,886.44	31,997.09	34,573.06
Value of Damage ($/per Metric Ton)	4,015.57	4,212.75	4,502.51

Port of Long Beach

Damage assessment for the Port of Long Beach is presented in table 13 through 16.

Containerized

Table 13. Port of Long Beach container terminal damage.

[TEUs, twenty-foot equivalent units; --, no data; %, percent]

Location	March 27, 2014 Throughput (TEUs)	Projected Throughput impacted on March 27 2014 (TEUs)	Value of Damage (U.S. Dollar)	Damage Assessment
Pier T Berth T132-T140	4,290	0	--	No damage
Pier G: Berths G226-G236	2,347	0	--	No damage
Pier F: Berths F6-F10	2,120	0	--	No damage
Pier J: Berths J243-J247, J266, J270	5,096	0	--	No damage
Pier A : Berths A88-A96	4,234	635	$21,000,000	15% loss to daily throughput value
Pier C: Berths C60-C62	1,065	160	$6,000,000	15% loss to daily throughput value. Significant number of containers on wheels (chassis)
Total	19,152	795	$27,000,000	

Dry Bulk

Table 14. Port of Long Beach dry bulk damage.

[--, no data; %, percent]

Location	Material	March 27 2014* Throughput (metric tons)	Projected Throughput impacted on March 27 2014 (metric tons)	Value of Damage (U.S. Dollar)	Damage Assessment
Pier D—Berth D46	Gypsum	205	31	$140,000	15% loss to daily throughput value; imported material
Pier D-Berth D32	Cement	100	--	--	No damage
Pier F—Berth F211	Petroleum Coke, prilled sulfur	1,954	33	$148,000	5% loss to daily throughput value; imported material
Pier F-Berth F208	Cement		--		No damage
Pier F—Berth F210	Salt		65	$292,000	10% loss to daily throughput value; imported material
Pier G-Berths G212-G214	Petroleum coke, coal, potash, borax, sodium sulfate, soda ash, concentrates, and prilled sulfur.	19,094	--	--	No damage
Pier B-Berth B82	Gypsum	377 metric tons	--	--	No damage
Total		21,730 metric tons	129	$580,500	

Liquid Bulk

Table 15. Port of Long Beach liquid bulk damage.

[--, no data]

Location	Cargoes Served	March 27 2014 Throughput (metric tons)	Projected Throughput impacted on March 27 2014 (metric tons)	Value of Damage (U.S. Dollar)	Damage Assessment
Pier T-Berth T121	Crude oil and petroleum products	49,220	--	$50,000 mooring damage	Damage to mooring hardware; crippled for 6 weeks; imported crude oil
Pier B—Berths B76-80	Petroleum products				No damage
Pier B Berth B82,83	Gasoline, ethanol, gasoline blend stocks, diesel, biodiesel	29,300	--	--	No damage
Pier B—Berth B84-B87	Crude oil, petroleum products, bunker fuel.				No damage
Pier F—Berths F209-211	Petroleum products and bunker fuel	6,350	--	--	No damage
Pier S Berth S101	Miscellaneous bulk liquid chemicals	5,580	--	$1,000,000	No damage to products, facility out of commission for a month, $1 million in building repair. Currently not in use. Most recently used as low-sulfur diesel import.
Total				$1,050,000	

Break Bulk

Table 16. Port of Long Beach break bulk damage.

[n/a, not applicable; --. no data]

Location	Equipment/ Facilities	March 27 2014 Throughput	Projected Throughput impacted on March 27 2014 (metric tons)	Value of Damage (U.S. Dollar)	Damage Assessment
Pier F Berths F204-F205	Steel products, plywood, and lumber.		--	--	No damage
Pier F—Berth F206, F207	Steel products, plywood, lumber, project cargoes, and large machinery.	1,209 metric tons	--	--	No damage
Pier F Berth F201	Standby berth		--	--	No damage
Pier D, Berth D50-D54	Crescent Warehouse Company	n/a	--	n/a	15% loss to daily throughput value. recently vacated.
Pier T, Berth T122	Lumber and Lumber products		--	$50,000	Mooring damage, 1 month down time. Import material.
Pier T Berth T118	Recyclable metal and steel products.	2,474 metric tons	--	$50,000	Mooring damage, 1 month down time. Export material.
Pier T-Berth T122	Lumber and lumber products.		--	--	No damage
Pier B Berth B82, B83	Automobiles, Office building, processing buildings, body shop and car wash	2,000 vehicles	2,000 vehicles	($24,000/vehicle) $48,000,000	100% vehicle damaged. Imported vehicles.
Total			2,000 vehicles	$48,100,000	

Notes: The average value lost for an automobile is taken to be $24,000/vehicle. The figure extrapolates from 2010 retail values of import vehicles according to the U.S. Census Bureau (2012a), reduced by 13 percent for retail markup per Kelley Blue Book (2013) and TrueCar (2013).

Port of Long Beach Damage Summary

Table 17. Port of Long Beach damage summary.

[TEUs, twenty-foot equivalent units; --, no data]

Cargo Type	Projected Throughput impacted on March 27 2014	Value of Damage (U.S. Dollar)
Containerized	795 TEUs	$27,000,000
Dry Bulk	129 metric tons	$580,500
Liquid Bulk	--	$1,050,000
Break Bulk	2,000 vehicles	$48,100,000
Total		$76,730,500

Port of Los Angeles

Damage assessment for the Port of Los Angeles is presented in tables 18 through 23. Refer to table 12 for average damage values per cargo type.

Containerized

Table 18. Port of Los Angeles container terminal damage.

[TEUs, twenty-foot equivalent units; --, no data; %, percent]

Location	Projected throughput on March 27, 2014 (TEUs)	Projected Throughput impacted on March 27, 2014 (TEUs)	Value of Damage (U.S. Dollar)	Damage Assessment
Berths 100-102	1,270	--	--	No Damage
Berths 121-131	2,590	--	--	No Damage
Berths 135-139	2,410	241	$8,314,500	10% loss to daily throughput value
Berths 206-209	1,200	--	--	No Damage, No longer used as terminal
Berths 212-225	2,575	--	--	No Damage
Berths 226-236	2,860	--	--	No Damage
Berths 302-305	4,100	--	--	No Damage
Berths 401-404	6,470	--	--	No Damage
Berths 405-406	1,270	--	--	No Damage
Total	25,000	241	$8,314,500	

Dry Bulk

Table 19. Port of Los Angeles dry bulk damage.

[--, no data; %, percent]

Location	Terminal features	Projected throughput on March 27, 2014 (metric tons)	Projected Throughput impacted on March 27 2014 (metric tons)	Value of Damage	Damage Assessment
Berths 165-166	Industrial borates	843	85	$382,000	10% loss to daily throughput, Out of commission for 2 weeks. Off-line for 2 weeks for cleanup. Exported material.
Berths 210-211	Handles all grades of ferrous and non-ferrous scrap metals	3,212	--	--	No Damage
Total		4,055	27.4	$382,000	

Liquid Bulk

Table 20. Port of Los Angeles liquid bulk damage.

[--, no data]

Location	Use:	Projected throughput on March 27, 2014 (metric tons)	Projected Throughput impacted on March 27, 2014	Value of Damage (U.S. Dollar)	Damage Assessment
Berths 118-120	Receiving exporting petroleum products	2,695	--	--	No Damage
Berths 148-151	Vessel unloading of partly or fully refined petroleum products	1,361	--	--	No damage. Containment walls or berms protect tanks
Berth 163	Marine oil	812	--	--	No damage to product. Facility 50% capacity for 1 month. Imported material
Berth 164	Fuels and lubricants	4,030	--	--	No damage to product. Facility 50% capacity for 1 month. Imported and exported material
Berths 167-169	Fuels and lubricants	5,237	--	--	No damage to product. Facility 50% capacity for 1 month. Imported and exported material
Berths 187-191	Liquid bulk chemical products	11,778	--	--	No damage to product. facility down 50% capacity for 1 month. Imported and exported material
Berths 238-240C	Fuels and lubricants	229	--	$50,000	Damage to mooring equipment, no product damage. Imported crude. Alternate berth available
Total		21,428	--	$50,000	

Automobile

The average wholesale value for automobile damage is taken to be $24,000/vehicle. The figure extrapolates from 2010 retail values of import vehicles according to the U.S. Census Bureau (2012a), reduced by 13 percent for retail markup per Kelley Blue Book (2013) and TrueCar (2013).

Table 21. Port of Los Angeles automobile damage.

[%, percent]

Location	Terminal features	Projected automobiles on March 27, 2014	Automobiles impacted on March 27, 2014	Value of Damage (U.S. Dollar)	Damage Assessment
Berths 195-199	Storage capacity up to 8000 vehicles	6,400	650	$15,600,000	10% vehicles damaged. Imported vehicles.

Break Bulk

Table 22. Port of Los Angeles break bulk damage.

[n/a, not applicable; --, no data; %, percent]

Location	Terminal features	Projected throughput on March 27, 2014 (metric tons)	Projected Throughput impacted on March 27 2014 (metric tons)	Value of Damage (U.S. Dollar)	Damage Assessment
Berths 49-53	Use: break bulk steel	n/a	--	--	No damage
Berths 54-55	Imported meats, Chilean fruit, kiwis, apples	327	--	--	No damage
Berths 174-181	Steel	5,357	535	$2,408,850	10% product damage, Building out of commission for 2 weeks. Imported material.
Total		5,684	535	$2,408,850	

Small Craft Basins

All marinas located where the East Basin and Cerritos Channel meet will experience significant damage. The majority of the marinas will experience some damage, as they will be directly exposed to the current velocities. Damage to small craft basins marinas is addressed elsewhere in this chapter.

Table 23. Port of Los Angeles marina damage.

Marina Name	Location	Slips	Slips Affected	Value of Damage
Al Larson's Marina	Berth 258	128	50	Addressed elsewhere in this chapter
Cabrillo Beach Yacht Club	Berth 35	184	50	
Cabrillo Way Marina	Berths 42-43	697	100	
California Yacht Marina-Cabrillo Marina	Berth 29-33	885	100	
California Yacht Marina	Berth 202	266	266	
Cerritos Yacht Anchorage	Berth 205	90	90	
Holiday Harbor-Fleitz Bros.	Berth 34	300	300	
Holiday Harbor	Berth 201	169	169	
Island Yacht Anchorage #1	Berth 205	22	22	
Island Yacht Anchorage #2	Berth 200X	116	116	
Leeward Bay Marina	Berth 201	190	190	
Lighthouse Yacht Landing	Berth 205	70	70	
Pacific Yacht Landing	Berth 203	178	178	
San Pedro Marina	Berth 80	85	20	
Yacht Centre-Newmarks	Berth 204	250	250	
Yacht Haven Marina	Berth 202	165	165	

Table 24. Port of Los Angeles damage summary.

[TEUs, twenty-foot equivalent units; --, no data]

Cargo Type	Projected Throughput impacted on March 27, 2014	Value of Damage (U.S. Dollar)
Containerized	241 TEUs	$8,314,500
Dry Bulk	27.4 metric tons	$382,000
Liquid Bulk	--	$50,000
Automobiles	650 metric tons	$15,600,000
Break Bulk	535 metric tons	$2,408,850
Small Craft Marina	2,000 slips	(elsewhere in this chapter)
Total		$26,755,350

General Damage Discussion

Mooring design of the terminals in POLA/POLB typically includes a mooring analysis for the proposed vessels that incorporates winds, waves, and current forcing to the moored vessels to compute loads on the mooring components, including mooring lines, bollards, and fenders. When mooring loads resulting from high currents representative of a tsunami are compared with the loads generated by design wind speeds, generally the loads resulting from the winds are the controlling factor for design purposes. This is particularly true for container vessels with high wind profiles due to the stacked containers. The currents can be more of a contributing factor for liquid bulk carriers, as their wind profile is less and the draft more significant. However, the bulk of the currents adjacent to the liquid bulk terminals in both ports do not generally appear to be sufficient to overload the mooring components to the extent that the vessels would become free floating. Some damage to the mooring components is expected and has been included in the assessment. Alternate moorings would be available to prevent loss of terminal function at Port of Long Beach Berths T118, 121, and 122.

Where automobiles are indicated as being damaged, it is assumed that the damage will be limited to the vehicles and they will not become free-floating debris items in the navigation channel. This assumption is based on the limited water depth over the automobile storage facilities, relatively small currents, and the fact that the storage facilities are located some distance inland from the pier headline. Removal of the vehicles following the tsunami will entail shipping them inland in the normal manner to scrap yards.

There is some commercial fishing activity in the Port of Los Angeles located within Fish Harbor and adjacent to Ports O Call. Damage to fishing vessels and other small craft is addressed elsewhere in this chapter. The inundation limits along the boundary of Fish Harbor are along the fringe of the basin and suggest some flooding of the waterfront area and possibly damaging some of the associated fish processing and shipping facilities.

Tsunami Impacts on Container Terminal Operations

With approximately 4 hours of warning before the first wave arrives in the San Pedro Harbor, it is realistic that there will be at least 2 days in which port operations will come to a halt. The first day during the tsunami propagation will consist of strategically and safely shutting down operations. The second day will consist of inspections of the facilities to identify any

damage. Some terminals may be up and running after the tsunami warning is cancelled on Saturday 29 March. Gate operations will cease and all personnel will follow evacuation procedures. All loading and unloading equipment will be disengaged to prevent damage.

Tsunami Impacts on Truck and Rail Movement

With a warning time of 3.5 hours, teamsters will have time to remove trucks to an offsite location away from the inundation areas. (Rail is addressed elsewhere in this chapter) Continued truck movement may involve movement of vehicles away from inundation areas to prevent damage or relocation of other equipment that may potentially be harmed. Once the port is evacuated, all truck movement will come to a halt until the tsunami warning is cancelled. After the third day, it is believed that there will be minimal impact on truck and rail movement due to a tsunami of this magnitude. The simulated tsunami inundation at the rail and road bridge to Pier 400 will come close to the soffit of the superstructure, but is not expected to impact the superstructure or damage the bridges. The high currents may dislocate some of the armor stone protecting the bridge abutments and channel area, but should not undercut the foundations. The armor stone was designed to accommodate expected high current speeds when constructed.

Damage to Lifelines

All electrical wiring and equipment inside vaults and pull boxes are continuously submersible. At the first warning of a tsunami, substations will be powered down to prevent any possible damage to equipment and protective devices. Drying out of equipment should only take a few days to a week. There does not appear to be significant damage to major SCE power vaults from water levels and inundation limits. Water runoff should only take a few days to clear and should have minimal impact to POLA/POLB operations.

Damage to Other West Coast Ports

The tsunami scenario impacts are modeled for other major ports along the Pacific coast including San Diego, Port Hueneme, San Francisco, Oakland, Richmond, and Redwood City. These are potential alternate ports where vessels could call when the Ports of Los Angeles and Long Beach are not available. However, these ports are not likely to be available during the tsunami event or possibly for days afterward. No detailed assessment of the tsunami damage to these other ports was conducted as part of this project. Some general observations are discussed in this section.

Damage to Other Southern California Ports

The Port of San Diego operates two marine terminals, neither of which would be inundated by the tsunami. They would be expected to have minimal damage. However, there are a large number of navy piers that may be flooded and vessels may be present. Navy procedures typically call for vessels to leave port if possible. Remaining vessels may have some damage to the mooring components due to the water level fluctuation and/or high currents. Supplies on piers may be floated off causing debris issues. The major issue within the Port of San Diego area is the numerous small craft basins that will likely sustain significant damage due to the high currents and lesser design criteria compared to commercial and naval facilities. For example, strong currents damaged docks and boats around Shelter Island during the 2011 Tohoku and 2010 Chile tsunamis (Wilson and others, 2012). Free-floating small craft are likely to create a

significant debris problem following the tsunami. Note that marina damage in San Diego is addressed later in this chapter.

Port Hueneme specializes in shipping break bulk cargo, palletized produce, and automobile imports and exports. The extent of the inundation is expected to cause damage to several warehouses and operations buildings. The automobile import/export terminal would not be flooded, and automobiles are not expected to be damaged. The detailed tsunami modeling indicates currents as high as 12 nautical miles per hour (kt) in the entrance channel, which is sufficient for possible scour of the channel and possible damage to the toe armor of the jetties. The scour will possibly deposit sediment in the interior of the harbor that will require maintenance dredging following the tsunami.

Damage to the Port of San Francisco

Farther north along the California coast, the ports in the San Francisco Bay (San Francisco, Oakland, and Richmond, and Redwood City) would also be affected by the tsunami. They would have 30 minutes less warning time than the southern California ports. In this hypothetical event, NOAA posts a tsunami watch for the San Francisco Bay within a few minutes after the earthquake (here, 11:54 a.m. PDT on Thursday March 27, 2014), and upgrades it to a tsunami warning at 2:05 p.m., 3 hours before the first wave's estimated arrival time at 5:02 p.m. At 2:05 p.m., NOAA estimates wave heights in San Francisco of 2.1 ft ± 0.6 ft (0.64 m ± 0.18 m; NOAA's simulated tsunami messages use U.S. units, so these are repeated here first) and a duration of 9 hr. The estimated wave height at San Francisco increases with later tsunami messages, reaching 2.7 ft ± 0.8 ft (0.82 m ± 0.24 m) at 5:02 p.m., 2.9 ft ± 0.9 ft (0.88 m ± 0.27 m) at 6:02 p.m., by which time a buoy at station 46026, 20 miles (17.4 nautical miles) west of the Golden Gate, has observed a maximum wave height of 3.4 ft (1.0 m), which ultimately reaches 3.7 ft (1.1 m). The warning is downgraded to an advisory at 8:02 p.m. on Friday 28 March, 32 hours after the earthquake. It is cancelled at 12 p.m. PDT on Saturday 29 March, 48 hours after the earthquake.

The tsunami model used in this study estimates wave heights in excess of 2m (6 ft) at the Golden Gate in approximately the 3rd wave about 90 minutes after the 1st, around 6:30 p.m., as illustrated in figure 36.

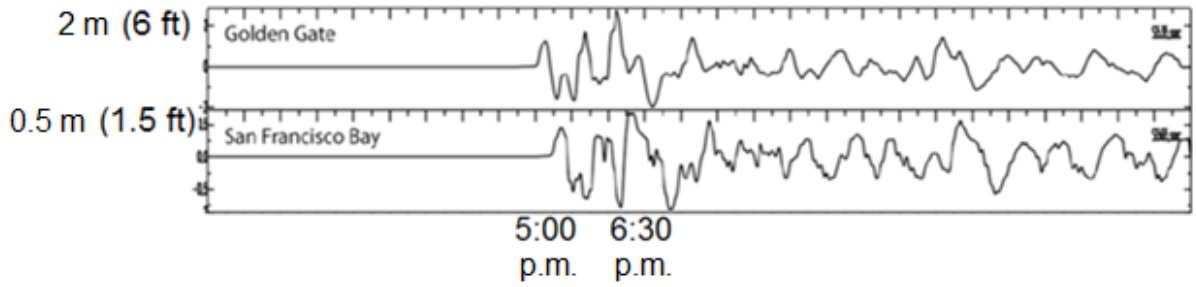

Figure 36. Marigrams in San Francisco Bay area for the SAFRR tsunami scenario (m, meters; ft, feet).

Maximum wave amplitudes above MHW+20 vary throughout the San Francisco Bay area, reaching 5 m (15 ft) in along the Pacific Coast and parts of the bay's shore, as shown in figure 37. The tsunami is expected to cause flooding along the San Francisco Embarcadero, with flow depths of 1–2 m (3–6 ft). Currents along the Embarcadero reach 5–10 m/sec (10–20 kt); see figure 38.

Damage to Port of San Francisco Headquarters Building

The Port of San Francisco has its offices at Pier 1, which is estimated as being flooded to a depth of 1–2 m (3–6 ft). The 1st floor of the office would be heavily damaged by that level of inundation. Crucial computer equipment is on the upper level of the port headquarters and so would probably escape damage, but the two 300 kilowatt (kW) generators are on the 1st floor and would be damaged. Commercial space in lowrise reinforced concrete shearwall buildings can take 3 months to repair after experiencing 130 m^3/sec^2 momentum flux (maximum depth does not occur at the same time as maximum velocity), so the headquarters would be inoperative for months during repair. The port does not have a backup operations facility, and would most likely operate at least temporarily out of the San Francisco Emergency Operations Center.

Commercial Real Estate at the Port of San Francisco

The port derives much of its revenue from the rental of commercial real estate ($59 million of $73 million total revenue in fiscal year 2011–2012), especially at Pier 39 and the Ferry Building, both of which are modeled as flooding to a depth of 1–2 m (3–6 ft, see figure 39) and maximum velocities of 5–10 m/sec (10–20 kt), and so would likely be inoperative for several months. Leases assign responsibility for cleanup, and may vary between tenants. It was unclear from conversations with port personnel whether the real estate division maintains emergency plans for such a contingency, although they do have radios for emergency communication and expect to warn tenants using their Cooper Industries notification system. Within the port's commercial real estate, the largest impacts would be to Pier 39 and Fisherman's Wharf, which are visited by 14 million tourists per year. The cruise terminal at Pier 27 is modeled as being vacant (no cruise ship there) at the time of the tsunami. Damage to the cruise terminal would likely displace cruise activities for up to a season.

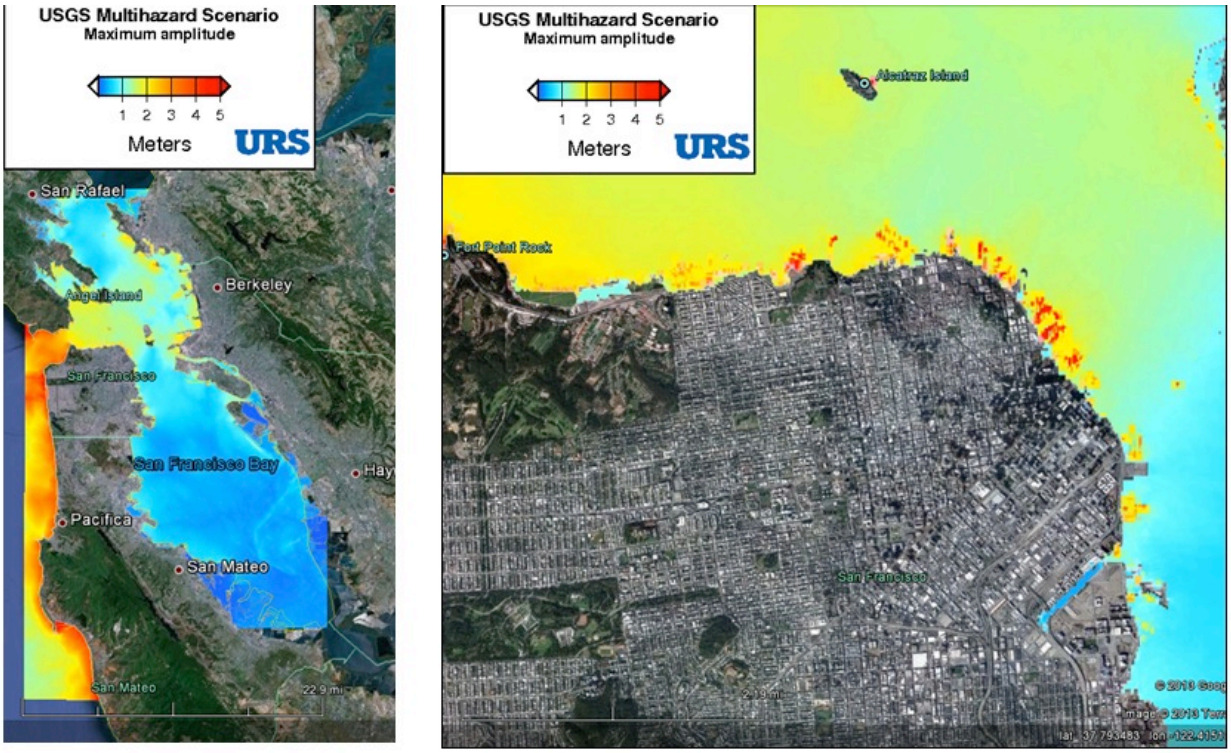

Figure 37. Wave amplitudes in the San Francisco Bay area for the SAFRR tsunami scenario.

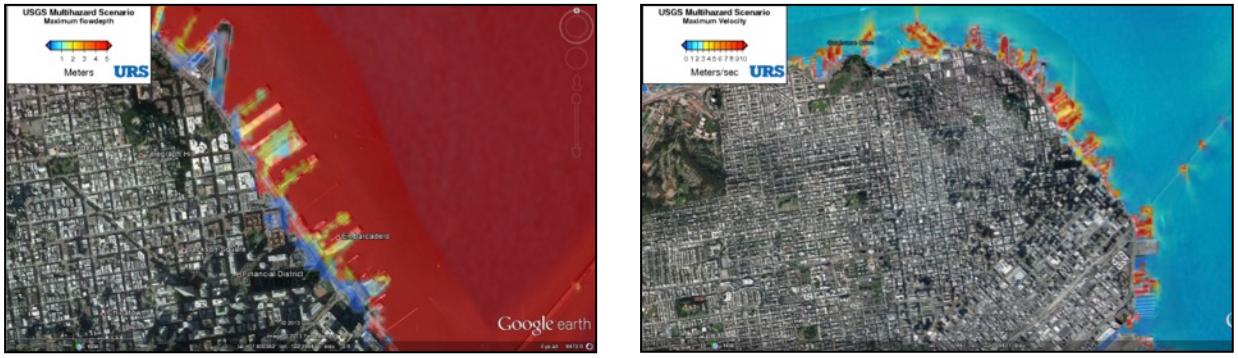

Figure 38. Flooding along the San Francisco Embarcadero reaches 1 to 2 meters and wave velocities reach 5 to 10 meters per second (10-20 knots) in the SAFRR tsunami scenario.

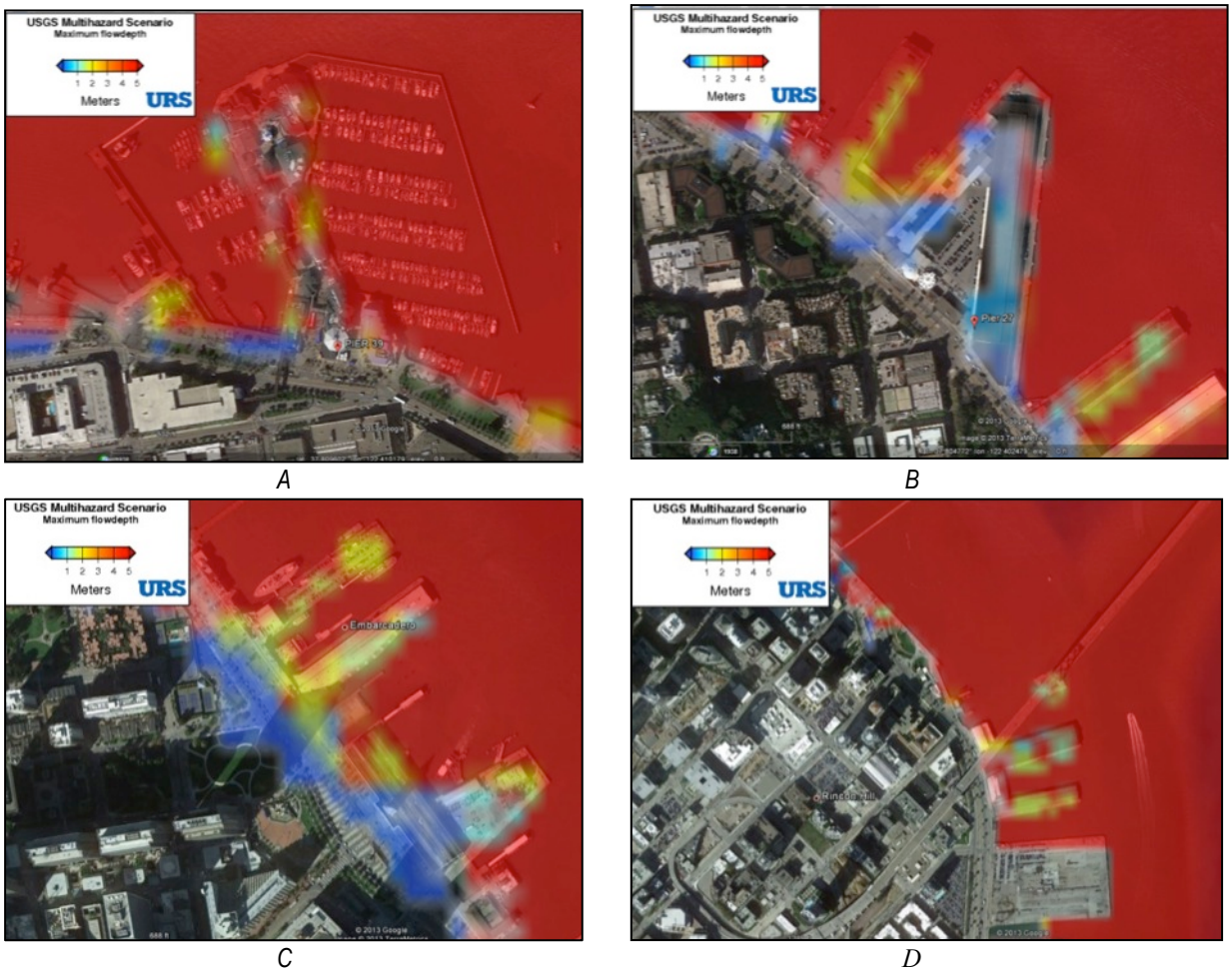

Figure 39. Inundation along the San Francisco Embarcadero in the SAFRR tsunami scenario: *A,* Pier 39; *B,* Pier 27; *C,* Pier 1 and Ferry Building; and *D,* Pier 26.

Ferry Operations

It is unclear whether the tsunami could damage the access gangways for ferries. As long as the collars do not get damaged, port personnel believe that ferry operations would not be impacted by damage, although debris on the piers at ferry berths would have to be cleaned up before ferry operations could resume.

Cargo Operations at the Port of San Francisco

The Port of San Francisco handles approximately 1 million tons of cargo annually (1.24 million in calendar year 2012) from approximately 40 cargo vessel calls annually at Piers 80, 94, and 96. Because these piers are occasionally flooded simply by high tides, they would certainly be flooded in the tsunami scenario. Most of the cargo is imported breakbulk (1.21 million tons—largely steel and aggregate) that port personnel believe would be undamaged by flooding. However, the cargo office would be damaged just as would be the headquarters building, along with equipment such as forklifts. There might be one or two cargo vessels berthed at the time of the tsunami. Port personnel believe that in the event of a tsunami warning, harbor staff would alert vessel masters to move their vessel to the southern part of the San Francisco Bay. As

previously noted, there would be approximately 3 hours between the time NOAA issued a tsunami warning for the San Francisco Bay and the arrival of the 1st wave. With currents near the waterfront of 5–10 m/sec (10–20 kt; see fig. 40), vessels that were unmoored but still near the waterfront when the tsunami first arrived would be nearly impossible to control, so the timely movement of vessels would be crucial to avoiding damage to the vessels and piers.

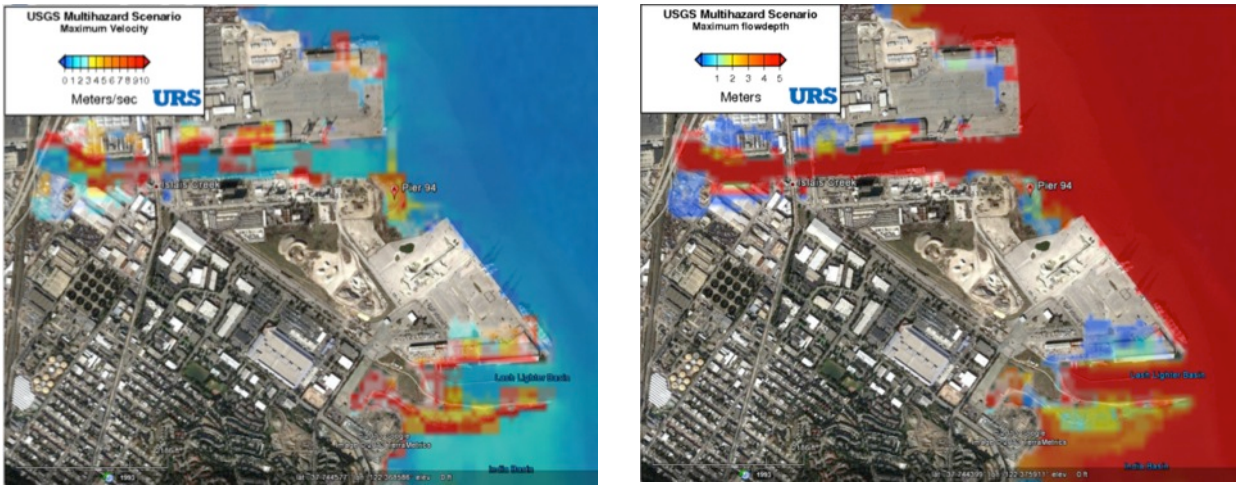

Figure 40. Velocities (left) and flow depth (right) at Port of San Francisco cargo piers in the SAFRR tsunami scenario.

Commercial Fishing Fleet

There are approximately 180 boats in the commercial fishing fleet at Pier 45. Port personnel believe that active boats would be moved to the southern bay, but since March is largely an idle time for the commercial fishing fleet, that would amount to only approximately 40 of the 180 boats. The inner lagoon, where 120 of the boats are berthed, is estimated to experience 2 to 8 m/sec (4–16 kt) currents, enough to damage or sink commercial boats remaining there. (Port personnel expect that no more than 20 percent of the owners of boats in the recreational marinas would be close enough to move their boats during the available warning time. Recreational marinas are addressed later in this chapter.) Pier 45 also has a fish processing and distribution facility, which is estimated to experience 1–2 m (3–6 ft) of flow depth and 5 to 10 m/sec (10–20 kt) velocity. This would be sufficient to cause heavy damage to the processing and distribution facility and render it inoperative for at least several months. Port personnel believe that dock repairs could render the fishing pier inoperative for a year, and that dock repairs might not be completed for as much as 2 years.

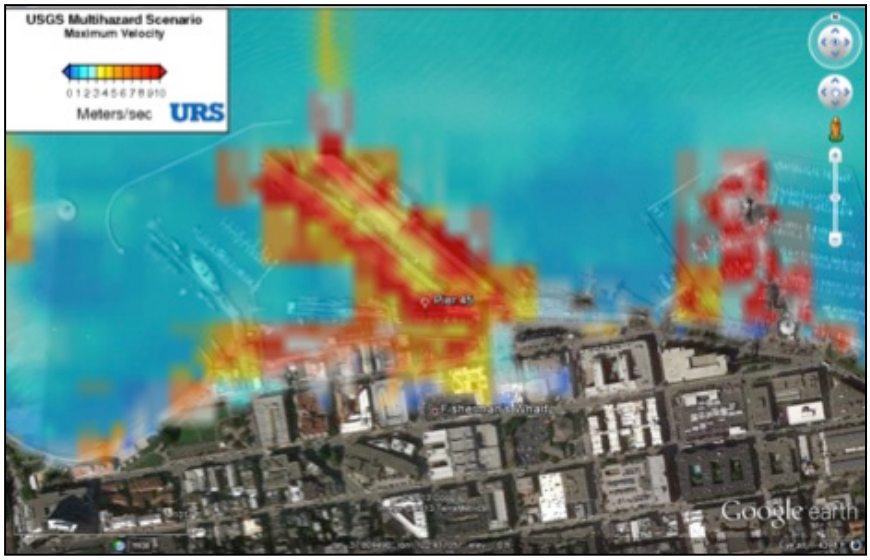

A

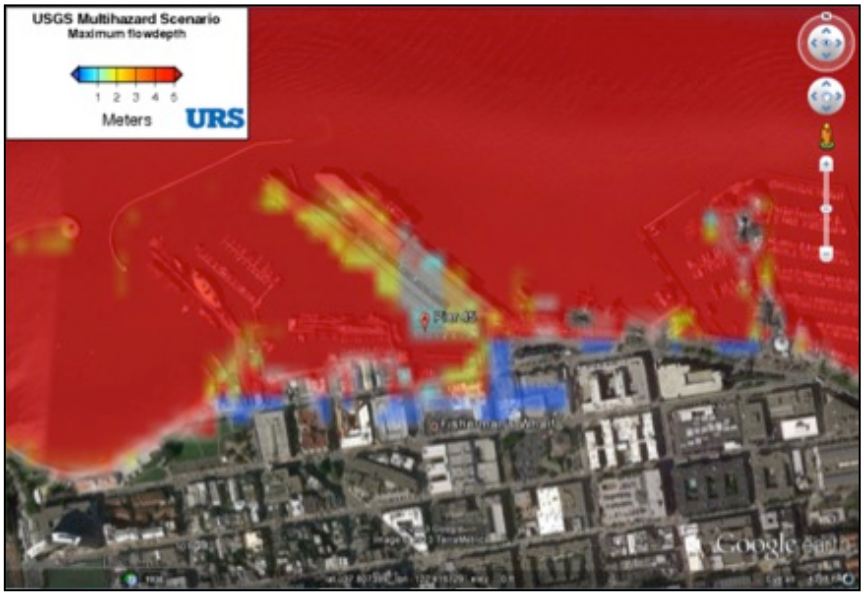

B

Figure 41. Velocities (*A*) and flow depth (*B*) at Port of San Francisco Pier 45 in the SAFRR tsunami scenario.

Seawall

The Port of San Francisco has a unique feature—an old seawall along much of its waterfront that is in various stages of structural integrity. We did not evaluate the potential for a tsunami to damage the seawall, but that may be worth investigating, especially at high-value locations or where crucial lifelines such as the Auxiliary Water Supply System, BART (Bay Area Rapid Transit), Muni (San Francisco Municipal Transportation Agency), or telecommunications are located near the seawall and could be damaged by its collapse.

Damage to Other San Francisco Bay Ports

The Ports of Oakland, Richmond, and Redwood City are also located within San Francisco Bay, which protects the ports from open coast swell conditions compared to the Ports of Los Angeles and Long Beach. Wave loads on structures and vessels are generally limited to shorter period, locally generated wind waves. Although these wind waves can be significant during storm activity, they have a significantly shorter wave period that generally decreases the loads. In general, design criteria are frequently controlled by currents and wind rather than waves. As such, the San Francisco Bay ports are likely better prepared for the current loads on vessels and structures during a tsunami. These commercial ports are also designed to the latest State engineering standards.

Figure 42 shows the extent of the maritime facilities in the Port of Oakland. As shown in figures 43 and 44, flow depths at piers and other port facilities are generally less than 0.5 m, and maximum currents are generally 1–2 m/sec (2–4 kt). Flooding is limited to the edges of wharves with the exception of the Ben E Nutter and TraPac terminals, where significant numbers of cargo containers and truck trailers are stored or parked.

Based on the inundation limits, it would be expected that a similar damage rate would occur as in the parts of the Ports of Los Angeles and Long Beach that are inundated. The total damage to these ports will generally be in proportion to their shipping volume compared to San Pedro Harbor, possibly somewhat higher in the Ben E Nutter and TraPac terminals where container yards and bulk areas are hypothesized to be flooded. There are also several small craft harbors throughout the area that are likely to experience more damage than the commercial facilities. These small craft will likely pose a significant debris and cleanup problem.

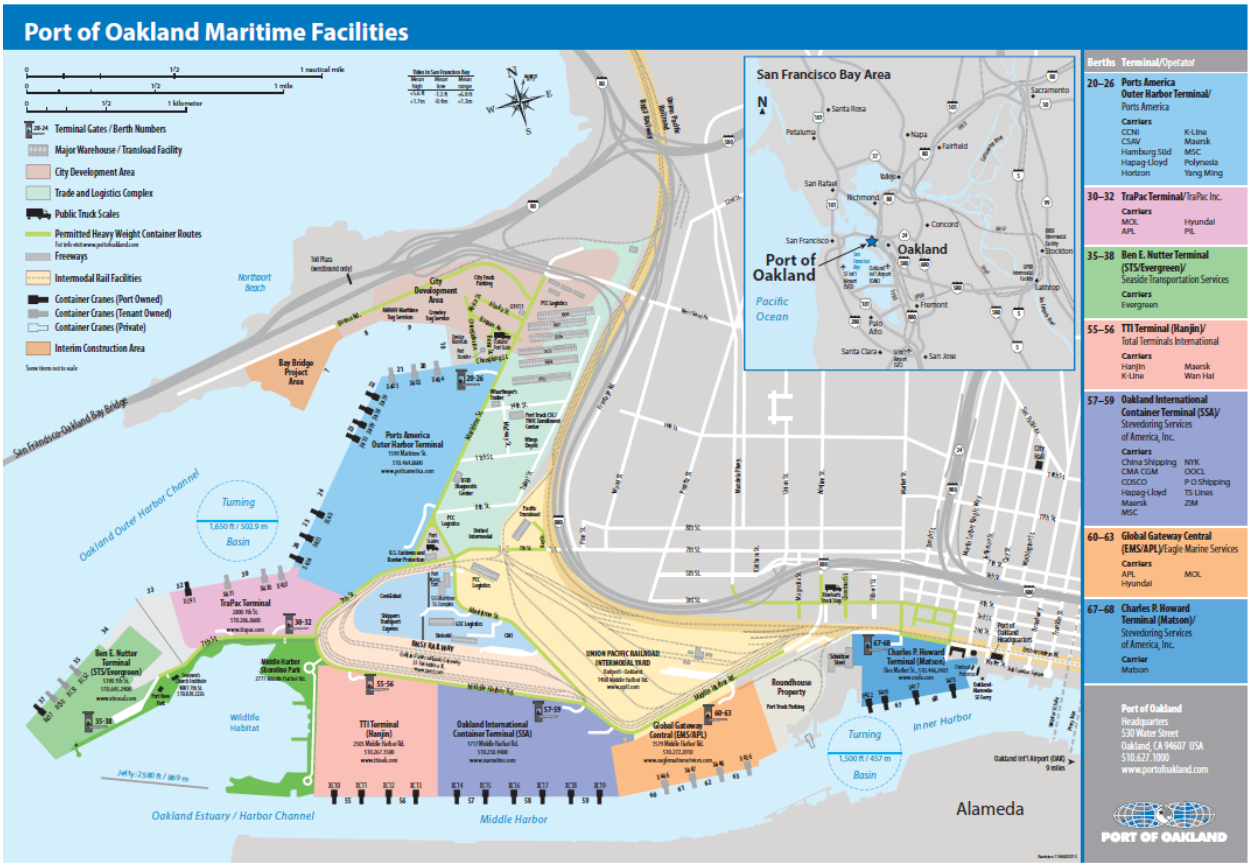

Figure 42. Port of Oakland maritime facilities map (Port of Oakland, 2013).

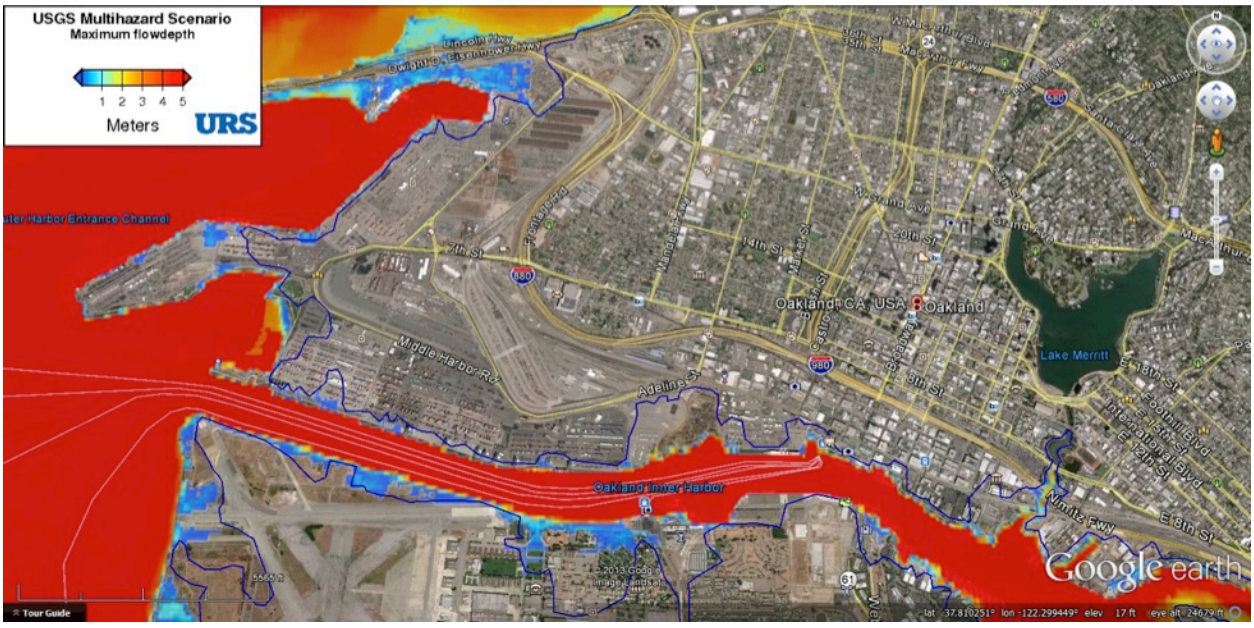

Figure 43. Flow depths and inundation line at Port of Oakland in the SAFRR tsunami scenario.

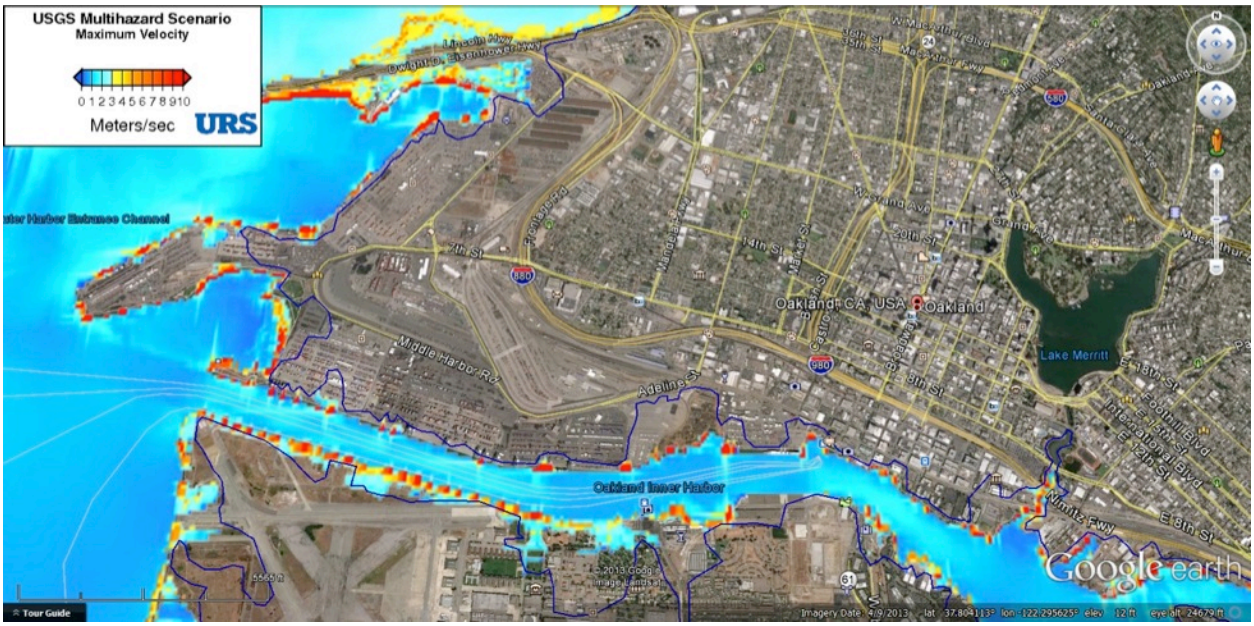

Figure 44. Current velocities in the Port of Oakland in the SAFRR tsunami scenario.

Resilience Strategies

On the basis of the somewhat limited overall damage to infrastructure in the Ports of Los Angeles and Long Beach, there are limited opportunities for improved engineering strategies. The most significant area of the Ports of Los Angeles and Long Beach to be flooded is in the area of Pier A at the Port of Long Beach. There will be damage to imported vehicles and damage to containers. The Port of Long Beach is well aware of the low area and has made an economic decision to not raise the land area. Operations buildings in this area have raised foundations to limit the risk of flooding and associated damage to infrastructure. Personnel evacuation procedures need to be developed for the safety of people working in the area. Given the lead-time for the proposed scenario, there should adequate time to shut down operations in this area and safely evacuate all personnel.

One design feature that could possibly be reviewed and improved on is the containment dikes around pipelines and tank farms. The crest of these containment dikes could be designed such that inundation will not occur within the contained areas. This will limit the damage to the facilities and reduce the likelihood of environmental damage from oil spills. Most of the tank farms are protected by containment dikes, but elevations should be confirmed against the proposed tsunami elevations. This may also entail more detailed modeling of hydrodynamics in the vicinity of the containment dikes and walls.

The bulk of the resilience strategies consist of developing and exercising a response plan in the event of a tsunami warning. There are several procedures that could be implemented to mitigate damage from the provided scenario. The most crucial issue to be addressed is the safety of the vessels because any freely floating vessel or even any vessel underway during the extremely high currents presents a risk to the vessel and port facilities. The current operations plan developed by the U.S. Coast Guard and the port pilots is to keep any approaching vessels from entering the port following receipt of a tsunami warning. Any vessels that can be safely removed from the harbor should be removed. During the Chile tsunami of 2010, some vessels in

Chilean ports were able to successfully leave port despite the tsunami arrival time of less than 30 minutes after the seismic event. This should be incorporated in the plan. However, there needs to be a reasonably accurate estimate of the arrival time to minimize the risk of vessels being caught navigating during tsunami arrival. Priority for removing vessels should be given to bulk liquid vessels to minimize environmental risk of spills during the tsunami.

In addition to removing vulnerable vessels during the tsunami-warning period, further investigations of vessel maneuvering during high currents should be conducted. Some work was conducted along these lines in Headland and others (2006) suggesting reasonable success in maneuvering vessels during a tsunami.

Possibly the most important procedure to be developed is to shut down all operations as quickly as possible once the tsunami warning is received. This would include shutting down pumps to liquid bulk tankers and disconnecting hoses. Container cranes should be shut down and safely stored with arms up to minimize the possibility of vessels striking them. Power should be shutdown to reduce or eliminate damage to the power trenches or the cranes. Terminal substations should also be shutdown wherever possible to reduce or eliminate damage to these substations. For dry bulk terminals, the conveyors should be shut down to reduce damage to the motors, which can be flooded in some cases. Nonessential personnel should begin evacuation immediately.

For those vessels remaining in POLA/POLB through the tsunami, tugboats should be deployed to assist in maintaining control of the vessels at their respective berths. Vessels should deploy additional mooring lines where possible. These mooring lines will have to be tended by ship personnel during the tsunami to allow the vessels to rise and fall with the water level so that mooring components such as bollards, mooring lines, and fenders are not overloaded or damaged. This can be accomplished by either manually controlling the shipboard winches or setting the shipboard winches to constant tension where possible instead of breaking the winches. For the tsunami scenario defined in this project, engineering judgment and experience with previous tsunami events within POLA/POLB suggests no damage to any of the vessels within the harbor other than small craft (with one exception discussed later). This conclusion was reached after extensive discussion of the scenario with senior engineers at the ports and senior engineers from design consulting firms.

One additional opportunity to enhance resiliency: a plan to evacuate all nonessential personnel would need to be exercised. As discussed earlier, the ports would have 3.5 hours from the time NOAA first transmits it tsunami warning for San Pedro (at 2:05 p.m. PDT on Thursday Mar 27, 2014) until the forecast arrival of the tsunami at 5:35 p.m. In that time port operators, emergency response personnel and tenants would have to receive the message, understand its contents, and successfully take self-protective action such as shutting off power, removing or elevating crucial documents and other assets, and evacuating the port. Given experience in Hurricane Sandy (discussed next), that is not much time. The resiliency opportunity is to review, exercise, and enhance an evacuation plan as appropriate. The exercise could examine the potential for traffic congestion leaving the port, to check that all port personnel can safely evacuate in that period of time, and to think through potential delays or misunderstandings in decision-making and communication? We discuss policy issues more deeply elsewhere in this report. All of these preparedness, response and recovery plans would need to be regularly exercised to be reliable and effective.

Lessons for Ports from Hurricane Sandy

In March 2013 representatives of the Port Authority of New York and New Jersey (PANYNJ) discussed with SAFRR personnel the port's experience in Hurricane Sandy. They summarized emergency plans, physical damage and recovery activities, and major threats to life safety, focusing on PANYNJ port facilities in Port Newark, Port Elizabeth, Jersey City, Bayonne, Staten Island, and Brooklyn.

Emergency Plans

PANYNJ maintains a contingency plan in accordance with both Federal standards and industry best practices. It has 25 to 30 annexes covering various perils. The plan for hurricane focuses on wind impacts. Preparations deal with lowering stacks of containers to 3 high, battening loose items, not accepting berth applications, tying cranes together, and maintaining tugs on standby. The hurricane plan did not address storm surge, although the port does possess maps showing expected extent of flooding color coded by Saffir-Simpson Intensity (SSI). The logic appears to be that each SSI increment corresponds to an expected degree of storm surge and therefore flooding. (Since 2010, SSI has been revised as the Saffir-Simpson Hurricane Wind Scale to exclude flood ranges, storm surge estimations, rainfall, and location.) Hurricane Sandy produced greater storm surge than the model used to create the map predicted. In fact, until the day before landfall, the National Weather Service (NWS) estimated 6 to 7 ft of storm surge at the ports. At 11 a.m. Sunday October 28, 2012, the day before landfall, the NWS revised the estimate to 13 to 14 ft as a result of a change in the storm's direction. The terminal operators had just reconfigured containers to be stacked lower so as to minimize wind forces, thus putting more containers at ground level and more containers in the flood zone. Because containers are moved by union labor, which requires significant advanced notice to mobilize, it was too late to reconfigure the container stacks. Note that the port personnel with whom we spoke did not have topographic maps or other maps that would show inundation as a function of storm surge. They relied on maps that relied on a model that underestimated flooding in storm surge.

One relevant lesson for the Tsunami Scenario is that this scenario uses models that estimate earthquake magnitude, rupture area, hypocenter, rupture velocity, and various other parameters. Although it is useful for planning, it should not be considered to represent an upper bound of the environmental excitation, that is, the flow depths, currents, extent of inundation, and so on. Another lesson for emergency planning: port personnel indicated that Hurricane Sandy has reinforced the need to stay out of the habit of only reacting to the last event. They also advised that generally the only people who take flooding seriously are those who had personally experienced it in the past. Both of these observations seem relevant to operators of California facilities who do not have personal experience with tsunamis and flooding.

Physical Damage

Flooding destroyed 16,000 vehicles and thousands of containers (see fig. 45). The truck fleet was heavily damaged: port personnel estimate that up to 20 percent of drayage truck fleet was lost, approximately 2,000 of 10,000 trucks in the New York and New Jersey region that serve the port, and the fleet has not yet fully recovered. In addition, approximately 15 percent of the chassis fleet was destroyed. Mechanical and electrical equipment associated with sewer lift stations were damaged, as were traffic signals and railroad crossing equipment, so much so that rail traffic is still using flares and flagmen in March 2013; PANYNJ described the power grid

and electrical equipment as a “giant Achilles’ heel.” Some fuel tanks inside of earthen berms at the facilities along the Arthur Kill were emptied in advance of the storm to protect the stored product, but as a result when storm surge inundated them, the tanks floated off their foundations and were damaged. Tanks behind containment walls fared better. A buried propane tank floated to the surface but did not ignite. Container handling equipment was damaged, including straddle carriers, reach stackers, fork lifts, and electrical equipment on most gantries. Electrical equipment was repaired on enough gantry cranes and container handling equipment within 6 days that the port was able to return to business, although some are still being repaired in March 2013. These damages were the greatest hindrances to recovery. Note the resemblance between hurricane damage in figure 45 and tsunami damage shown in figure 19.

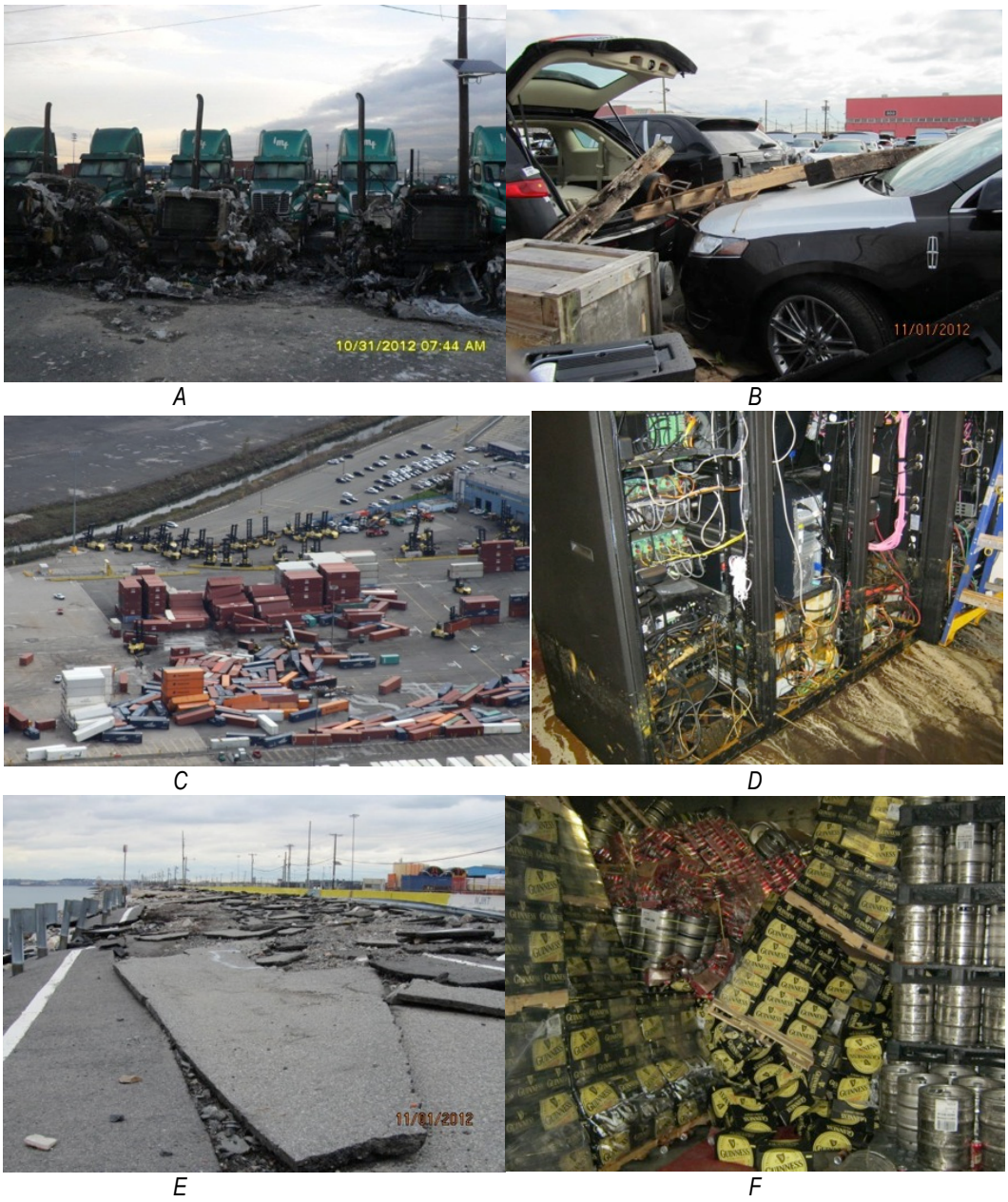

Figure 45. Photographs of damage from Hurricane Sandy at New York and New Jersey ports: *A*, flooding damaged 20 percent of the truck fleet, often by igniting fires and, *B*, destroyed 16,000 import vehicles. *C*, Flooding and wind damaged thousands of containers and much of the ports' cargo handling equipment; *D*, electrical and computer equipment were flooded and damaged; *E*, scour damaged pavements; and *F*, Flooding destroyed product in port warehouses. (Images from Port Authority of New York and New Jersey).

Recovery

Commercial power was available from the public utility an average of 5 days after landfall, though some tenants were not ready to receive power. However, power lines kept falling after the hurricane passed. As of March 2013, underground lines in certain locations

were still being replaced. PANYNJ is still seeing impacts of damage to electric power. PANYNJ speculated that latent damage could be observed for years. Sewer and firefighting were restored after 6 days. Telecom was still being restored in March 2013; a Verizon phone facility still was being restored. Lack of fuel caught many people off guard, but the PANYNJ had its own gas resources, which port personnel found invaluable. Channels and berths were surveyed within 3 days after landfall, and debris did not prevent ships from returning. Ships began to arrive 6 days after landfall, gates opened 7 days after landfall, and daylight-only restrictions were lifted 8 days after landfall. In that time, some ships diverted to Philadelphia, Norfolk, and Savannah. All facilities except the Brooklyn cruise terminal were in operation 8 days after landfall.

The Brooklyn cruise terminal shed was damaged with rollup doors staved in, its security equipment destroyed, and fixed gangways damaged. The Brooklyn cruise terminal returned to operation in December 2012. No pier damage has been observed yet. Port personnel indicated that it would be valuable in the future to have alternative operating space on high ground to conduct business, along with a stockpile of emergency generators, mobile guard booths, and other equipment needed for emergency operations. The relevance of these observations here is that many of the same damages are posited to occur in the present scenario, especially flooding and loss of vehicles and damage to electrical equipment. PANYNJ's advice regarding alternative operating space, mobile guard booths, fuel, and other emergency supplies may be relevant to California facilities.

Threats to Life Safety

There were no injuries or deaths on port facilities, though port personnel indicated that some emergency service personnel raced floodwaters as they evacuated. Had power not been shut down, people could have been injured or killed by electrocution. The PANYNJ offered the following advice to other port operators faced with the potential for inundation: shut down power, know when you have done all you can, and focus on evacuation, not waiting until the last minute to remove personnel.

Damage to Large Vessels in the Ports of Los Angeles and Long Beach

By Keith Porter

Previous Instances of Vessels Breaking Their Moorings

High wave amplitudes have lifted large vessels onto piers and breakwaters in past tsunamis, as discussed elsewhere in this report. Such amplitudes are not present in the SAFRR tsunami scenario in California ports. Another hazard exists: large vessels have broken their moorings in past tsunamis. For example, two U.S. Navy submarines moored in Guam parted their mooring lines when the tsunami from the 2011 Tohoku, Japan, earthquake caused currents there estimated to be less than 4 kt. In the 2004 Sumatra tsunami, the cargo vessel *Maersk Mandraki* broke its moorings and drifted for hours in the Port of Salalah, Oman. At approximately the same time as the Mandraki was pulled from its berth, the Maersk Virginia was hit by strong and erratic currents at the Port of Salalah entrance, pushing the vessel into a breakwater and causing minor damage. The captain of the Virginia waited for an additional 7 hours for currents to subside before attempting to reenter the port. A number of similar examples

of vessels parting their lines were recorded during the 2004 event in the Indian Ocean, with ships ranging from 50 to 290 m in length. Currents affecting the Mandraki are difficult to estimate but were likely in the range of 6–8 kt (Okal and others, 2006a,b,c).

Once a vessel becomes unmoored in strong currents, it may be difficult to regain control. In the 2004 Sumatran tsunami, a vessel attempted to leave Port Blair, South Andaman Islands during a strong current and could not exit the port (Eskijian, written commun., March 2, 2013). In the 2011 Tohoku earthquake and tsunami in the port of Hachinohe, Aomori, the 56,752-ton deep-sea scientific drilling vessel *Chikyu* was damaged when her crew lost control of the vessel (CDEX Web Magazine 2012; fig. 46). Her captain was informed that the tsunami wave amplitude would be 1m, and he decided to keep the *Chikyu* moored to its pier. He was then warned that the wave amplitude would be 9 m, not 1m, and he decided to depart. He had the crew cut the mooring lines. The vessel had just cut loose when the tsunami struck. Currents were too high and too erratic for the crew to control the vessel. The ship collided with piers and damaged one of its propulsion pods. For such an event to occur in the Ports of Los Angeles and Long Beach would require that vessels were still in the harbor or moored when the tsunami struck, and the currents there were substantial and adversely aligned with respect to vessels.

Figure 46. Photograph of Drilling Vessel *Chikyu,* which was damaged in the 2011 Tohoku earthquake and tsunami (from Wikimedia Commons).

Once its crew loses control of a ship, it can collide with other vessels or piers, it can become grounded, and possibly sink. There are 39 instances recorded at *http://shipwrecklog.com* (accessed June 2013) during the period June 2011 through May 2013 of container vessels becoming grounded or colliding with piers, wharves, or docks. Among these instances, three were accompanied by leakage of oil or other pollution (*Bareli* March 16, 2012; *Celina* March 9, 2012; and MV *Rena* October 5, 2011), and two of these sank (*Bareli* and MV *Rena*). So sinking of a container ship (as in the case of the MV *Rena*; fig. 47*A*) is rare, even when the ship runs

aground or collides with other vessels or piers. Far more common is that the vessel is undamaged and or is quickly refloated, as in the case of the *Norfolk Express* (fig. 47*B*).

A ***B***

Figure 47. *A*, Photograph of MV *Rena* aground on Astrolabe Reef, New Zealand, on October 13, 2011 (from Wikimedia Commons); *B*, Photograph of the Norfolk Express (from http://www.havariekommando.de).

Would ships still be moored 4 hours after the tsunami warning is issued? The U.S. Coast Guard Vessel Dispersal Plan (Laferrierre, 2011) specifies procedures for the dispersal of vessels from the Ports of Los Angeles and Long Beach in emergency situations, including earthquakes and other natural disasters. It does not specify particular triggers or guidance in terms of tsunami warning time, wave amplitudes, or other factors. It calls on vessel masters to use pilots and tugboats to get underway whenever possible, but it also allows vessel masters to leave port without a tug or pilot if they deem it necessary.

Vessels at Risk

The Ports of Los Angeles and Long Beach can routinely contain 30 to 40 large vessels at any time. With current pilot staffing and available tugs, port pilots estimate that they can remove 5 to 8 ships per hour from the harbor, suggesting that it could take 4 to 8 hours to evacuate the port once decision is made, if all ordinary protocols are followed, and if vessel masters do not decide to leave port without tug or pilot. (Tugs are the limiting factor, rather than pilots.) Recall that the Ports of Los Angeles and Long Beach would have 3.5 hours of warning. It therefore seems plausible that vessels would still be moored when the tsunami struck. If such a vessel were then subjected to strong currents, it could part its moorings.

It seems plausible that currents in excess of 6 kt would be sufficient to cause a ship to break its mooring lines. There is at least one berth at Pier J where tsunami currents exceed 6 kt (fig. 48), in a direction perpendicular to a moored vessel that ordinarily intrudes slightly into the channel near a constriction that would cause high currents. The situation is similar to the berth where the *Maersk Madraki* broke loose in 2004 (Okal and others, 2006a,b, and c). The scenario therefore hypothesizes that such an event occurs. We imagine either the U.S. Coast Guard decides not to disperse the port or it takes some time to decide to issue the order to disperse, and ship's masters decide not to evacuate on their own accord. These conditions might exist because of limited guidance in the dispersal plan or the sense that the tsunami warning does not provide enough information to warrant dispersal.

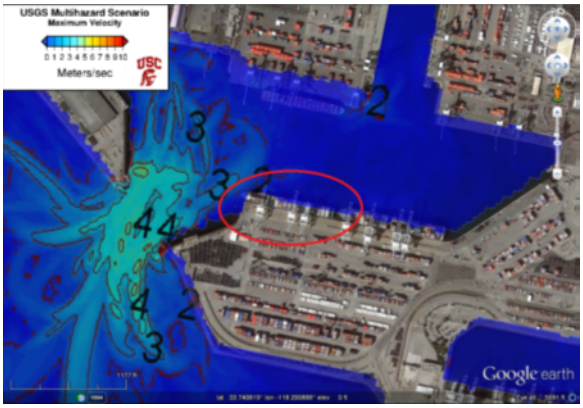

Figure 48. Image showing one location in the Port of Long Beach near a berth where tsunami currents exceed 6 knots (3 meters per second) in the SAFRR tsunami scenario (base image from Google Earth).

Damage to Large Vessels in the SAFRR Tsunami Scenario

We hypothesize that a vessel in the Port of Long Beach moored at Pier J parts its mooring lines and its crew cannot regain control before it collides with nearby piers. We have performed a simulation of the trajectory of an object originating at that berth. The simulation shows the current exceeding 6 kt at that berth at 7:10 p.m. on Mar 27, 2014. The object, representing the imagined unmoored vessel, comes close to Pier J and Pier G several times during the next 20–30 minutes, apparently close enough to damage the vessel and pier if the crew cannot regain sufficient control (fig. 49). The simulation is somewhat simplified: the vessel's inertia and dimensions are neglected, as are the effects of any remaining mooring lines. However, the simulation illustrates the potential for the vessel to impact Pier J or G or both, perhaps several times, and possibly impact other vessels still moored at Pier G.

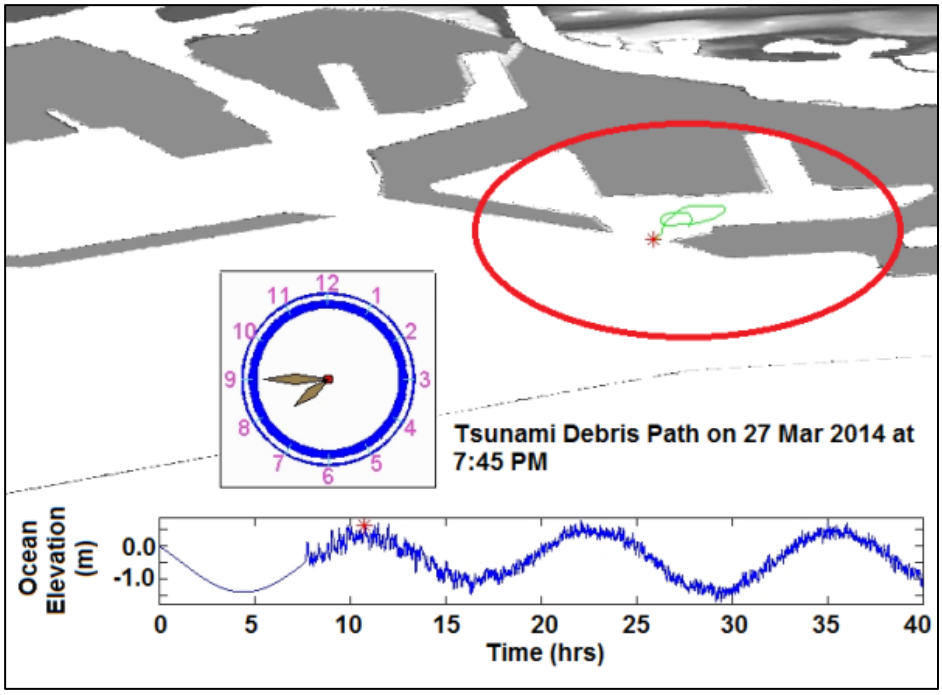

Figure 49. Diagram showing motion of a particle representing a vessel in the Port of Long Beach moored at Pier J that parts its mooring lines and collides with nearby piers in the SAFRR tsunami scenario. The particle released from the selected berth when the current exceeds 6 knots. The trajectory shown covers the time on March 27, 2014, from 7:10 p.m. (when first released) to 7:45 p.m. (by which time the vessel has either been brought under control or has already collided with one or more piers). (hrs, hours; m, meters.)

It seems realistic therefore that the impact would damage the vessel, Pier J (a container berth), and a crane at Pier J. (The vessel, experiencing some combination of surge, sway, heave, and yaw, damages the crane, which is located within 1m of the edge of the pier and cannot be moved away from the edge of the pier). In this scenario, the vessel does not sink, and is removed once the tsunami warning is lifted. As a result, the vessel does not create any navigation issues that cannot be worked around beyond the 2 days during which the port is shut down. Nor does it experience a fuel spill or cause other pollution. That the vessel does not sink or cause a spill is consistent with 92 percent of groundings recorded by shipwrecklog.com during June 2011 through May 2013, although clearly the possibility exists. After the tsunami, it could take two weeks for a structural engineer to certify the pier as safe (or several months to repair it if otherwise) and several months to repair or replace the damaged crane. The two adjacent berths are used with the remaining 6 cranes, producing a modest reduction in shipping capacity, and there are no other lingering effects of the vessel damage.

Opportunities to Enhance Resilience

The foregoing scenario suggests an opportunity to enhance port resiliency by reviewing the U.S. Coast Guard Dispersal Plan, perhaps adding guidance for decision-making in the event of tsunami that varies with warning time and estimated wave amplitudes, and considering the berths that are likely to experience the highest velocities in an adverse direction. It might be

valuable to test a procedure for dispersing major vessels from the ports within 3.5 or fewer hours. The test could include a tabletop exercise in which pilots, the U.S. Coast Guard, and a representative of other actors in the port dispersal plan imagine a warning has just been issued, and test their ability to carry out the plan. It could be with small craft standing in for major vessels, and could be incorporated into a regular exercise for tsunami preparedness. Such an activity might be particularly valuable if the scenario depicted here—a single vessel that does not sink and only damages one pier—might realistically be exceeded in a real tsunami.

Damage and Restoration of Marinas and Small Craft

By Keith Porter, Patrick Lynett, and Rick Wilson

Introduction and Purpose

This section presents an estimate of tsunami effects on small craft in the scenario. It is based on an inundation line and current velocities modeled by SAFRR scientists, knowledge of the locations of marinas drawn from remote sensing (Google Earth), and observations of historic tsunami damage to similar vessels. The objectives of this section are as follows:

- Summarize the locations and sizes of marinas exposed to loss.
- Identify the most common damage modes observed in past tsunamis.
- Estimate the damageability of vessels and floating docks, that is, quantify the conditions under which damage is assumed to occur.
- Describe repair activities and estimate the repair duration and repair costs for each mode of damage.
- Combine the foregoing to identify particular locations where it is realistic for damage to occur in the scenario. Estimate repair costs, repair durations, and traffic delays.
- Identify options for enhancing resiliency.
- Identify research needs.

Assets Exposed to Loss

There are approximately 58 coastal marinas and small craft harbors within the areas studied. We examined satellite imagery dated March 2011 to estimate the number of boats. In some cases we adjusted the estimates where harbor websites provided number of slips, in which case we factored number of slips by the apparent ratio of boats to slips in the satellite imagery. We provided the estimates to harbormasters by email and adjusted the numbers when corrected by the harbormasters. The Google Earth imagery does not show boundaries between adjacent marinas in the same harbor that are managed by distinct organizations, and we could find no other statewide map that distinguished between adjacent marinas, so the figure of 46 marinas refers to geographically distinct, as opposed to legally distinct, marinas.

An estimate of the number of boats in harbor on March 27, 2014, is shown in table 25, along with an approximate range of maximum tsunami wave velocity in each marina (denoted “Max V” in the table), and maximum wave height above mean higher high water (“Max D”). The table shows that the marinas in the study area contain on the order of 43,000 boats, mostly tied to floating docks. Velocities are in m/sec (to convert to knots, multiply by 2). Heights are in meters above mean higher high water. Records noted “USC estimate” are those where a finer-

resolution model was used to estimate velocities. “Pilings overtop” means that the tsunami wave is estimated to overtop the pilings. If the dock floats up over the top of the piling, it is no longer restrained from lateral movement. Pilings are designed to be tall enough to restrain the dock under tidal fluctuations, but a tsunami can raise the dock higher and allow it to float free. See for example figure 50. In the present case, we have indicated that pilings are overtopped where any of the following is true: (A) wave amplitude exceeds 2.0 m above mean higher high water, (B) the harbormaster has indicated that the pilings will be overtopped, or (C) an examination of Google Earth Street View imagery suggests that the pilings are too short for the tsunami amplitude.

Figure 50. Photograph of a concrete dock piling (from Wikimedia Commons).

Table 25. Marinas in study area, from north to south.

Name	Latitude °N	Longitude °E	Boats	Docks	Max V (m/sec)[a]	Max D, m[b]	Pilings overtop
Crescent City Harbor	41.745	-124.187	100	2	5-10	3.0	Yes
Trinidad Harbor	41.054	-124.144	50	0	5-10	4.0	Yes
Humboldt Bay Harbor	40.808	-124.163	450	12	4-8	1.0	No
Dolphin Isle Marina	39.4297	-123.798	70	1	0-2	2.5	Yes
Noyo Harbor	39.4239	-123.8058	230	5	4-5	2.5	Yes
Porto Bodega Marina	38.3331	-123.0522	36	1	2-4	2.5	Yes
Spud Point Marina	38.3304	-123.0564	250	5	3-5	2.5	Yes
Inverness Yacht Club	38.1027	-122.8566	76	2	0-2	1.5	Yes
Marina Bay	37.916	-122.353	300	6	2-4	2.0	No
Point Richmond	37.908	-122.382	400	8	2-4	2.0	No
Clipper Yacht Harbor	37.870	-122.496	350	7	3-6	1.5	No
Berkeley Marina	37.866	-122.318	1,100	22	3-6	1.0	No
Sausalito Yacht Harbor	37.860	-122.482	900	18	2-4	1.0	No
Emeryville Marina	37.839	-122.313	700	14	3-6	2.0	No
Treasure Isle Marina	37.816	-122.371	100	2	4-8	2.0	No
Fisherman's Wharf, San Francisco	37.810	-122.417	300	6	4-8	2.0	No
Pier 39 San Francisco	37.810	-122.411	300	6	4-8	2.0	No
Ft Mason, San Francisco	37.807	-122.433	350	7	4-8	2.0	No
San Francisco Marina Yacht Harbor	37.805	-122.445	150	3	4-8	2.0	No
Alameda Grand Marina	37.782	-122.251	1,900	38	2-4	1.0	No
South Beach Harbor, San Francisco	37.781	-122.385	700	14	2-4	1.0	No
Mission Bay, San Francisco	37.772	-122.386	20	1	2-4	1.0	No
San Leandro Marina	37.703	-122.193	455	8	2-4	1.0	No
Sierra Point Marina, Brisbane	37.673	-122.384	500	10	2-4	1.0	No
Oyster Point Marina, Brisbane	37.667	-122.383	500	10	2-4	1.0	No
Coyote Point Yacht Harbor, Burlingame	37.589	-122.320	250	5	2-4	1.0	No
Pacific Shores Marina, Redwood City	37.513	-122.196	100	2	1-2	0.5	No
Port of Redwood City	37.508	-122.208	100	2	1-2	0.5	No
Bair Island Marina	37.502	-122.220	300	6	1-2	0.5	No
Pilar Point Harbor	37.496	-122.480	300	6	4-8	4.0	Yes
Santa Cruz	36.964	-122.002	1,000	20	3-6	3.5	Yes
Moss Landing	36.807	-121.785	610	12	1	1.0	No
Monterey Harbor	36.605	-122.892	200	4	4-8	3.0	Yes
Morro Bay Harbor—floating docks	35.366	-120.856	300	6	3-6	2.0	Yes
Morro Bay Harbor—moorings and piers	35.366	-120.856	200	0	3-6	2.0	No
Port San Luis	35.167	-120.742	40	1	3-6	4.5	Yes
Santa Barbara Harbor	34.404	-119.688	1,200	24	4-8	2.0	Yes
Ventura Harbor	34.246	-119.260	1,200	24	4-8[c]	2.5[(c)]	Yes
Channel Islands Harbor	34.171	-119.209	4,000	80	3-6	1.5	Yes
Marina Del Ray	33.972	-118.452	4,000	80	2-4	1.0	No
Redondo Beach Marina	33.8469	-118.3983	1,480	30	1-2	1.5	Yes
POLA Berths 200-205	33.766	-118.248	1,516	30	1-2[c]	1.0	No
Downtown Marina	33.761	-118.193	85	10	1-2[c]	2.0	No
Long Beach Shoreline Marina	33.758	-118.184	1,764	32	1-2[c]	2.0	No
Alamitos Bay	33.747	-118.116	1,200	24	4-8	1.0	No

Table 25. Marinas in study area, from north to south.—Continued

Name	Latitude °N	Longitude °E	Boats	Docks	Max V (m/sec)[a]	Max D, m[b]	Pilings overtop	
Fish Harbor	33.734	-118.267		60	3	2[c]	2.0	No
Al Larson Marina	33.733	-118.268		128	3	2-3[c]	1.0	No
San Pedro Marina Port of Los Angeles Berth 80	33.730	-118.275		80	11	1-2[(c)]	2.0	No
Surfside	33.724	-118.066		1,000	20	4-8	1.0	No
Cabrillo marinas (Port of Los Angeles Berths 29–43)	33.719	-118.275		2,066	41	2-4[c]	1.0	No
Newport Bay	33.598	-117.893		1,000	20	4-8	0.5	No
Dana Cove	33.456	-117.697		2,400	45	4-8	2.0	No
Oceanside	33.209	-117.396		9,00	18	5-10	3.0	Yes
Quivira Basin	32.762	-117.239		1,200	24	2-4	1.0	No
Harbor Island	32.726	-117.215		1,100	22	2-3[c]	1.0	No
Shelter Island	32.708	-117.236		1,300	26	2-4[c]	1.5	No
Embarcadero Marina	32.707	-117.169		450	9	3-6	1.0	No
Chula Vista Marina	32.623	-117.104		800	16	2-4	1.0	No
Total				**11,593**	**258**			

[a]Max V = maximum velocity, meters per second (m/sec). For knots, multiply by 2.

[b]Max D = maximum wave amplitude, meters (m) above mean higher high water. Note 1 m ≈ 3 feet.

[c]USC (University of California) estimate from finer-resolution model.

Vulnerability

Historical Damage Data

Wilson and others (2012) record the following damage modes were observed in California after the 2010 Chile earthquake and the 2011 Tohoku earthquake, generally boats were damaged or sunk and docks damaged or destroyed. Associated with each observation is some measure of the currents or wave amplitudes accompanying the damage. Although the relationship between strong currents and damage can vary greatly within and between harbors, the results in the table indicate that boat damage could occur when velocities reach 4 or 5 m/sec (8 to 10 kt). For some harbors, like Crescent City and Santa Cruz, 1 in 5 damaged boats sank when velocities were in the range of 4–8 m/sec (8–16 kt; see fig. 51).

Figure 51. Photograph of boats sunk by the tsunami generated by the 2011 Tohoku, Japan, earthquake within Crescent City, California's, small boat basin (photograph by Rick Wilson).

Dock damage may also occur at about the same velocities depending on the location of the dock in the harbor, because currents vary throughout the harbor. Age matters because dock materials can degrade over time. Orientation of the docks matters, because the currents that flow parallel to a dock, impose lower bending moments (a sort of prying action) on its connections than do currents that flow perpendicular to it. Piling height matters because the tsunami can overtop short pilings, as previously mentioned. A detailed structural analysis of the docks and moored craft under the scenario currents could provide a better estimate of dock damage and an indication of which are most susceptible to tsunami damage.

Table 26. Damage modes recorded by Wilson and others (2012).

[m, meters; m/sec, meters per second]

Damage mode	Example	Tsunami effects
Vessel collision when vessels break free of moorings	Santa Cruz 2010	5 m/sec, 2.2 m tidal fluctuation
Vessels almost run aground while returning to harbor	Santa Barbara 2010	4.5 m/sec, 0.9 m tsunami wave amplitude
20 damaged docks, $300,000-500,000 repair cost	Ventura 2010	6-7 m/sec
8m sailboat swamped, damaged beyond repair; rescue of passengers required	Mission Bay 2010	3m standing wave at Bay entrance
Part of a dock destroyed. 25 m, 100-ton fishing vessel tore its dock from its moorings	Shelter Island, San Diego Bay 2010	1m tsunami amplitude; 5 m/sec current
All docks heavily damaged or destroyed ($20 million in damage), 16 boats sunk, 47 damaged. Sediment removal took 10 months. Repair work ongoing after 15 months. Interestingly, post-Tohoku repairs upgraded the marina for an assumed surge of 2.5 m (Trenkwalder, 2013, oral commun.). The present scenario estimates 3 m of surge above mean higher high water	Crescent City 2011	2.5 m tsunami wave amplitude, 4.5 m/sec
Dock and infrastructure damage at openings to 2 harbors	Noyo River 2011	No info
Minor damage to docks and boats	San Francisco Bay 2011	0.3—1.5 m wave amplitude
23 of 29 docks significantly damaged or destroyed. 14 boats sunk, dozens damaged. Repair work ongoing after 15 months.	Santa Cruz 2011	1.6-1.9 m wave amplitude, 7 m/sec currents
Docks sheared their wooden piles at metal ring connectors; $1.75 million repair costs.	Moss Landing 2011	2 m tsunami tidal fluctuation
Damaged to several boats, docks, and maritime infrastructure	Morro Bay 2011	1.6m peak tsunami amplitude, 2.5 m peak-to-trough tidal fluctuation. 7 m/sec in confined parts of the harbor
Harbor personnel injured helping boaters to dock; $150,000 dock damage	Ventura 2011	1.3 m tsunami amplitude
Boat, dock, and harbor infrastructure damage $130,000. Four people knocked off shoreline rocks	Mission Bay 2011	<1 m tsunami amplitude
Police pontoon boat dragged under a dock and sunk—$40,000. Minor hull damage to 2 other police boats whose moorings broke.	Shelter Island, San Diego Bay 2011	

Because wave heights in the SAFRR scenario event are 3 to 4 times larger than the 2010 and 2011 events, especially north of Point Conception, marinas and harbors would likely face more significant tsunami hazards. Extreme fluctuations in water level caused by the tsunami could cause damage to boat keels and dock and boat connections. With significant flow depths and inundation of dry land around harbors expected, dock connections could float above the tops of piles causing docks (and attached boats) to float freely within the harbors. Free-floating boats and docks would become tsunami debris capable of additional damage to surrounding structures. Harbor infrastructure (for example, electrical lines, sewage, and petroleum pipelines) could also become significantly damaged by loose docks and boats. Offshore moorings could also conceivably be damaged, either by dragging the anchor (commonly a concrete block attached to a mooring line and buoy) or by parting (breaking) the mooring line.

Testing and cleanup of hazardous materials could delay restoration of harbors. For example, after the 2011 tsunami, reconstruction efforts in Crescent City Harbor were delayed by over 10 months due to complications in permitting and sampling of the 150,000 cubic-meters of sediment deposited in the basin by the tsunami (Wilson and others, 2012). A larger tsunami scenario, like that of the SAFRR project, would cause similar damage and sediment movement to dozens of harbors in the State, would likely cause even longer delays because regulatory and recovery resources would be stretched very thin. Environmental problems are addressed in greater detail elsewhere in the scenario study.

Fragility Functions for Velocity-Induced Damage

There is some standard practice in earthquake engineering on how to create a mathematical model of the damageability of an object subjected to seismic excitation. See for example Porter and others (2007). In that procedure, the objective is to create an idealized mathematical model of damageability. Typically (though not always) the model is a lognormal cumulative distribution function of the capacity of the object to resist a specified damage state, in terms of a scalar measure of environmental excitation, termed an intensity measure (IM). The damage state is commonly defined in terms of the observable evidence of damage and the repair required to restore the object to its pre-event condition. The evidence is commonly tabulated in terms observations either of the actual level of excitation causing each instance of damage to occur (type-A data, where A refers to actual excitation), or the number and fraction of instances where the damage state was exceeded, and the maximum excitation associated with each observation (type-B data, where B refers to bounding excitation). There are other kinds of damageability evidence described in Porter and others (2007) that are not relevant here. These include type-C (capacity) data, where specimens were subjected to varying levels of excitation but none were damaged; type-D (derived) fragility, which applies engineering first principles to estimate the excitation at which a modeled specimen fails; and type-E (expert opinion) data, which represents a last resort absent types A–D data.

We assume vessel and dock damage can be modeled as a function of tsunami velocity using the convention of a capacity parameter idealized as a lognormal random variable with some reasonable logarithmic standard deviation; it is common to use 0.4, absent better data. The evidence offered by Wilson and others (2012) are insufficient to create a strongly defensible fragility function, but at least they suggest some reasonable parameter values. Only two set of observation are sufficient to plot damage (fraction of vessels damaged or sunk) versus intensity: Crescent City (2011) and Santa Cruz (2011). We estimated number of boats exposed to the tsunami from satellite imagery prior to the tsunami, and divided the reports of damaged or suck

boats by the estimated number of boats exposed. For Santa Cruz, we interpreted "dozens" to mean 120; results are sensitive to this assumption. We fit fragility functions through points averaged from these data, as shown in figure 52. (A maximum-likelihood method could also be used to determine parameter values, but that approach seems excessively refined for such crude data.) The fragility functions for "boat at least damaged" and "boat sinks" are thus respectively:

$$P\left[D_{boat} \geq 1 \middle| V = v\right] = \Phi\left(\frac{\ln(v/6.5)}{0.4}\right) \quad (1)$$

$$P\left[D_{boat} = 2 \middle| V = v\right] = \Phi\left(\frac{\ln(v/9.9)}{0.4}\right) \quad (2)$$

where $P[D \geq d|V = v]$ denotes the probability that any given boat reaches or exceeds damage state d (that is, $d = 1$ means damaged, $d = 2$ means sunk), V is the maximum tsunami wave velocity in the marina measured in m/sec, and Φ is the normal cumulative distribution function. Figure 52 illustrates these curves and a fragility function for dock damage, whose form is similar:

$$P\left[D_{dock} = 1 \middle| V = v\right] = \Phi\left(\frac{\ln(v/3.5)}{0.4}\right) \quad (3)$$

Equations (1) and (2) are used to estimate the probability that a boat is damaged but not sunk, as follows:

$$P\left[D_{boat} = 1 \middle| V = v\right] = P\left[D_{boat} \geq 1 \middle| V = v\right] - P\left[D_{boat} = 2 \middle| V = v\right] \quad (4)$$

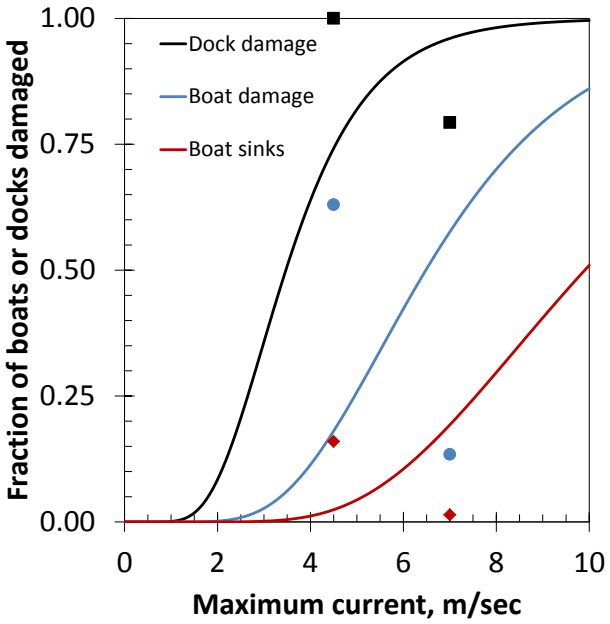

Figure 52. Graph showing fragility model for boats and docks in the SAFRR tsunami scenario. This model considers only current velocities. Elsewhere we recognize that boats secured to docks whose pilings are overtopped experience much greater damage. Dots represent data; curves are roughly fit to them. Though the data are sparse, the curves are plausible. (m/sec, meters per second.)

Repair Costs Conditioned on Damage

Ideally each damage state is defined unambiguously, in quantitative terms of observed symptoms of damage and a clear set of repair measures required to restore the object to its pre-event condition. Except in the case of "boat sinks," the foregoing fragility functions lack that clarity. Qualifiers such as "slight," "minor," or "significant" still beg the question of what repairs are required and how much they cost, questions that are not answered by the available evidence. The following costs conditioned on damage state are therefore order-of-magnitude estimates. The replacement cost for a boat can be taken as approximately uniformly distributed between $25,000 and $75,000, although higher and lower prices exist, based on a sample of 2010–2013 model-year boat listings within 50 miles of San Francisco at *http://www.boattrader.com* (accessed May 15, 2013). We use Boat Trader's average price of $50,000 for the same sample. Damage is assumed to cost 20 percent of the replacement cost. The average cost to repair a damaged dock is taken as $6,000, based on a reported $114,000 to repair 20 damaged docks in the Berkeley marina after the 2011 Tohoku tsunami (Hardinger, written commun., 2012). If the dock is damaged, one repair is required per 50 slips, again based on Berkeley's experience in 2011. Replacing concrete modular floats is estimated to cost $100 per square foot ($ft^2$) (Trenkwalder, 2013, oral commun.). Each slip requires approximately 300 ft^2 of dock, based on sample California marinas. Thus, destroyed docks are assumed to cost $30,000 per slip to demolish and replace. Replacement of a pile could also approach $10,000 to $15,000 (Trenkwalder, 2013, oral commun.).

Damage Resulting from Overtopped Pilings

With high tides and tsunami wave heights together sometimes exceeding 4m, a strong potential exists for docks to float off their pilings. Piling heights vary between marinas, and some are relatively short, so we queried harbormasters about piling heights, asking them whether the wave heights estimated by URS would cause docks to float off their pilings. Where harbormasters replied that docks would float off their pilings, or where harbormasters did not reply but wave heights were at least 2.5m above the reference water level, that is, above mean high water plus 20 cm (MHW+20), we assumed that pilings are overtopped. In such a case, all boats are assumed to be damaged, half of them sink, an assumption that several harbormasters agreed with and none disagreed with. We have also assumed that among docks that float off, 25 percent can be salvaged, and the other 75 percent require replacement, as suggested by an engineer involved in post-Tohoku marina repairs (Trenkwalder, 2013, oral commun.), who says that floats would be damaged from impact from loose boats or other floats, cleats breaking wales (as a result of cross-grain bending), and utilities (potable water and power) would be damaged from loss of structural support. Repairs would typically consist of replacing timber wales, reusing salvaged floats, reattaching salvaged cleats, and reconnecting utilities. We estimate the cost to replace or repair freed docks at \$80/ft^2· 300 ft^2/slip, where we use \$80 rather than \$100 because 25 percent of floats at freed docks could be salvaged with some cost, say \$20/ft^2, for the salvage effort.

Restoration Time

To assess restoration time, we inquired of 26 California harbormasters about restoration of damage under the scenario tsunami and about their experience in the 2011 Tohoku tsunami. Replies were limited, so the following restoration model is speculative, although consistent with four harbormasters' experience in 2011. Harbormasters of marinas where the majority of docks were damaged but not destroyed reported repairs taking 1 to 2 months. They speculated that if all of their docks were destroyed, repairs could take 1 to 3 years, especially municipal marinas where repair funding would be an issue. Conceivably repair durations might be briefer in a future tsunami through streamlining of the regulatory process and by applying lessons learned from Tohoku, but we have assumed that the speed of recovery is similar to 2011.

We therefore offer the following simple restoration model, illustrated in figure 53. In Equation (5), $R(t)$ refers to the fraction of the marina operating normally t days after the tsunami alert or warning is lifted, f_1 is the fraction of docks that are damaged but not destroyed by the tsunami, and f_2 is the fraction of docks destroyed by the tsunami, meaning that they have to be demolished and replaced. Equation (6) says that damaged docks are restored linearly with time, and completely restored within 30 days. Equation (7) says that it takes 3 months to demolish and arrange financing to replace destroyed docks, and then the remainder of 2 years to complete the replacement.

$$R(t) = (1 - f_1 - f_2) + f_1 \cdot g_1(t) + f_2 \cdot g_2(t) \tag{5}$$

$$\begin{aligned} g_1(t) &= \frac{t}{30} \quad t \le 30\,days \\ &= 1 \quad\quad t > 30\,days \end{aligned} \tag{6}$$

$$
\begin{aligned}
g_2(t) &= 0 && t \le 90\,days \\
&= \frac{t-90}{640} && 90\ days < t \le 730\ days \\
&= 1 && 730\,days < t
\end{aligned} \tag{7}
$$

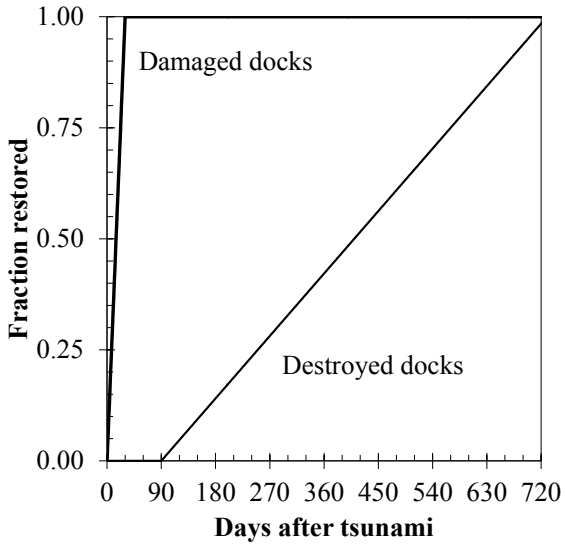

Figure 53. Graph showing restoration of damaged and destroyed docks after the SAFRR tsunami scenario.

Damage to Marinas and Small Craft in the SAFRR Tsunami Scenario

Taking the exposed quantities and velocities shown in table 25 and the vulnerability relationship just proposed, one can estimate the following consequences:

- 8,900 boats are damaged and are repairable. This amounts to 1 in 5 boats in the study area.
- 6,600 boats sink (about 1 in 7).
- 360 docks are damaged and are repairable (about 1 in 2; docks sizes vary, but a typical dock might comprise 50 slips).
- 170 docks are destroyed and must be replaced (1 in 5).
- The total expected value of loss is approximately $700 million, of which approximately $420 million is boat repair and replacement, $280 million in dock repair and replacement. This total represents approximately 20 percent of the estimated replacement cost of all small craft and floating docks in the study area. (Of this total, $20 million was already mentioned in the section on the Port of Los Angeles, so the total excluding this figure is $680 million.)
- Note that we have not estimated the cost associated with sediment transport such as dredging and environmental remediation. These costs could be substantial, conceivably in the hundreds of millions of dollars. Nor does the tsunami modeling address all harbors throughout the State.

Considering that perhaps 40 percent of boats in Crescent City and 80 percent of Santa Cruz's docks were damaged in the 2011 Tohoku tsunami, these figures (1 in 3 boats damaged or

sunk) in a tsunami pointed more directly at California does not seem unrealistically high, and it may be low. These figures omit potential damage to offshore moorings.

Using the foregoing model, it is estimated that two thirds of the loss comes from five large harbors with high enough waves that pilings are overtopped: Channel Islands Harbor (short pilings confirmed by harbormaster), Redondo Beach Marina (not confirmed, but pilings look shorter than the 1.5 m wave height above MHW+20 modeled here), Santa Barbara Harbor (short pilings confirmed by harbormaster), Ventura Harbor (not confirmed, but 2.5 m waves above MHW+20 strongly suggests overtopping) and Santa Cruz Harbor (not confirmed, but 3.5 m waves above MHW+20 strongly suggests overtopping). Channel Islands accounts for 1 in 4 of all of the damaged or sunk boats; and together with the next five (Redondo Beach, Santa Barbara, Ventura Harbor, Dana Cove, and Santa Cruz), these six harbors account for 2/3rd of all damaged or sunk boats. As shown in figure 55, this is not just a Northern California event: marinas from one end of the State to the other can be heavily damaged by a single tsunami. The figure shows the 10 marinas that contribute the most to the total economic loss postulated by the scenario because they are large and have high wave heights or velocities.

Boat damage can pose a navigation hazard. The Cabrillo marinas (POLA Berths 29-43) and the marinas at POLA Berths 200-205 would have approximately 90 damaged boats and 5 sunk. If any of the damaged or sunk boats broke loose from their slips, they could represent a navigation hazard to large ships in the Port of Los Angeles, as illustrated in figure 54. Shelter Island and Harbor Island similarly represent a potential threat to the Port of San Diego, contributing 30 damaged boats and 2 sunk. The Alameda Grand Marina near the Port of Oakland might have 45 damaged boats and 3 sunk. Marina Bay near the Port of Richmond is hypothesized to have 7 damaged boats, 1 sunk.

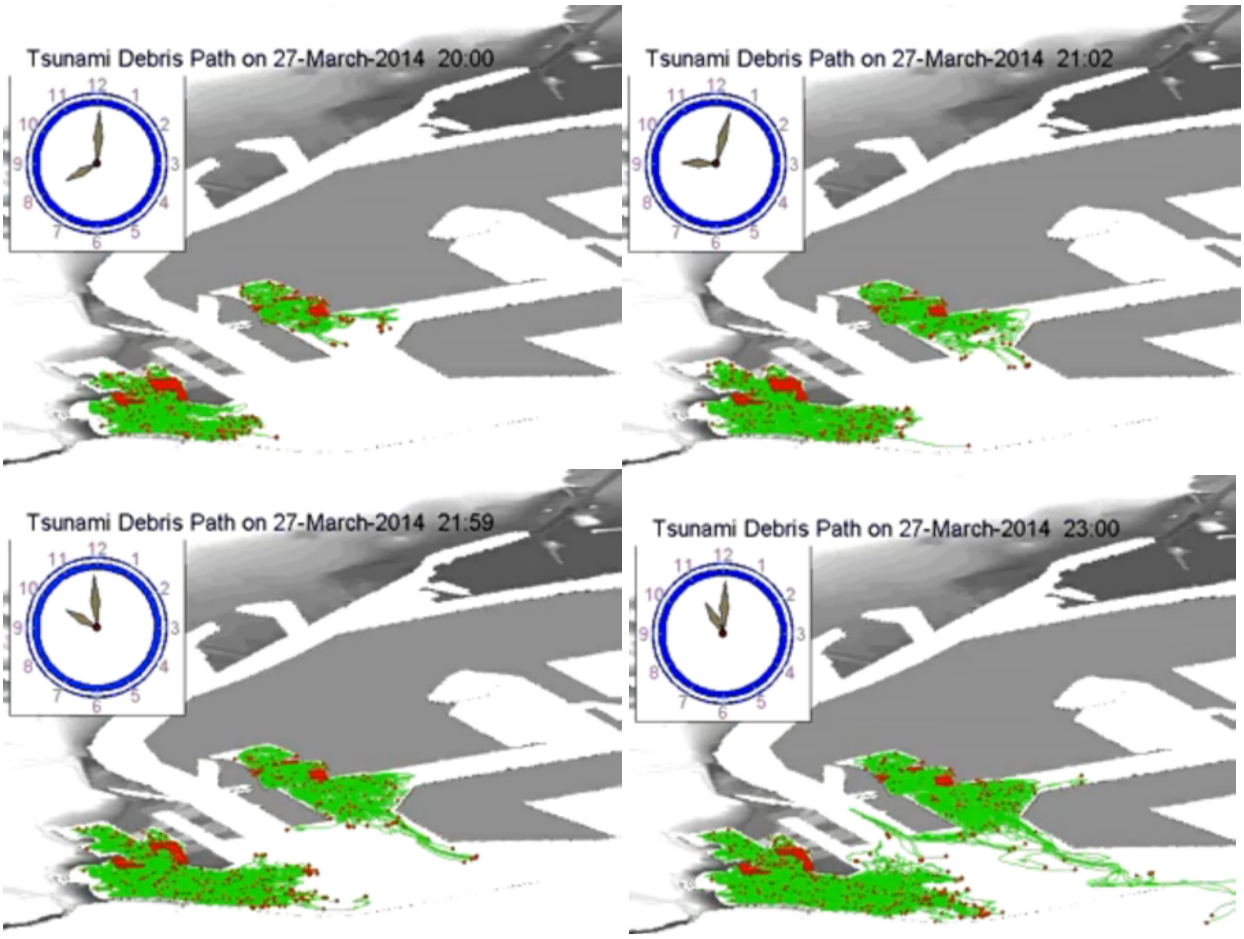

Figure 54. Diagrams of paths of hypothetical floating debris from Port of Los Angeles marinas 3.5 to 6.5 hours after the first arrival of the SAFRR tsunami.

The most significant repair delays would be attributable to removing potentially contaminated debris and sediment, especially if testing and permitting were required, but we have not estimated sediment transport so no particular locations are identified here where this would be an issue.

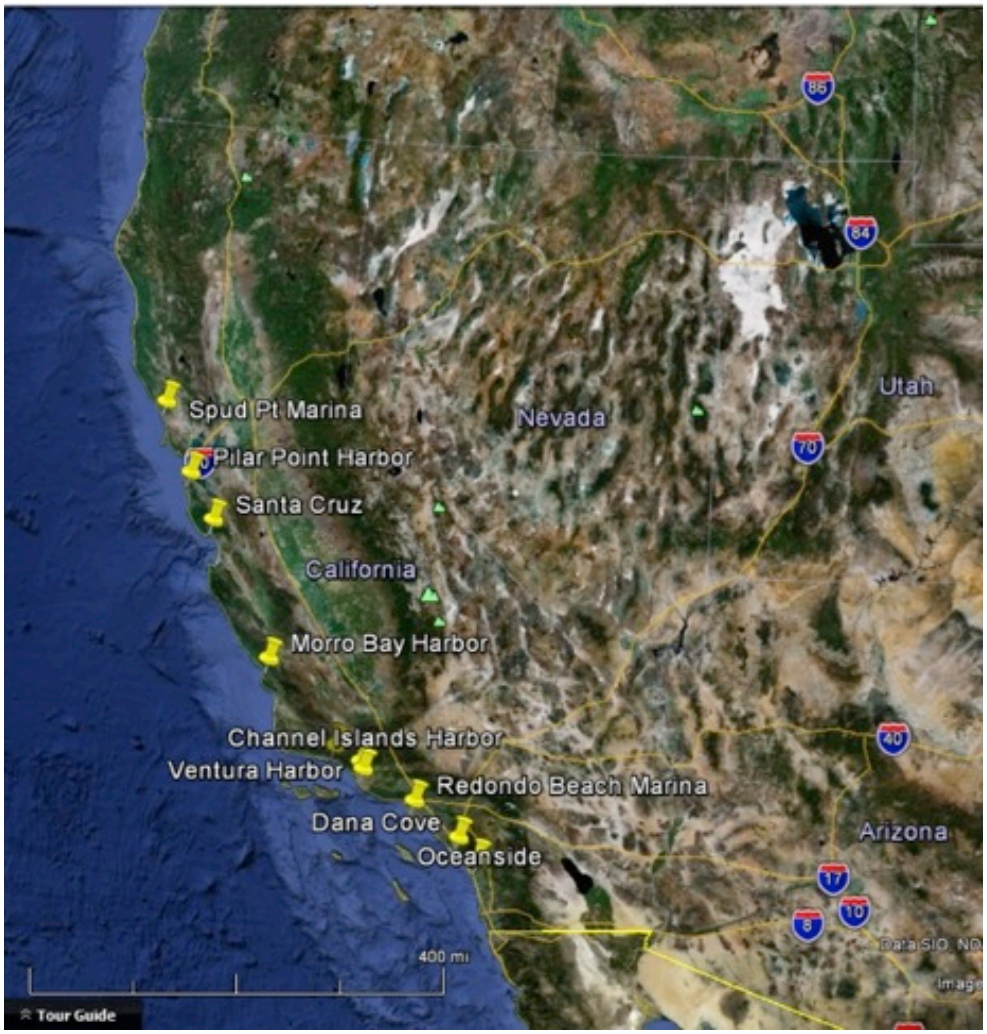

Figure 55. Most of the losses to marinas in the SAFRR tsunami scenario are to the 10 marinas shown on this map, attributable to high current velocities or high wave heights (base image from Google Earth).

Repair of breakwaters, rock slope protection, and dredging will add substantially to losses in the tsunami. In the 2011 Tohoku earthquake, the Crescent City Marina experienced 2.5 m surge and 12-kt velocities. This undermined rock slope protection and deposited close to 80,000 cubic yards of sand and debris in the marina basin. The required dredging and rock slope protection repair costs totaled approximately $6 million, according to Trenkwalder (2013, oral commun.). We have not estimated sediment transport nor identified particular locations of likely damage to breakwaters and slope protection, but these are likely and could add $100 million in losses.

Resiliency Opportunities

Boat and dock damage could be greatly reduced by increasing the heights of pilings; more than half the damage is attributed to docks floating off their pilings (though boats could be damaged by current velocities as well). It is practical to add height to most kinds of pilings, although doing so raises strength concerns. Boat damage could also be reduced by moving boats

offshore or to safe anchorage during the warning period, or by removing them from the water onto trailers, but this seems impractical for more than a small number of boats in most recreational boating communities. Most boat owners would not likely be on or near their boats when the warning was issued. U.S. Coast Guard personnel voiced the opinion that moving large numbers of boats out of their harbors simultaneously would tend to cause more life-safety threats than warranted by the potential property savings. The boats would have to stay out of the harbor for at least 12 hours, which means until the morning of March 28, and which would be problematic for many boat owners with families to care for and require solid advance planning in terms of understanding the need for taking enough fuel, food, water, and having the navigational skill to remain at sea for extended periods. The Coast Guard would be hard pressed to support so many boats all hastily put to sea, all likely in a bunch, all night. In addition, damage within harbors could prevent boats from returning.

Research Needs

Future tsunamis can be more severe than California's recent experience in the Tohoku and Chile tsunamis, so absent significant changes to the vulnerability of boats and docks, California's marinas will experience greater damage in more-severe tsunamis. The research needs discussed here are about refining models of that damage. That is, these research needs address improvements in our ability to estimate asset fragility, to better understand damage mechanisms, and to better inform risk mitigation decisions.

There is a good deal of simplification in the marina damage model presented here. Fragility functions are based on only two observations. Standard procedures call for several more. We intend these fragility functions to represent plausible relationships for purposes of developing a scenario; they are not offered for other purposes. However, the paucity of data used to derive the fragility functions reflects limited literature, not limited experience: California marinas have recently enough experienced tsunamis that have caused such extensive damage to boats and docks that it should be practical to find sufficient data to produce high-quality fragility functions that could be used in loss estimation. It would also be worthwhile to quantify the damageability of offshore moorings for small craft.

Repair costs for damaged docks are based on limited repair-cost data from Berkeley and from catalog prices of docks. An additional effort to collect more cost data on docks and boat repair would be desirable. Results are largely proportional to these guesses, by which we mean that if the estimate of the average repair cost for a damaged boat is high or low by a factor of two, so is the estimate of total loss. Velocity observations are aggregated, with single midrange values for entire marinas, despite that the velocity may vary significantly within a marina. Boat and dock orientation and interaction could relate to damageability in ways that are not reflected in these two observations.

Piling heights are in many cases based on Google Earth Street View from nearby streets. It was necessary in these cases to judge the tidal stage from the photos and to estimate how much piling height would remain above the water at mean higher high water. Results are sensitive to these judgments. If we overestimated piling heights, and in fact they were uniformly half as tall above MHW+20 than we judged, then the property damage could be $400 million more ($1.1 billion total property damage): 12,000 boats would be damaged and 11,000 sunk, meaning that half of California pleasure boats in the study area would be damaged or sunk. But lacking a high-resolution velocity model and more-detailed harbor infrastructure and damage data, the foregoing is as much as is practical.

More could be done. There has been a good deal of research on the tsunami fragility of buildings, but the authors could find none on the fragility of boats (in the sense of a mathematical relationship between tsunami wave velocity or amplitude and damage to small craft). Such a relationship would be valuable given the number of craft exposed and the hazard they may pose to navigation if damaged. Standard procedures exist for the derivation of earthquake-related fragility functions for building components; these have been easily adapted to boat damage due to tsunami. The data collection procedures for earthquake damage to building components could similarly be applied to boats damaged by the next tsunami. We have sought and received from California harbormasters anecdotal data on marina restoration times in past tsunamis, but it has been said that the plural of anecdote is not data. A more exhaustive survey with high response rates would be required to draw deeply defensible conclusions about the factors that affect repair time and to create a good mathematical model.

Additional research and assistance regarding piling heights and boat movement or evacuation are also clear needs. The California State Tsunami Program is focusing on this type of work for maritime communities by studying safe depth and distance required for offshore evacuation and strong tsunami currents within harbors in order to provide consistent guidance from findings to harbor authorities, emergency planners, and the public.

Building Damage

By Keith Porter

Introduction and Purpose

This section presents an estimate of tsunami effects on buildings from the SAFRR tsunami scenario. It is based on a map of flow depths and momentum flux by URS Corp., modified by an inundation line produced by the California Geological Survey (CGS). Where the inundation line extends farther inland from the URS map, flow depth is estimated to be 1.5 ft. Where the inundation line is closer to the shore than the URS map, the URS map is clipped to exclude the portions that CGS believes are not inundated. It also draws on a preliminary tsunami vulnerability model developed for the National Institute of Building Sciences (NIBS) as part of NIBS' efforts to create a HAZUS-MH tsunami loss model.

The objectives of this portion of the study are as follows:

- Summarize the value and location of buildings exposed to loss
- Summarize and illustrate common forms of building damage in tsunamis
- Summarize the development of tsunami vulnerability functions from the HAZUS-MH draft damage model
- Estimate the repair cost and repair duration of these assets
- Identify options for enhancing resiliency
- Identify research needs

Estimating Assets Exposed to Loss

HAZUS-MH offers a nationwide default building-stock inventory, but it can be difficult to use outside of HAZUS-MH (as is sometimes desirable): it is encoded in 15 tables in 2 Microsoft Access databases for each of 50 States. A Microsoft Access database is developed

here that links to the HAZUS-MH tables, and includes 54 scripted query language (SQL) queries, a macro to perform them all, and a number of supporting tables, for the purpose of extracting the HAZUS-MH inventory to a single de-normalized table, which is more practical for use in the present study. The table shows by Census block, tract, county or State: square footage of construction, building value, content value, and number of indoor occupants at 2 p.m., 2 a.m., and 5 p.m. The quantities are distributed by HAZUS-MH occupancy classification, structure type, and design level.

Let us denote the quantities of square footage, building value, and content value by A, Vb, and Vc, respectively. We begin by distributing square footage, building value, add content value by census block, occupancy class, and material, as follows:

$$A_{block,occ,matl} = A_{block,occ} \cdot Pct_{matl|occ} \tag{8}$$

$$Vb_{block,occ,matl} = Vb_{block,occ} \cdot Pct_{matl|occ} \tag{9}$$

$$Vc_{block,occ,matl} = Vc_{block,occ} \cdot \frac{Pct_{matl|occ}}{100} \tag{10}$$

In these equations, $Pct_{matl|occ}$ is used to distribute square footage and value equally. There does not appear to be any documentation to indicate whether the *Pct* values in the HAZUS-MH tables refer to square footage, building value, content value, or other factors, but HAZUS-MH does not appear to have any data to distinguish the percentage of one quantity, such as square footage, from that of another, such as building value. The same percentages are used regardless of which quantity is being distributed. This may be a somewhat crude assumption: fraction of area may be very different from fraction of value in highly disparate occupancies. However, it seems sufficient considering other sources of error in risk analyses. Once the area and values have been distributed to the level of block, occupancy class, and material, they are then further distributed to the level of structure type and design level as follows:

$$A_{block,occ,type,design} = A_{block,occ,matl} \cdot Pct_{type,design|matl} \tag{11}$$

$$Vb_{block,occ,type,design} = Vb_{block,occ,matl} \cdot Pct_{type,design|matl} \tag{12}$$

$$Vc_{block,occ,type,design} = Vc_{block,occ,matl} \cdot Pct_{type,design|matl} \text{ ,} \tag{13}$$

where $Pct_{type,design|matl}$ denotes the fraction of square footage in the given material represented by the given particular structure type and design level.

In a parallel effort, URS Corp staff estimated flow depth and momentum flux on a 30m gridded basis; these raster data were imported to a GIS for further analysis. U.S. Geological Survey (USGS) staff intersected the URS maps with census block boundaries and masked out water features, meaning that the portions of census block in water were removed from the portions on land. The USGS staff then calculated the remaining fraction of each census block with positive flow depth ("inundated fraction"), and estimated the average flow depth and momentum flux in the inundated fraction of each census block. The inundated fraction of each census block area was assumed to be the same fraction of building value with some inundation. This fraction was applied to building area, building value, content value and occupancy, to estimate the quantities of buildings and occupants with positive flow depth.

By this process, it appears that the tsunami has positive flow depths in 1800 city blocks, affecting 100 million square feet of buildings valued at $13 billion (replacement cost new, only including the subset of buildings in the inundated portion of coastal census blocks) and $8 billion of contents (replacement cost new, same subset). See table 27 for inventory totals by county. These totals include only the scenario inundation zones in the study area, not areas that would be inundated in such a scenario but that fell outside the study areas.

Buildings that are wetted by the tsunami in this scenario (and that are in the study area) represent approximately 37 percent of the inventory inside the maximum inundation zone developed by the California Governor's Office of Emergency Services (Cal OES). As noted elsewhere in this report, Cal OES's maximum inundation zone represents an envelope of inundation from many large distant and local-source tsunamis that could affect California, not just a single tsunami. That fact accounts for part of the difference between this tsunami and the Cal OES maximum inundation zone. Much of the rest is because the Cal OES inundation zone is delineated for the entire California coast, whereas our model only examines a portion of the coast. See table 28 for our estimate of the inventory inside Cal OES's maximum inundation zone. As shown in the table, this tsunami is a statewide event, not just a northern or southern California disaster: counties along the entire coast have significant inundation compared with the Cal OES inundation zone.

Forms of Building Damage

Buildings affected by tsunamis tend to be damaged by the following mechanisms, illustrated in figures 56 and 57:

1. Hydrodynamic pressure of the moving water damages building finishes and structural members, potentially causing local pressure-related damage to building components or displacement of the entire building. This damage can be due to either the inflow or outflow of water. Figure 56 shows instances of damage from Japan in 2011 where buildings were completely swept away.
2. Wetting of building and contents components that are subject to water damage, such as carpets, electrical wiring, wall finishes, computers and other contents.
3. Soiling of building and contents by soil deposited by tsunami flows.
4. Impact or deposition of water-borne debris.
5. Fire or release of hazardous materials. These issues are addressed elsewhere.
6. Buoyancy can lift and transport a building from its foundation.
7. Scour can erode soil around the building, especially at corners.

Figure 56. Photographs of apparent effects of hydrodynamic pressure on buildings in Japan affected by the 2011 Tohoku tsunami (photographs by Keith Porter).

Figure 57. Photographs of wetting, soiling, and deposition of debris in buildings in Japan affected by the 2011 Tohoku tsunami (photographs by Keith Porter).

Creating Tsunami Vulnerability Functions

Physical damage and repair costs for buildings and contents can be estimated as functions of tsunami loading, commonly measured in terms of momentum flux (m) and flow depth (f). The result is referred to here as a vulnerability function. We considered two sources for these: a draft analytical model in development for the HAZUS-MH tsunami model (Kircher, written commun., 2012) and recently published empirical relationships derived from experience in the 2011 Tohoku tsunami (Suppasri and others, 2013).

The model offered by Suppasri and others (2013) is based on a survey by the Ministry of Land, Infrastructure and Transportation of Japan, with more than 250,000 structures surveyed. The set of data has details on damage level, structural material, number of stories per building and location (town). It provides a set of fragility functions that depict the probability of reaching or exceeding each of six qualitatively defined damage states as a function of inundation depth. It offers the advantage of drawing on a very large survey of building damaged by tsunami flows.

The HAZUS-MH draft model relates damage state, repair cost, and duration of loss of functionality to both depth (for nonstructural components and contents) and momentum flux (for structural components) for U.S. construction. It borrows from riverine and coastal flood damage models developed by the U.S. Army Corps of Engineers and others over several decades and supplements these with analytical models that use engineering first principles to estimate structural forces, resistance, damage, and loss. It offers the advantages of transparency, application of a great deal of U.S. domestic damage experience in floods, ability to estimate quantitative measures of performance (repair cost and loss of functionality), and consistency with developing U.S. codes. For these reasons, we employ the HAZUS-MH model here. Note that we do not use the HAZUS-MH vulnerability functions in HAZUS-MH; the software has not been distributed yet. Rather we use the vulnerability functions in a database outside of HAZUS-MH. Note also that the HAZUS-MH Tsunami module is still under development, and that significant changes could occur prior to release of production software.

In HAZUS-MH, a vulnerability function applies to a single combination of model building type (16 types related to construction material and lateral force resisting system), height (low rise, mid-rise, or high rise), code era (precode, low code, moderate code, high code), and occupancy type (33 varieties of residential, commercial, industrial, agricultural, religion, government, and education). The vulnerability functions reflect an uncertain discrete damage

state D for each building component (structural, nonstructural, and contents) and an expected value of repair cost conditioned on damage state. The probability mass function of the uncertain damage state is evaluated using fragility functions in the form of a lognormal cumulative distribution function that reflects the assumption that components have an uncertain capacity to resist each damage state, and that the capacity is lognormally distributed. The duration of loss of function ("downtime") is assumed to be a function of structural damage state. The vulnerability functions for building, contents, and downtime are denoted here by MDF_B, MDF_C, and MDF_T, respectively, and are evaluated as follows.

$$\begin{aligned} MDF_B(m,f) = &\sum_{d=2}^{4} P\left[D_S = d \,|M = m\right] \cdot E\left[L_S \,|D_S = d\right] \\ &+ \sum_{d=2}^{4} P\left[D_N = d \,|F = f\right] \cdot E\left[L_N \,|D_N = d\right] \end{aligned} \tag{14}$$

$$MDF_C(f) = \sum_{d=2}^{4} P\left[D_C = d \,|F = f\right] \cdot E\left[L_C \,|D_C = d\right] \tag{15}$$

$$MDF_T(m,f) = \sum_{d=2}^{4} P\left[D_S = d \,|M = m\right] \cdot E\left[L_T \,|D_S = d\right] \tag{16}$$

,

where

$$\begin{aligned} P\left[D_S = d \,|M = m\right] &= \Phi\left(\frac{\ln\left(m/\theta_{S,d}\right)}{\beta_{S,d}}\right) - \Phi\left(\frac{\ln\left(m/\theta_{S,d+1}\right)}{\beta_{S,d+1}}\right) \quad d \in \{2,3\} \\ &= \Phi\left(\frac{\ln\left(m/\theta_{S,d}\right)}{\beta_{S,d}}\right) \quad d = 4 \end{aligned} \tag{17}$$

$$\begin{aligned} P\left[D_N = d \,|F = f\right] &= \Phi\left(\frac{\ln\left(f/\theta_{N,d}\right)}{\beta_{N,d}}\right) - \Phi\left(\frac{\ln\left(f/\theta_{N,d+1}\right)}{\beta_{N,d+1}}\right) \quad d \in \{2,3\} \\ &= \Phi\left(\frac{\ln\left(f/\theta_{N,d}\right)}{\beta_{N,d}}\right) \quad d = 4 \end{aligned} \tag{18}$$

$$\begin{aligned} P\left[D_C = d \,|F = f\right] &= \Phi\left(\frac{\ln\left(f/\theta_{C,d}\right)}{\beta_{C,d}}\right) - \Phi\left(\frac{\ln\left(f/\theta_{C,d+1}\right)}{\beta_{C,d+1}}\right) \quad d \in \{2,3\} \\ &= \Phi\left(\frac{\ln\left(f/\theta_{C,d}\right)}{\beta_{C,d}}\right) \quad d = 4 \end{aligned} \tag{19}$$

M = uncertain momentum flux (ft^3/sec^2)

m = a particular value of M

F = flow depth (ft)

f = a particular values of F

D_S = damage state of structural components, $D_S \in \{0, 1, 2, 3, 4\}$. Only damage states 2, 3, and 4 are assumed to contribute to tsunami loss.

D_N = damage state of nonstructural components, $D_N \in \{0, 1, 2, 3, 4\}$. Only damage states 2, 3, and 4 are assumed to contribute to tsunami loss.

D_C = damage state of contents, $D_C \in \{0, 1, 2, 3, 4\}$. Only damage states 2, 3, and 4 are assumed to contribute to tsunami loss.

d = particular value of D

P[A|B] = probability that A is true given that B is true

E[A|B] = expected value of A is true given that B is true

$E[L_S|D_S = d]$ = mean damage factor of structural component in damage state d (damage factor = structural repair cost as a fraction of building replacement cost new, where the building comprises the structural and nonstructural components), and $d \in \{2, 3, 4\}$. Estimates of $E[L_S|D_S = d]$ are tabulated in NIBS and FEMA (2009). They vary by occupancy class.

$E[L_N|D_N = d]$ = mean damage factor of nonstructural components in damage state d (damage factor = nonstructural repair cost as a fraction of building replacement cost new), $d \in \{2, 3, 4\}$. Values are tabulated in NIBS and FEMA (2009) and vary by occupancy class. For tsunami, they are the sum of the nonstructural drift-sensitive and nonstructural acceleration-sensitive values from the earthquake methodology.

$E[L_C|D_C = d]$ = mean damage factor of contents in damage state d (damage factor = content repair cost as a fraction of content replacement cost new), $d \in \{2, 3, 4\}$. Values are tabulated in NIBS and FEMA (2009) and vary by occupancy class. Half the value of contents is assumed to be recoverable after earthquake shaking but not after tsunami, so these values are taken as double the earthquake-related quantities tabulated in NIBS and FEMA (2009).

$E[L_T| D_S = d]$ = mean duration of loss of function of a building whose structural component is in damage state d, $d \in \{2, 3, 4\}$. It is calculated as the product of repair time, denoted here by BCT_d and a factor MOD_d between 0.0 and 1.0 that reflects the fraction the repair time after which the building is functional again, even if repairs are ongoing. Median values of BCT_d and MOD_d are tabulated in NIBS and FEMA (2009) and vary by occupancy class. NIBS and FEMA (2009) does not suggest the form of the probability distribution of BCT conditioned on d. There is an information-theory justification for assuming that, given a damage state d, BCT_d is uniformly distributed between two bounds. Under this condition, the median value of BCT_d is also its mean value, which we denote here by $E[BCT|D_S=d]$. The HAZUS-MH developers offer MOD_d as point estimates and do not suggest any distribution (or discuss uncertainty for that matter), so we treat it as a point estimate as well. Thus,

$$E\left[L_T \middle| D_S = d\right] = E\left[BCT \middle| D_S = d\right] \cdot MOD_d \tag{20}$$

$\beta_{S,d}$ = median capacity of structural component to resist damage state d, $d \in \{2, 3, 4\}$; values are estimated in Kircher (written commun., 2012) and vary by model building type, height, and code era

$\zeta_{S,d}$ = logarithmic standard deviation of capacity of structural component to resist damage state d, $d \in \{2, 3, 4\}$; tabulated in Kircher (written commun., 2012) and vary by model building type, height, and code era

$\beta_{N,d}$ = median capacity of nonstructural component to resist damage state d, $d \in \{2, 3, 4\}$; tabulated in Kircher (written commun., 2012) and varying by model building type and height, but not code era.

$\zeta_{N,d}$ = logarithmic standard deviation of capacity of nonstructural component to resist damage state d, $d \in \{2, 3, 4\}$; tabulated in Kircher (written commun., 2012) and varying by model building type and height, but not code era.

$\theta_{C,d}$ = median capacity of contents to resist damage state *d*, $d \in \{2, 3, 4\}$; tabulated in Kircher (2012) and varying by model building type and height, but not code era.

$\beta_{C,d}$ = logarithmic standard deviation of capacity of contents to resist damage state *d*, $d \in \{2, 3, 4\}$; tabulated in Kircher (written commun., 2012) and varying by model building type and height, but not code era.

The vulnerability functions were evaluated at 51 levels of momentum flux $m \in \{10^0, 10^{0.1}, 10^{0.2}, \ldots 10^5\}$ cubic feet per second squared (ft^3/sec^2) and 51 levels of flow depth $f \in \{10^0, 10^{0.1}, 10^{0.2}, \ldots 10^5\}$ ft for each combination of model building type, height, code era, and occupancy class, for a total of approximately 10,000 vulnerability functions (4008 each for structural and downtime, and 1002 each for nonstructural and contents, which do not vary by code era.). A sample set of vulnerability functions is shown in figure 58, for a large woodframe multifamily dwelling of moderate-code construction, such as a 1950s-era apartment building along the San Francisco Pacific shoreline. Here are some sample calculations for losses to a large woodframe building (W2) moderate code, multifamily dwelling (RES3) at $m = 1{,}000$ ft^3/sec^2 (for structural vulnerability) and $h = 10$ ft depth (for nonstructural and contents vulnerability).

From Kircher (written commun., 2012),

$\theta_{S,2} = \theta_{S,3} = \theta_{S,4} = 571$ $ft^3/$

$\beta_{S,2} = \beta_{S,3} = \beta_{S,4} = 0.83$

$\theta_{N,2} = \theta_{N,3} = 12$ ft

$\theta_{N,4} = 24$ ft

$\beta_{N,2} = \beta_{N,3} = 0.78$

$\beta_{N,4} = 0.65$

$\theta_{C,2} = \theta_{C,3} = 3$ ft

$\theta_{C,4} = 15$ ft

$\beta_{C,2} = \beta_{C,3} = 0.78$

$\beta_{C,4} = 0.65$

$m = 1000$ ft^3/sec^2

$h = 10$ ft

From NIBS and FEMA (2009),

$E[L_S \mid D_S = 2] = 0.023$

$E[L_S \mid D_S = 3] = 0.117$

$E[L_S \mid D_S = 4] = 0.234$

$E[L_N \mid D_N = 2] = 0.05 + 0.027 = 0.077$

$E[L_N \mid D_N = 3] = 0.25 + 0.08 = 0.33$

$E[L_N \mid D_N = 4] = 0.5 + 0.266 = 0.766$

$E[L_C \mid D_C = 2] = 2 \cdot 0.05 = 0.10$ (that is, 2x the earthquake loss)

$E[L_C \mid D_C = 3] = 2 \cdot 0.25 = 0.50$

$E[L_C \mid D_C = 4] = 2 \cdot 0.5 = 1.0$

Evaluating Equation (17),

$P[D_S = 2|M = 1000] = P[D_S = 3|M = 1000] = 0$

$P[D_S = 4|M = 1000] = 0.75$

Evaluating Equation (18),

$P[D_N = 2|F = 10] = 0$

$P[D_N = 3|F = 10] = 0.32$

$P[D_N = 4|F = 10] = 0.09$

Evaluating Equation (19),

$P[D_C = 2|F = 10] = 0$

$P[D_C = 3|F = 10] = 0.67$

$P[D_C = 4|F = 10] = 0.27$

$$P\left[D_N = d \,\middle|\, F = f\right] = \begin{cases} \Phi\left(\dfrac{\ln\left(f/\theta_{N,d}\right)}{\beta_{N,d}}\right) - \Phi\left(\dfrac{\ln\left(f/\theta_{N,d+1}\right)}{\beta_{N,d+1}}\right) & d \in \{2,3\} \\ \Phi\left(\dfrac{\ln\left(f/\theta_{N,d}\right)}{\beta_{N,d}}\right) & d = 4 \end{cases} \tag{21}$$

Figure 58 shows for example that once depth reaches the top of the 2nd story of the building, the depth-sensitive contents are a complete loss, whereas nonstructural damage is about 50 percent of the building value. Note that although content vulnerability applies to content value, both nonstructural vulnerability and structural vulnerability are expressed as a fraction of *total* building replacement cost new structural plus nonstructural, so they add. However, because they do not have the same intensity measure type—nonstructural is sensitive to flow depth, structural to momentum flux—the curves cannot be summed on a two-dimensional (2-D) chart. Once momentum flux exceeds approximately 1,000 ft^3/sec^2—such as say 10 ft depth and 10 ft/sec velocity, or 3m depth and 3m/sec or 6 kt velocity—the repairs take 18 months.

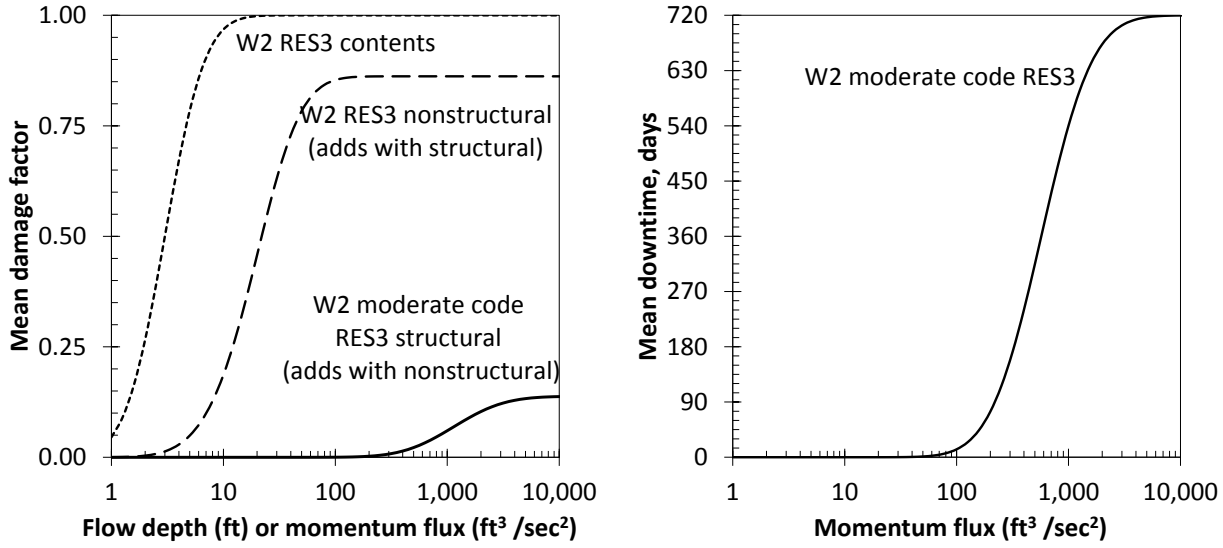

Figure 58. Graphs of sample tsunami vulnerability functions for a large wood-frame building (W2) being used as a multifamily dwelling (RES3) of moderate-code construction. (ft^3/sec^2, cubic feet per second squared).

Building Damage in the SAFRR Tsunami Scenario

Vulnerability functions were applied to the estimates of value exposed using the mapped average flow depths and momentum flux by census block (masked to exclude water and portions of the census blocks not inundated). The tsunami affects approximately 1840 census blocks statewide, including 100 million square feet of buildings valued at $13 billion and $8.4 billion of contents. These estimates assume that building value is uniformly distributed over the normally dry portion of each census block. The scenario produces approximately $1.8 billion in building and content damage, mostly contents. These figures represent 2.2 percent of building value and 18 percent of content value lost in wetted buildings. See table 27.

The reader should bear in mind that the HAZUS-based analysis gives the expected value from a probabilistic estimate of loss, considering a variety of uncertainties. To illustrate, imagine that there were some buildings valued at $10 million and inundated such that they had a 1-percent chance of $1,000,000 loss and 99-percent chance of $0 loss. The expected value of loss is $10,000. It is hard to imagine a particular outcome in which $10 million of building value is damaged by tsunamis and then is repaired for $10,000, but that is not what the $10,000 represents.

Table 27. Building damage in the SAFRR tsunami scenario.

[M, million; ft^2, square feet; %, percent]

County	Wetted building area, million ft^2	Wetted building value, $M	Content value in wetted buildings, $M	Building loss, $M	Content loss, $M
Alameda	11.1	$1,453	$1,066	$20.0	$164.4
Contra Costa	1.3	$153	$128	$1.7	$19.0
Del Norte	1.2	$107	$66	$4.4	$17.2
Humboldt	4.9	$499	$331	$12.9	$62.1
Los Angeles	10.2	$1,294	$743	$23.4	$139.8
Marin	9.7	$1,526	$927	$33.6	$170.1
Mendocino	0.9	$97	$61	$0.9	$8.9
Monterey	2.9	$359	$228	$12.0	$51.9
Orange	17.4	$2,286	$1,293	$26.4	$206.6
San Diego	18.9	$2,205	$1,259	$60.9	$240.0
San Francisco	11.1	$1,651	$1,252	$55.1	$257.2
San Luis Obispo	0.8	$86	$49	$1.6	$8.4
San Mateo	5.3	$767	$505	$28.4	$91.2
Santa Cruz	4.8	$621	$355	$14.9	$69.2
Ventura	2.2	$241	$138	$2.3	$20.9
Total	**103**	**$13,345**	**$8,401**	**$298.4**	**$1,526.9**
% of wetted value				**2.2%**	**18.2%**

Table 28. Building and content value in California Governor's Office of Emergency Services' (Cal OES) maximum inundation zone.

[M, million; %, percent]

County	Wetted building area million ft^2	Wetted building value $M	Content value in wetted buildings $M	Scenario building + contents value as % of value in Cal OES max. inundation zone
Alameda	52	$6,996	$5,053	21%
Contra Costa	3	410	315	39%
Del Norte	3	295	198	35%
Humboldt	13	1,436	996	34%
Los Angeles	21	2,738	1,633	47%
Marin	24	3,729	2,274	41%
Mendocino	1	139	94	68%
Monterey	6	822	495	45%
Orange	61	7,850	4,764	28%
San Diego	28	3,365	2,063	64%
San Francisco	16	2,547	1,954	64%
San Luis Obispo	2	215	128	39%
San Mateo	14	2,034	1,398	37%
Santa Barbara	0	42	24	
Santa Clara	3	350	411	
Santa Cruz	13	1,775	1,101	34%
Solano	1	80	52	
Sonoma	1	117	60	
Ventura	3	390	210	63%
Total	**265**	**35,330**	**23,223**	**37%**

Resiliency Opportunities

The figures in table 27 are fairly modest in the aggregate as California natural disasters go—less than $2 billion—but would undoubtedly be painful to those affected, especially those who are uninsured or underinsured and lack the resources to repair damage. One opportunity to enhance resiliency is to ensure that people living in or doing business in potentially inundated areas are aware of the National Flood Insurance Program or commercial flood insurance. Another opportunity is to provide coastal communities with the California Geological Survey's maps of the potential extent of tsunami inundation, to inform those communities' decisions about their zoning plans. The State is working on probabilistic inundation maps for land-use planning that might help to identify areas that are more susceptible to tsunami inundation.

Research Needs

As with marinas, future tsunamis can be more severe than California's recent experience in the Tohoku and Chile tsunamis, so absent significant changes to the protection and vulnerability of coastal buildings, they will experience greater damage in more-severe tsunamis. Just as with marinas, the research needs discussed here are about refining models of that damage: improving our ability to estimate building fragility, improving our modeling of damage and loss, and making better-informed risk-management decisions.

It would be valuable to compare the HAZUS estimate of exposed building value with the finer-resolution database of businesses and dwellings prepared by others on this project. It would also be valuable to compare the developing HAZUS vulnerability model with an empirical one that was published after this study was complete. The HAZUS database reflects the census of

population and housing, which publishes its data by census block, not by street address. Coastal development might not be uniformly distributed over the census block, as was assumed here. Buildings along waterfronts and in marinas might cluster near the shore, whereas coastal buildings that do not have a function related to the water might be located farther from the shore.

Damage and Restoration of Roads and Roadway Bridges

By Keith Porter

Introduction and Purpose

This section presents an estimate of tsunami effects on Caltrans (California Department of Transportation) highways and bridges from the SAFRR tsunami scenario. It is based on an inundation line and current velocities modeled by SAFRR scientists, knowledge of the locations and elevations of highways and coastal bridge embankments drawn from remote sensing (Google Earth), observations of historic tsunami damage to similar assets, and an approximate analysis that considers Federal Highway Administration (FHWA) and Caltrans design guidelines. It draws on a half-day discussion between SAFRR staff and eight Caltrans engineers in Sacramento on Oct 3, 2012, and a review of this memo by Caltrans engineers (Mark Yashinsky and Steve Ng) and USGS staff (Ann Wein). The objectives of this memo are as follows:

Summarize the State and local road and bridge assets exposed to loss.

Identify the most common damage modes observed in past tsunamis.

Estimate the damageability of these assets, that is, quantify the conditions under which damage is assumed to occur.

Describe repair activities and estimate the repair duration and repair costs for each mode of damage.

Combine the foregoing actions to identify particular locations where it is realistic for damage to occur in the scenario. Estimate repair costs, repair durations, and traffic delays.

Identify options for enhancing resiliency.

Identify research needs

An important issue that is not addressed here is road closure of evacuation routes. This topic represents a gap that will be addressed in another part of the scenario study.

Assets Exposed to Loss

There are approximately 54 coastal highway bridges and 12 stretches of low-elevation highway and local roadway (less than 5 meters or so) within the study area. These are clustered around Eureka, the San Francisco Bay, and along the south coast from Ventura to San Diego, as shown in figure 59. In the figure, bridges are colored yellow and roads are red.

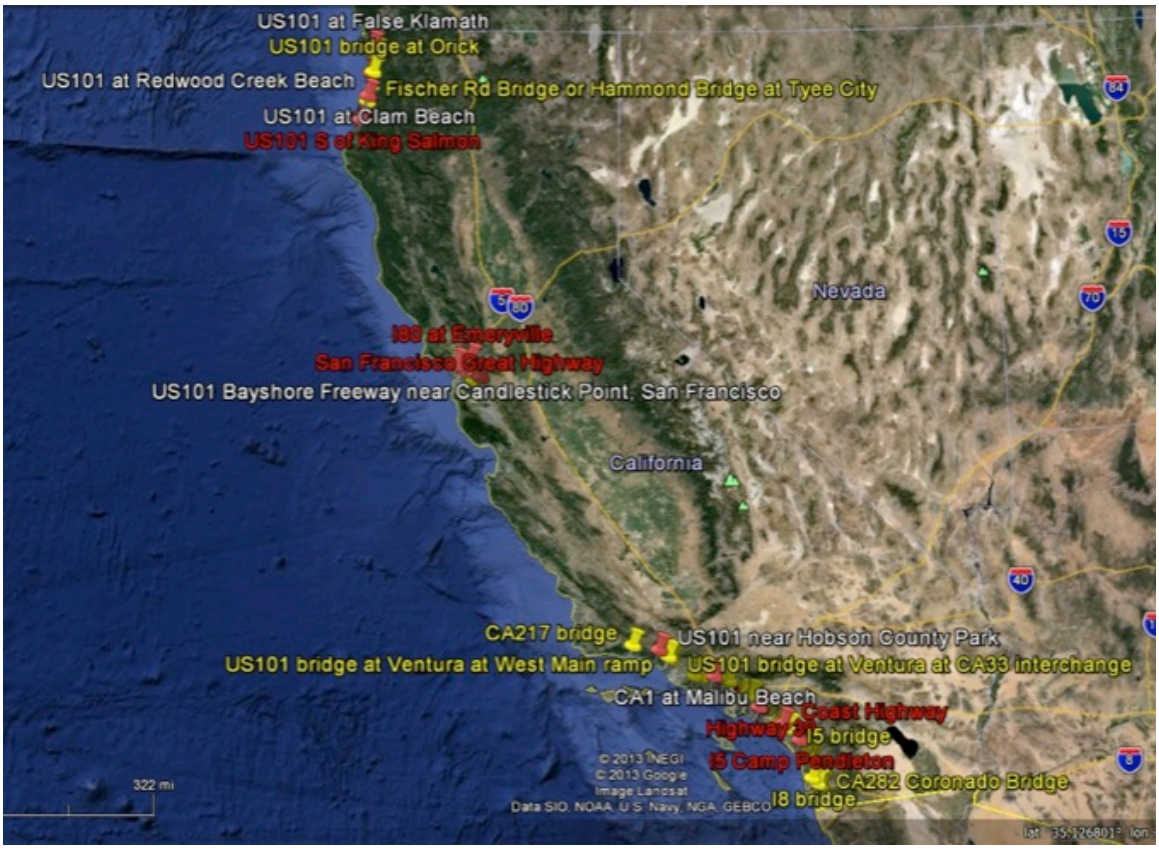

Figure 59. Map of coastal bridges and low-elevation roads in the SAFRR tsunami scenario study area. Only a subset are damaged in the scenario (base image from Google Earth).

Damage Modes

The relevant damage modes that have been observed in past tsunamis or identified in Caltrans Memo to Designers 20-13 (2010) includes:

Scour damage to embankments and erosion of fill. This is expected to occur where the embankment is located at or near channel banks, and the embankment obstructs the flow. According to FHWA (2011), vortices form near embankments and piers. See figure 60 for examples.

Scour damage to roads. This is expected to occur where the roadway is on a levee or embankment and tsunami flows can form vertical vortices on the downstream side or horizontal vortices on the upstream side, especially near culverts. Even in locations with high flow depth and velocity, where the road is level with or below the adjacent ground and offers no soil embankment to scour, it seems to resist tsunami damage. See figure 61 for an illustration of a coastal road near Shinchi, Japan, scoured away by the Tohoku tsunami. See figure 62 for a road near the Port of Sendai that was not damaged by the tsunami. Similar to FHWA (2011) comments about vortices near piers and embankments, we hypothesize that the difference between these two sites was the presence or absence of a crown that would cause the road to intrude into the flow and thereby create scour-producing vortices.

Hydrodynamic pressure on or buoyant uplift of bridge superstructures, as in figure 63. This damage mode is not expected to occur in the present scenario because no Caltrans or local bridge appears to be affected by waves reaching the bridge superstructure.

Scour damage to bridge pier foundations. Caltrans engineers, especially Ng, expect that this damage mode is unlikely to occur in the present scenario. The expected tsunami waves are less than the design considerations for normal riverine discharge design. The events of Tohoku would appear to confirm this.

Impact from debris. Floating debris (for example, boats, buildings, and trees) could strike bridge piers and might need to be cleared away. Vessels impacted bridges in the Tohoku tsunami, as shown in figures 64 and 65. Navy Way at the Port of Los Angeles is the location where there are large enough vessels nearby to cause damage significant enough to carry away a bridge superstructure. The ports, however, have stated that it is unlikely and perhaps unrealistic that large ships would become unmoored or lose control while underway, though they do not completely discount the possibility. Such an impact is considered here to be a possibility, but is not explicitly included as part of the scenario.

Figure 60. Photographs of embankment scour at Route 45 bridge (Takada Bypass) over Route 141 (Hamaiso Highway) due to the 2011 Tohoku tsunami (photographs by Charles Scawthorn).

Figure 61. Photographs of tsunami damage from the 2011 Tohoku, Japan, tsunami: Left, About 1 mile of Route 38 north of Shinchi was washed away by the 2011 Tohoku tsunami. Right, Roads throughout the Port of Sendai were largely undamaged despite high currents and depths; they had no embankments that could generate scouring vortices. (Photographs by Keith Porter.)

Figure 62. Photographs showing a contrast in tsunami scour potential resulting from roadway elevation. The left image is a view looking north from a commuter railway platform on the Sendai, Japan, plain. Before the 2011 Tohoku tsunami, it had had rail on both sides of the platform; now only a short stretch on the east (ocean) side and large scour pits on the west (landward) side. There is no sign of the railbed or rail. On the right is a nearby road, largely undamaged, on the seaward side of the rail line. The road is largely undamaged. (Photographs by Keith Porter.)

Figure 63. Photographs of bridges whose superstructures were pushed or floated off their piers in the 2011 Tohoku, Japan, tsunami (photographs by Charles Scawthorn).

Figure 64. Photograph of example from the 2011 Tohoku, Japan, tsunami of how small craft represent a debris hazard for bridges; the Miyako Bridge across the Hei River in the City of Miyako (photograph by Junichi Hoshikuma).

Figure 65. Photograph of damage from a barge impact on the Jokawa Bridge over the Higashimatsushima River in the 2011 Tohoku, Japan, tsunami that destroyed the middle span and damaged the other spans (photograph by Junichi Hoshikuma).

Estimating Damageability

The focus here is on damage modes 1 and 2. Let us begin with damage mode 1, scour damage to bridge abutments. Commercial and public scour models exist for the risk analysis or design of bridges, dams, and reservoirs, but they appear to be inappropriate for the present use. Some do not take event-specific input data (for example, HYRISK). Others require bridge and abutment geometry and materials data that are unavailable or prohibitively time consuming to analyze on a wide scale (for example, Flow-3D). The present project takes a more approximate approach to estimating damage. This level of detail seems appropriate to the task of estimating a realistic level of damage, which can then be used to determine whether and where detailed analysis is required.

FHWA (2011) offers advice regarding design against this failure mode, stating that "Available technology has not developed sufficiently to provide reliable abutment scour estimates for all hydraulic flow conditions that might be reasonably expected to occur at an abutment. Therefore, engineering judgment is required in designing foundations for abutments." This is an important modeling gap, but despite the gap it is still necessary to select a threshold current depth and velocity at which scour damage would reasonably occur. At a minimum, it can be seen as a first cut at a plausible level of damage. (If that damage potential seems to be substantial, the result can at least motivate the development of analytical models supported by field observation and laboratory testing.)

For Froude number (V/gy) < 0.80, where V denotes velocity at the contracted section, g denotes acceleration due to gravity, and y denotes depth of flow, Federal Highway Administration (2011) recommends D_{50} (median stone diameter) of

$$\frac{D_{50}}{y} > \frac{K}{S_S - 1}\left(\frac{V^2}{gy}\right), \tag{22}$$

where K depends on abutment geometry but is approximately 1.0 and S_S is the specific gravity of riprap, which we take as 2.4. We are not interested in design of riprap but in the analysis of the potential for scour damage knowing D_{50}, y, V, and other factors. In equation 22, depths cancel. Let us assume as a first estimate a median stone diameter of 0.3 m. We substitute 0.3 for D_{50} and solve for V, which results in the following expression:

$$V < \sqrt{\frac{(S_S - 1) \cdot g \cdot D_{50}}{K}} \tag{23}$$

It evaluates as

$$V < \sqrt{\frac{(2.4 - 1) \cdot 9.81 \frac{m}{\sec^2} \cdot 0.3m}{1.0}} \tag{24}$$
$$V < 2m / \sec$$

Which suggests that if D_{50} = 0.3 m, the design is sufficient to resist scour damage as long as V_{max} < 2 m/sec. Checking the Froude number at say V = 2 m/sec, (2/9.81) < 0.8 y limits the applicability of equation 24 to y > 0.25 m. For V = 5 m/sec, y > 0.6 m/sec, so the expression seems general enough for present purposes. That is, we do not need to consider the case of the Froude number exceeding 0.80.

We assume that the design guideline is conservative, perhaps with a safety factor of 3, so the median capacity of an embankment with D_{50} = 0.3 m to resist scour might be V = 6 m/sec, meaning 50-percent chance of scour at 6 m/sec. The capacity scales with $D_{50}^{0.5}$, meaning that with D_{50} 1/4th the assume diameter, that is, 3-inch diameter stone, the median capacity is halved to 3 m/sec. This seems to be a reasonable threshold for such an approximate analysis, where we do not actually know whether there is any riprap at all on any given embankment. It also satisfies intuition; a 3-m/sec flow feels like it could scour an embankment with a cover of 3-inch diameter stones.

Turning to damage mode 2, because roads are not necessarily armored in any way, let us assume soil conditions, say D_{50} = 0.01 m and S_S = 1.2. This yields V < 0.14 m/sec. Even with some added conservatism, it suggests that any flow over an elevated roadway where vortices can form on the downstream side is likely to cause scour damage.

To recap, for purposes of estimating realistic damage to bridge embankments and roadways in the SAFRR tsunami scenario, we assume that embankment scour occurs to bridges where the embankment obstructs the flow and V > 3 m/sec. Any flow over an elevated roadway (elevated in the sense that vortices can form on the downstream side) is assumed to cause scour damage.

Repair Duration

The degree of damage and duration of repair is more problematic, especially here where we are limited to a very approximate analysis for a number of roads and bridges and little scope to consider site-specific information. Degree of damage would seem to depend on some integral involving velocity over duration of flow. For convenience, we assume that all cases are the same. Bridge embankment scour requires say 4 days to backfill and repave. Roadway scour requires

say 1 day per 1,000 feet to repair in a rural area, say 1 day per 2,500 feet in an urban area with high traffic demand. In the case of a rural road with an alternate route and the existing alignment is at high risk to repeated tsunami damage, let us add 3 months for decision-making to select the new alignment

Traffic disruption is likely to be briefer than repair duration, especially where alternate routes are available. Let us assume that, where an alternate route is available, traffic is merely slowed and not cut off, and that we need not quantify the delay. Otherwise, traffic is stopped for the duration of the repairs: 3 days for a bridge embankment and 2 days per 1,000 ft of roadway.

Repair Costs

The General Accounting Office estimates the cost of highway construction at $1 to $9 million per lane-mile, with costs varying widely (GAO, 2003). Let us assume that roadway repair costs on the order of $5 million per lane-mile. This figure was judged reasonable by Caltrans staff in a October 3, 2012, panel discussion, and further supported by construction cost statistics for new highway construction in Florida, adjusted for location. We assume the repair of a bridge abutment damaged by scour costs $150,000. (This assumes a crew of 12 working 32 hours at a cost to the State of $150 per hour, the figure doubled to include material and equipment, and a 25-percent premium for urgency.)

Damage to Roads and Bridges in the SAFRR Tsunami Scenario

We compared the criteria described above to the locations of highways and highway bridges and the modeled inundation line and current velocities estimated elsewhere in this study. Figure 66 shows damage locations; they are clustered near Eureka, in the San Francisco Bay, and along the south coast from Malibu to just north of San Diego. In the figure, damaged roads are shown in red and damaged bridge embankments are in yellow. This is a subset of the assets shown in figure 59. Table 29 details roadway damage at six locations where the scour conditions described above are met. Table 30 details the scenario's hypothetical scour damage to bridge embankments.

The total length of damaged roadway is approximately 5 miles. The width of the damaged road varies from place to place. The total damage is approximately 20 lane-miles. The repair cost is approximately $100 million. Traffic delays are none to 2 days, but two stretches of U.S. 101 might take 3–4 months to repair to allow for decisions about rerouting. Public assistance grants would probably provide $80 million from the Federal government to perform repairs, with the remaining $20 million borne by the State.

As shown in table 30, bridge embankment scour damage is hypothesized to occur at 12 locations, 7 of them on to CA1 between Malibu and Costa Mesa. The table shows velocities at each bridge location, which are generally in the range of 3–10 m/sec. It also shows wave heights for information purposes (generally 1–2 m), though these are not used to identify damage locations. Bridge embankments not listed in the table either do not intrude into the channel, or have velocities below 3 m/sec. The table also shows estimated repair costs. Total repair cost is $3 million. All but one have alternate routes available.

There are several stretches of highway and local roadway that are wetted, but not with the required scour conditions—elevated roadway with soil on upstream or downstream side that can be eroded by vortices. These include stretches of the Pacific Coast Highway, CA39, CA75, CA92, US101 and the San Francisco Great Highway. These stretches do not appear in table 29.

There are a few bridges slightly inland of the coast where embankments intrude into the current (according to the inundation line), but the velocity model does not reach.

Tables 29 and 30 note which hypothetical damage locations are part of the Strategic Highway Network (STRAHNET). STRAHNET is a network of highways deemed to be important to the United States' strategic defense policy and which provide defense access, continuity and emergency capabilities for defense purposes. They could be important to the supply chain for emergency supplies. As with other damage locations, where STRAHNET routes are damaged the traffic would be detoured to local roads. There is no program that distinguishes STRAHNET routes from any other route, so the fact that a route is STRAHNET would have no bearing on decisions to improve the tsunami resistance of the route before a disaster (called "betterment" by Caltrans).

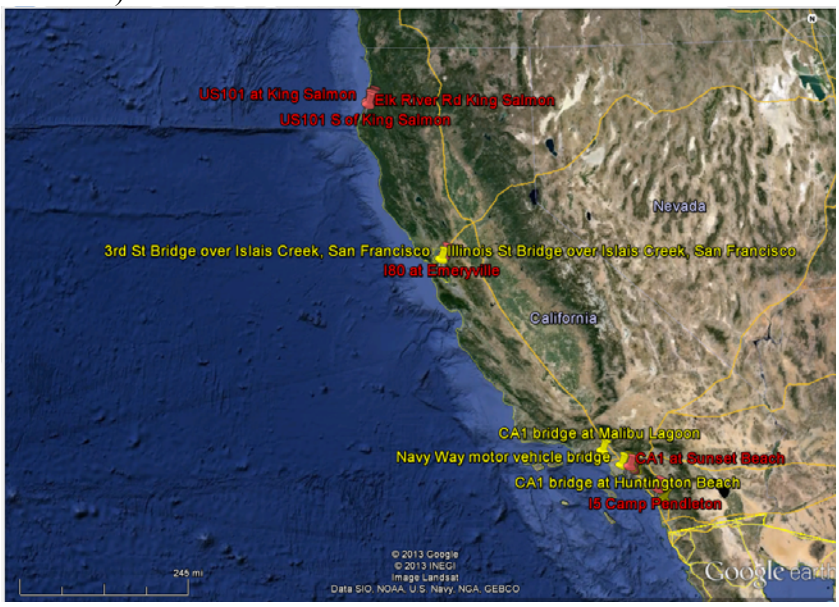

Figure 66. Map of SAFRRR tsunami scenario bridge and roadway damage locations. Road damage is shown in red, bridges in yellow. This is a subset of the assets shown in figure 59. (Base image from Google Earth.)

Table 29. SAFRRR tsunami scenario highway scour damage.

[*sn*, Strategic Highway Network, STRAHNET; mi, miles; ft, feet; $M, millions of dollars]

Location	Length	Lane-miles	Alt route	Realign	Delay	Repair days	Cost, $M
US101 Eureka ***(sn)***	1 mi, 4 lanes	4.0	Yes	Maybe	No	95 days	$20
US101 King Salmon ***(sn)***	1,000 ft, 4 lanes	0.8	No	No	1 day	1 day	$4
US101 S of King Salmon ***(sn)***	1 mi 4 lanes	4.0	Yes	Maybe	No	95 days	$20
I80 Emeryville ***(sn)***	1 mi, 2 of 10 lanes	2.0	Yes	No	No	2 days	$10
I5 Camp Pendleton ***(sn)***	2,000 ft, 4 of 8 lanes	1.6	Yes	No	No	2 days	$8
CA1 Costa Mesa	3,000 ft, 6 lanes	3.6	Yes	No	No	3 days	$18
CA1 Sunset Beach	1 mi, 4 lanes	4.0	Yes	No	No	3 days	$20
Total	**4.6 mi**	**20**					**$100**

Table 30. SAFRRR tsunami scenario bridge embankment scour damage.

[*sn*, Strategic Highway Network, STRAHNET; mi, miles; ft, feet; $M, millions of dollars; m, meter; m/sec, meters per second. Wave heights are above mean high water plus 20 centimeters (MHW+20)]

Location	Latitude °N, Longitude °W	Velo-city m/sec	Wave height, m	Alternate route	Delay days	Repair days	Cost $M
US101 Bucksport (2 ends) ***(sn)***	40.7550, 124.1903	5-10	1	No	3	3	$0.30
3rd St., San Francisco (2 ends)	37.7474, 122.3874	8-10	1.5	Yes	No	3	$0.30
Illinois St., San Francisco (north end)	37.7475, 122.3862	8-10	1.5	Yes	No	3	$0.15
CA1 Malibu Lagoon (2 ends)	34.0346, 118.6815	3-10	1.5	Yes	No	3	$0.30
CA1 Marina (north end)	33.7630, 118.1154	5-10	1	Yes	No	3	$0.15
CA1 Anaheim Bay (2 ends)	33.7319, 118.0849	4-10	1	Yes	No	3	$0.30
CA1 Huntington Beach (north end)	33.6833, 118.0357	5-7	2	Yes	No	3	$0.15
CA1 Costa Mesa (2 ends)	33.6331, 117.9610	5-7	1-2	Yes	No	3	$0.30
CA1 Costa Mesa b (2 ends)	33.6310, 117.9575	5-7	1	Yes	No	3	$0.30
CA1 Costa Mesa c (north end)	33.6168, 117.9047	7-10	0.5	Yes	No	3	$0.15
I5 Camp Pendleton (south end) ***(sn)***	33.2065, 117.3940	3-5	2	Yes	No	3	$0.15
US101 Cardiff (2 ends) ***(sn)***	33.0161, 117.2809	7-10	2	Yes	No	3	$0.30
Total							$2.85

Resiliency Opportunities

Caltrans has strategies for quickly restoring roads and bridges. As with previous disasters such as fires, earthquakes, and floods, Caltrans has contractors bid the days and cost for a repair or replacement. An economist determines the cost for each day the road is closed and the bidder with the lowest total bid is awarded the contract. Only a few contractors are asked to bid for each job to keep the process efficient. The governor declares a state of emergency so the contracting process is abbreviated and does not require an Environmental Impact Statement (EIS).

One other opportunity to enhance resiliency might be to review plans with local officials about changing the alignment or increasing the elevation of roads that are particular exposed to tsunami damage. Two such stretches were identified here. Discussions and planning before a disaster might reduce decision-making delays in the event of an actual tsunami. Another opportunity might be to examine bridge embankments like those identified here for future improvements. As noted earlier, this study does not address evacuation routes and road closures during the warning period.

Research Needs

The scenario depicted here relies on simplifications about damageability, especially about threshold levels of velocity causing embankment scour. It suggests that a large Alaskan teletsunami could cause on the order of $80 million in damage affecting 16 lane-miles of highway and 13 bridges. These figures are offered to understand the order of magnitude of damage for such a tsunami and for design emergency response plans. They can inform community decisions about emergency planning, but they do not represent the results of a detailed engineering analysis.

Caltrans and the Pacific Earthquake Engineering Research (PEER) Center are pursuing such analyses. They are supporting tsunami hazard work being done by URS Corp. The CGS is preparing to make detailed maps of wave elevation and velocity for different return periods provided by URS. Caltrans will write bridge design procedures for tsunami loading, in part using computer modeling of fluid-structure interaction with the finite-element software LS-DYNA by researchers at Oregon State University's (OSU) NEES facility. (NEES refers to Network for Earthquake Engineering Simulation, a program of the National Science Foundation). Caltrans will determine whether a Cascadia subduction event produces larger tsunami loads on bridges as part of its research program.

PEER is considering a project or example to frame a new performance-based tsunami engineering (PBTE) methodology. The SAFRR tsunami scenario might be an ideal case study. Among the data needs for such a methodology would be detailed maps (perhaps by lidar) of existing bridges and coastal roads, necessary to apply scour models to roads and bridge abutments. Such an effort might also require a database of fragility and repair-cost data, along the lines of PEER's prior work developing 2nd generation performance-based earthquake engineering (PBEE-2) methodology.

Finally, note that the Federal Emergency Management Agency and California counties are developing an Earthquake and Tsunami Response Plan for the West Coast, focusing on the consequences of a Cascadia subduction earthquake and tsunami. This study may address highway and bridge damage in northern California counties as well as Oregon and Washington. The FEMA effort and the present one share common concerns but address different scenarios. The interested reader is referred to the project Facebook page at *https://www.facebook.com/RCTWG?filter=3* (accessed November 1, 2012).

Damage and Restoration of Railroads in the SAFRR Tsunami Scenario

By William Byers

Significant to extreme damage to railroads has been documented in 94 earthquakes and slight or minor damage in 20 others. The earliest of these was the 1859 magnitude 7.6 Copiapo, Chile, earthquake. There are doubtless other earthquakes that caused railroad damage for which documentation was not found or does not exist. In 11 of the 94 earthquakes, significant to extreme damage was caused by earthquake-generated tsunamis. These earthquakes were all in subduction zones and had magnitudes ranging from 7.3 to 9.5. Nine were inter-plate. One involved a normal rupture in the subducting slab. It is possible that the tsunami associated with

this last-mentioned earthquake was caused by an under-ocean landslide. The tsunami in one other subduction zone earthquake of undetermined type caused some railroad damage.

Most railroad damage from tsunamis was in the same area as other earthquake damage but the tsunami generated by the December 26, 2004, Sumatra earthquake caused severe railroad damage, including washing a train off the track at a location over 1,000 miles away in Sri Lanka.

Four of the 94 earthquakes causing major railroad damage generated tsunamis which either did not affect railroads or caused only slight damage as there were no railroads in locations significantly impacted by the tsunamis. Of the 79 earthquakes that did not generate tsunamis, nine were inter-plate thrust earthquakes in subduction zones, 26 were in subduction zones but not identified as inter-plate. Seven of these were in the subducting slab and eight in the overriding plate. The locations, relative to the plate interface, of the other 11 fractures were not determined.

On the basis of this sample, there is an appreciable risk of railroad damage from earthquake-generated tsunamis, including tsunamis generated by remote earthquakes. For comparable wave heights, damage from tsunamis can be expected to be similar to that from hurricane storm surges. Information on railroad damage is available for Hurricanes Alicia in 1983, and Ike in 2008 (Byers, 2011) and Katrina in 2005. Storm surges at selected locations of railroad damage were estimated to be in the order of 9 feet (as much as 4 feet above the track over a distance of about 5 miles) for Alicia; 20 to 28 feet (up to 20 feet above the track over a distance of about 100 miles) for Katrina; and 14 feet (as much as 10 feet above the track over a distance of about 15 miles) for Ike.

The tsunami associated with the March 11, 2011, Tohoku, Japan, earthquake provides extreme examples of the types of railroad damage normally associated with tsunamis. These are illustrated by figures 67 through 70. Similar, but in many cases less extreme, damage was caused by other tsunamis. Bridge spans were also washed off piers in the 1908 Messina earthquake (Davison, 1936). There was also, less severe, bridge damage in the 1946 Nankai earthquake (Okamoto, 1984). Rolling stock was overturned or derailed in the 1922 Atacama, Chile (Willis, 1929), the 1964 Alaska (Sturman, 1973), the 2004 Sumatra and the 2010 Maule, Chile (Chile Railways, 2010) earthquakes. Tracks and embankments were submerged and/or washed out: in the 1908 Messina (12 miles) (Morris, 1909), the 1922 Atacama (Willis, 1929), the 1933 Sanriku (Okamoto, 1984), the 1946 Nankai (Okamoto, 1984), the 1964 Alaska (Sturman, 1973), the 1964 Niigata (Kawasumi and others, 1968) and the 2010 Maule, Chile (Chile Railways, 2010), earthquakes. Debris was deposited on tracks in varying quantities and signal systems damaged in most, if not all, tsunamis. Railroad car ferry loading facilities were damaged in the 1964 Alaska (Sturman, 1973), and the 1968 Tokachi-oki (Okamoto, 1984) earthquakes. Damage from earlier tsunamis is shown in figures 71 through 73. Hurricane storm surge damage depended on both the height of the surge and the types of construction exposed. It included debris on tracks, washed out ballast, track washed out-of –line, track washed off bridges and moderate to extreme bridge damage. Examples of relatively limited damage are shown in figures 74 and 75.

Figure 67. Photograph of overturned passenger cars in Komagamine, Japan after 2011 Tohoku, Japan, tsunami. Wave height at location unknown. (Photograph by Charles Scawthorn.)

Figure 68. Photograph of overturned passenger train locomotive in Komagamine, Japan, after the 2011 Tohoku tsunami (photograph by Charles Scawthorn).

Figure 69. Photograph of displaced steel girder span near Rikuzen Takata after 2011 Tohoku, Japan, tsunami (photograph by Charles Scawthorn).

Figure 70. Photograph of damaged piers of the JR Rail Viaduct crossing the Tsuya River, Japan, after the 2011 Tohoku tsunami (photograph by Shideh Dashti).

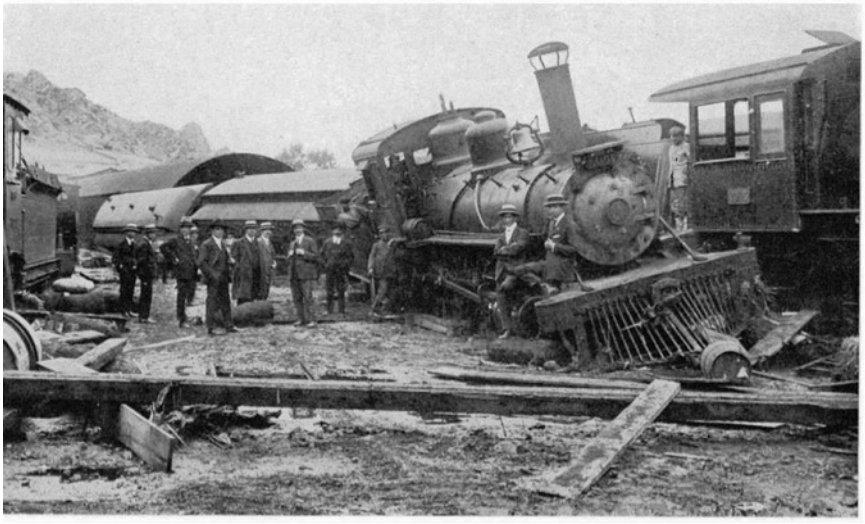

Figure 71. Photograph of Coquimbo rail yard after 1922 Atacama, Chile, tsunami. Run-up height is given as 26 feet but elevation of yard is not known. Estimated wave height in the yard is between 5 and 15 feet. (Photograph from Willis, 1929.)

Figure 72. Photograph of overturned locomotive at Seward after 1964 Alaska tsunami. Run-up height at Seward after the 1964 Alaska tsunami was about 40 feet. (Photograph from Sturman, 1973.)

Figure 73. Photograph of Seward yard after 1964 Alaska tsunami. Estimated wave height in the Seward yard is between 25 and 35 feet (photograph courtesy of National Oceanic and Atmospheric Administration, National Geophysical Data Center).

Figure 74. Photograph of open deck trestle damage from 1983 Hurricane Alicia in the United States. Deck shifted by return flow. Surge depth was about 3 feet above track, about 5 feet above bottom of deck. (Photograph by William Byers.)

Figure 75. Photograph of track damage from 2008 Hurricane Ike in the United States. Surge depth was about 3 feet above track (photograph by Ross Ruckel).

Tsunami damage is the result of one or more of three mechanisms that are shared to a greater or less extent by other types of flooding. Submergence to various depths occurs to the limit of inundation. Erosion of soil and other granular material requires a minimum depth but depends primarily on the velocity and duration of flow. Direct wave effects result from buoyancy, lateral pressure of the wave, upward pressure when the surface of the wave rises against exposed horizontal surfaces and impact from floating debris.

It is impossible to know where trains will be at the time of the hypothetical tsunami, but for the sake of depicting a particular outcome it is useful to assume some particular location for trains. To that end, it is assumed here that, at the time the tsunami warning is issued, trains and other movable railroad equipment will be located as shown in a Google Earth image from March 2012. However, with the amount of warning anticipated, there should be no trains in locations subject to damage. Article 1.2.2.4—Tsunamis in chapter 9 Seismic Design for Railway Structures of the American Railway Engineering and Maintenance-of-Way Association Manual for Railway Engineering (AREMA, 2012) contains the following recommended practice:

After a tsunami warning is issued to the railroad, train dispatchers shall notify all trains and engines within the areas vulnerable to the tsunami to move out of those areas before the estimated arrival of the tsunami. To the extent possible all other equipment should also be moved. The movement should be to the closest location at an elevation deemed to be safe. This movement may be in reverse of the train's normal movement.

For any remotely generated tsunami, train dispatchers would have plenty of time to get all trains moved to safe areas. However, damage to track and other fixed facilities and to any equipment remaining on inundated yard tracks or side tracks can be expected. The extent of damage depends on the depth of inundation, the velocity and, for erosion of ballast or embankment, the duration of the velocity.

Removal of wave deposited debris will probably be required on a major portion of any tracks inundated to a depth of one foot or more. Ballasted track would probably not be significantly damaged if inundated to a depth of less than one foot. Ballast has been protected from erosion by hurricane storm surges with a depth in the order of 5 feet by asphalt injection but the cost would probably not be justified for tsunamis due to their low frequency of occurrence at vulnerable locations. Track alignment has been maintained well enough to allow limited operation under storm surges as great as 10 to 15 feet by anchoring to piles located on both sides of the track at about 300 foot spacing (Byers, 2011) but, again, the cost would not be justified. At the ports of Los Angeles and Long Beach, and at some other locations, tracks are encased in concrete paving with its surface at the same level as the top of rail. Track in concrete paving would probably withstand inundation to a depth of several feet unless the pavement is undermined. At these locations, debris would be removed as part of clearing the paved area. However, it might be necessary to remove debris from the flangeways (the openings parallel to the rail that are made through platforms, pavements, track structures to permit passage of wheel flanges). This would probably be done by high-pressure flushing.

Electrical/electronic components of signal systems are typically about 2 feet above the track. If the water depth significantly exceeds this value, it would damage or destroy the instrument cases in which these components are housed. Electric motors of switch machines would be submerged by near the top of rail. Unless struck by debris, signal masts would probably survive wave heights in the order of 5 to 10 feet.

Damage to bridges will require a wave of appreciable amplitude. Very few railroad bridges have shallow foundations on erodible material. Typically they have deep foundations

consisting of driven piles or reinforced concrete drilled piers or are founded on rock. Old timber bridges built in the early 1900s typically have pile depths of approximately 25-30 feet and may be subject to scour when currents exceed 6 to 8 kt. New bridges typically consist of concrete or steel superstructures supported by driven steel piles or reinforced concrete drilled piers, typically with sufficient depth to avoid scour. We examined bridges rail bridges along the entire coast in the study area and found one case where velocities were significant enough to cause scour: the Santa Margarita River (Trestle) bridge near Camp Pendleton. At this bridge, 10 kt currents could potentially cause scour around the 30-feet piles, though it seem unlikely to be sufficient to cause the failure of the bridge. Therefore, scour is an unlikely mode of failure along the Coastal Rail Corridor. We found no cases where the wave was high enough to impact the bridge soffit, and therefore superstructure displacement also seems unlikely.

An open deck timber trestles trestle had its deck washed out of line by a relatively low hurricane storm surge with a maximum height of about 5 feet above the track. Attachment of the deck to the bents was probably broken during inward flow and final misalignment occurred during outward flow of the surge. Unanchored track was washed out under a surge estimated as being in the order of 3 feet over the track. Track anchored to piles at intervals of about 300 feet remained essentially in alignment after a surge of about 14 feet over the track (Byers, 2011).

If water reaches a depth significantly greater than 3 inches above the top of rail, traction motors of locomotives are subject to damage. Locomotives, cars with loads of particularly high value or hazardous materials and other particularly important equipment would be moved to high ground. This is based on railroads' policies for removing equipment from Galveston Island in advance of hurricanes during the period when Galveston was a major port and rail terminal. However, a number of both loaded and empty cars may still remain vulnerable in ports or low elevation yards and side tracks adjacent to the coast. If water reaches a depth significantly greater than 8 inches above the top of rail, bearings and brakes of cars are subject to damage. If the crest of the wave is over about 2 feet above the top of rail, lading in double stack container cars and hopper cars is subject to water damage. If the crest of the wave is over about 4 feet above the top of rail, lading in most cars is subject to water damage and there is a risk of derailing standing cars, particularly empty cars. At the crucial depths where a type of damage begins, a small change in water depth can cause a disproportionate change in total damage.

In addition to the areas vulnerable to the scenario tsunami, there are near-by areas that would be vulnerable to greater wave amplitudes or to similar tsunamis arriving at a higher tidal stage. Tidal ranges for many of the vulnerable areas are appreciable. Data for several tide gages along portions of the California coast with adjacent railroads are shown in table 31.

Table 31. Tide gages near several coastal stretches of railway.

[max., maximum; min., minimum; ft, feet]

Location of Tide Gage	Difference between max. high and min. low tides	
	Typical Day	Typical Year
Port Chicago (on Sacramento/San Joaquin River Delta)	5 ft	6.9 ft
Richmond	5 ft	9.6 ft
San Francisco	5 ft	9.5 ft
Monterey	4 ft	9.2 ft
Santa Barbara	4 ft	9.0 ft
Los Angeles	4 ft	9.2 ft
San Diego	4 ft	9.5 ft

Inundation limits and modeled flow depths given in the scenario are used to estimate damage. Even if there is no damage or inundation of railroad facilities, there will be interference with normal operation and associated costs during the period that the tsunami warning is in effect and while post-tsunami inspections of tracks are being performed. Damage will be discussed from north to south.

There are no longer operated rail lines at vulnerable locations in California north of the San Francisco Bay area. (There is a vulnerable line in Washington along Puget Sound.)

At Richmond, slightly more than one half mile of a rarely-used track to the former Atchison, Topeka and Santa Fe Railway (AT&SF) car ferry slip would be inundated to a maximum depth of about two to three feet. Before reaching the BNSF Railway Richmond yard, the wave would have to pass through a short tunnel. Entrance and exit head losses, friction in the tunnel along with limited duration of the wave and a large area for dissipation upon leaving the tunnel would prevent inundation of any significant depth in the yard. (A 5-foot higher wave would inundate about 3½ miles of additional track at 4 locations in Richmond and Oakland.)

The Union Pacific (UP) operates a line from the San Francisco Bay area to Los Angeles that runs parallel to the coast at a number of locations from near Watsonville to Ventura. There is also a branch to Santa Cruz. At some locations, the line is very close to the coast and low enough to be vulnerable to tsunamis. The line carries both freight and passenger trains. Both the UP and BNSF have lines between the San Francisco Bay area and Los Angeles that run through the Central Valley, would not be affected by a tsunami, and would serve as detour routes.

At Santa Cruz, about 0.1 mile of track in a concrete paved street would be inundated to a depth of less than one foot. (A 5-foot higher tsunami would increase the maximum depth by 5 feet and the length involved by one half mile.)

Near Carpinteria, there is a 0.9 mile stretch of main track with 3 ballasted deck bridges that would be inundated to a maximum depth of about 3 feet. Considerable washed out ballast, some track severely misaligned or washed off embankment, and insignificant bridge damage can be expected at this location. There would also be immersion damage to some signal system equipment. (A 5-foot higher wave would increase this segment by 0.8 mile and add 2.3 miles of main track in segments near Summerland and Ventura, including a 700 foot bridge that would not be damaged and a 152 foot open deck trestle which would have minor damage, as well as 1.8 miles of tracks and the bearings on three cars at the U.S. Navy's construction battalion facility at Port Hueneme.)

In addition to freight trains, thirteen passenger trains, including 11 commuter trains, operate over the track near Carpinteria. Four of these are scheduled to pass the affected area between the time of the earthquake and the arrival of the tsunami. The first of these is scheduled to clear the area by 12:48 p.m. and would probably be allowed to proceed normally if running on time. Later trains would probably be held at safe locations until after the tsunami's arrival. Freight trains, which do not have defined schedules, would be dispatched in a similar manner.

Considering the time required for mobilization and performing the work, the line could be expected to be out-of-service for up to three days, depending on the availability of ballast and track surfacing equipment. Although through movements would be prevented during this period, intermediate points could be served from one end or the other. If equipment and train crews are available, separate sections of passenger trains could be run north and south of the damaged area and through passengers transferred between sections by bus. Freight could be moved through the connection on the appropriate side of the track closure.

The area of greatest rail vulnerability involves tracks and equipment at the Ports of Los Angeles and Long Beach. Track damage would be limited as tracks in the areas of greater inundation depth and velocity are primarily in concrete slabs and not subject to damage from washed out ballast. Damage to containers and their contents should be considered as part of the damage to the ports unless the containers are loaded on cars. Damage to containers and contents on cars is a part of railroad damage. No estimate will be made of the value of lading in containers but it should, on average, be similar to that in other loaded containers in the ports.

All movement of cars into the port would be stopped when the tsunami warning is received. There will be sufficient time to move all cars in the port area that are coupled to locomotives to safe locations as the locomotives are removed. Although they may not meet the requirements of the definition, these movements will be referred to as “trains”. Remaining cars are vulnerable to damage related to the depth of inundation. Significant inundation of tracks occurs at locations “A”, “B” and “C” in figure 76.

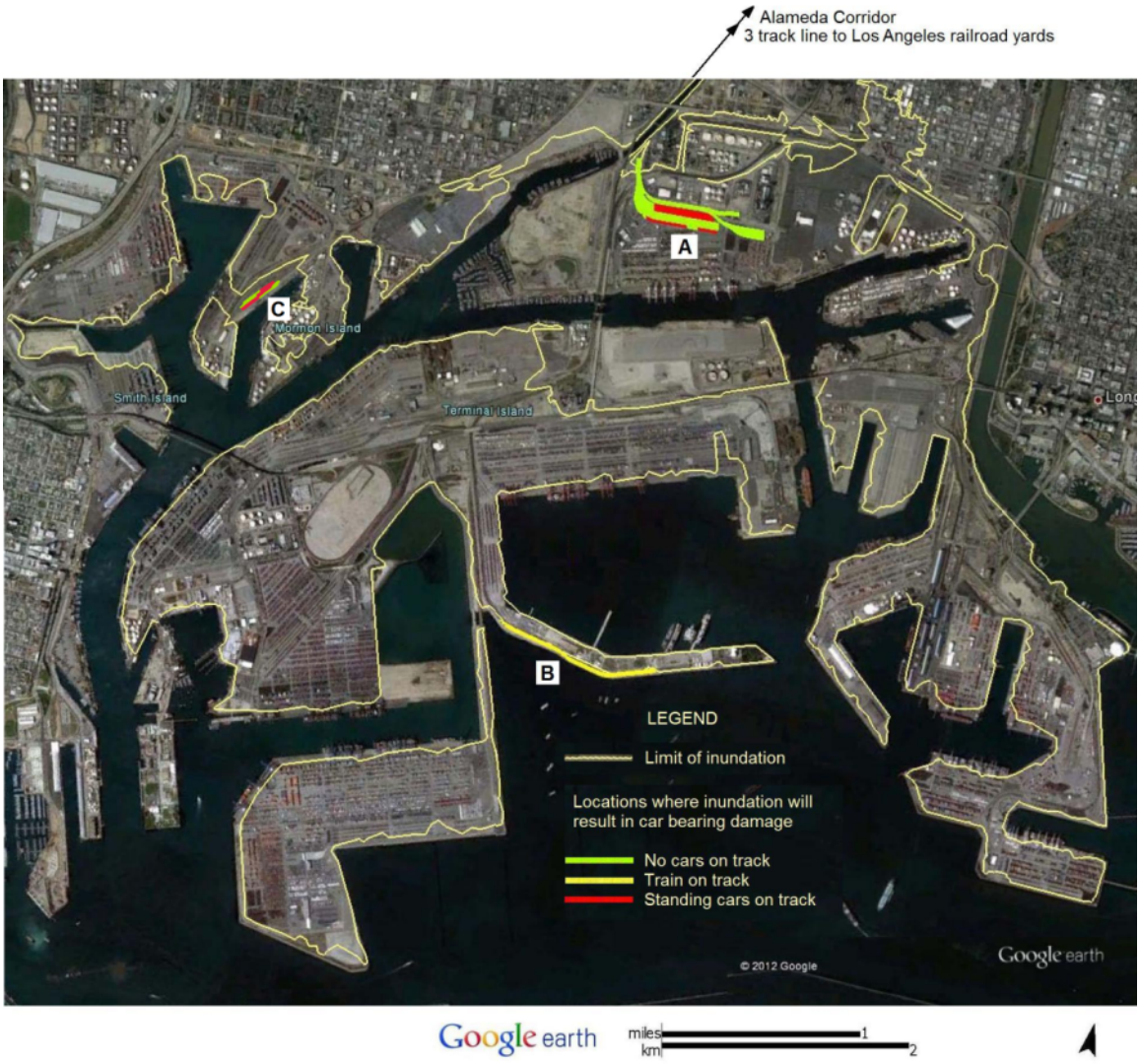

Figure 76. Map of conditions, when SAFRR tsunami warning is received, at locations in ports of Los Angeles and Long Beach where inundation will be deep enough to damage cars left standing on track (base image from Google Earth).

Details of the region at Location "A" with water depth great enough to cause wheel-bearing damage are shown in figure 77. This depth is less than the depth that would cause track damage. Segments of track with inundation depth great enough to cause damage are colored—green if unoccupied, red if occupied by either loaded or empty cars. This amounts to nearly five miles of track with about ¼ mile on ballast and the rest in concrete slabs. Track repairs would be relatively light, involving cleaning flangeways after trash is removed from the slabs as part of general port cleanup and any necessary restoration of ballast, lining and surfacing of the track on ballast.

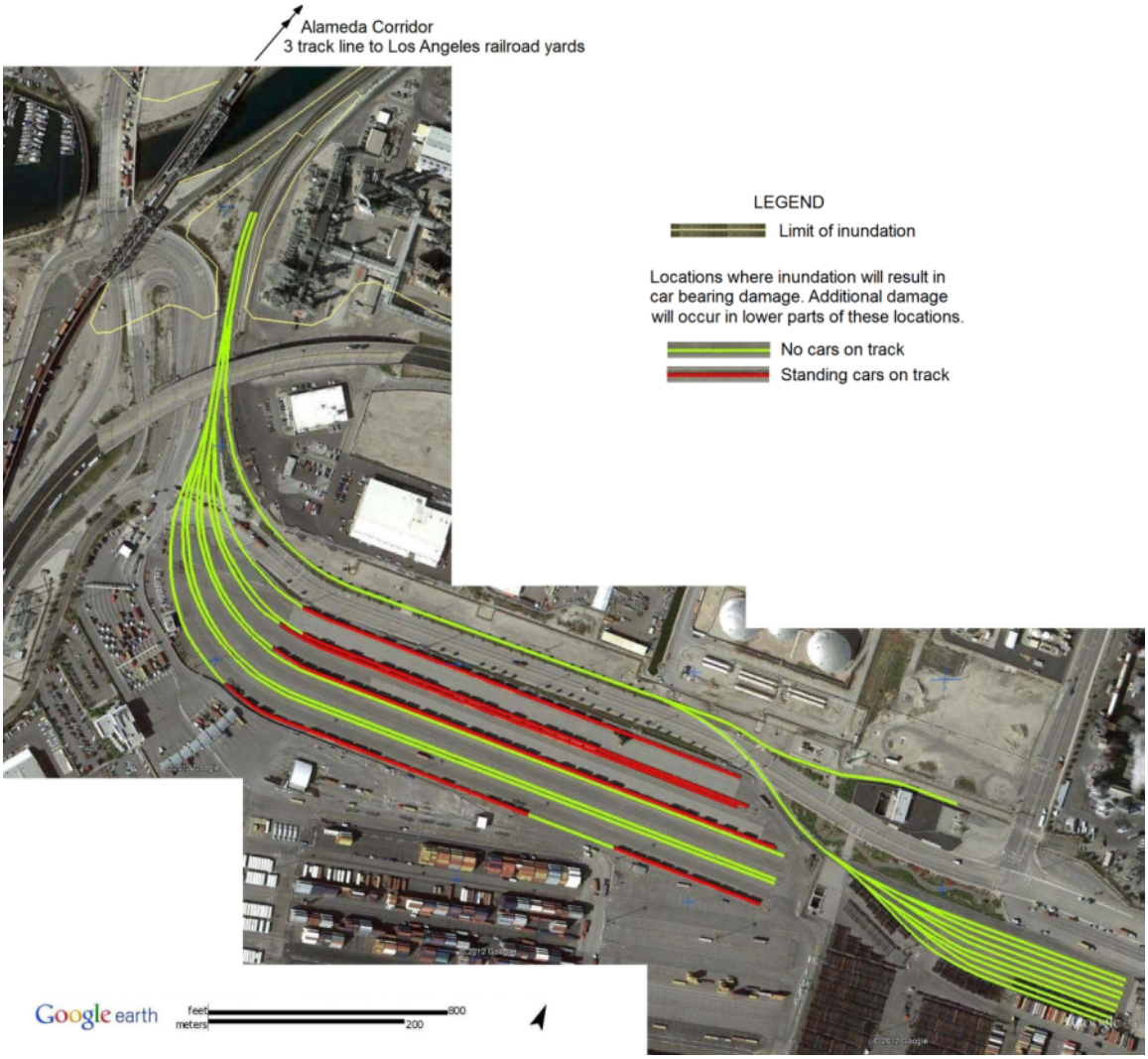

Figure 77. Satellite image annotated with details of location "A" (see fig. 76) at time of the SAFRR tsunami warning (base image from Google Earth).

Any car wheel bearings that are submerged must be reconditioned (or replaced) according to interchange rules. As a practical matter, this normally involves replacing the entire wheelset and shipping the damaged wheelset to a shop for reconditioning. Thirty two cars for transporting containers, including 4-axle cars, 8-axle articulated cars and 12-axle articulated cars, will require replacement of 316 wheelsets. Water depths will be great enough to damage vulnerable lading in 149 containers on loaded cars. The extent of damage depends on the nature of the lading that cannot be determined by viewing the exterior of the typical container. It can vary from a bulk commodity or other situation in which wetting of the bottom part of the contents destroys the value of all of the contents to material in water-tight drums that would be unaffected by partial immersion. It is reasonable to assume that no more than 10 to 20 percent of these containers would either be empty of have lading that would not be subject to water damage. Value of damaged lading will not be estimated but, on average, should be similar to the average value of lading in other containers at the ports.

The "train" at Location "B" would be moved to a safe location but cars would remain at Location "C". Seventeen cars at Location "C" would have water damage to the bearings of 68 wheelsets.

AMTRAK, Metrolink, and North County Transit District operate a line between Los Angeles and San Diego that follows the coast between San Clemente and San Diego owned in part by Metrolink in Orange County, by North County Transit District in Northern San Diego County, and by Metropolitan Transit System in Southern San Diego County. The line carries Amtrak and commuter trains during the day and BNSF freight trains at night. Except for short stretches of BNSF track in San Diego, which are a few feet above the tsunami run-up elevation, the tracks are NOT well above any tsunami inundation. No railroad damage is expected in this area.

The estimated cost of repairs to fixed property—track, bridges and signals—is slightly over one million dollars. Repairs to cars will have a similar cost. The cost of train delays and less efficient operation during the repair period could equal the cost of repairs to railroad property. This is in addition to the damage to lading in 120 to 135 loaded containers. (Damage to containers is addressed in the section dealing with the ports.)

Agricultural Damages

By Jamie Ratliff and Anne Wein

With more than 25 million acres of active farmland National Agricultural Statistics Service (NASS) (2009), California is one of the largest agricultural producers in the United States. Tsunamis like the proposed scenario can potentially adversely impact agriculture. Agriculture in California, though mostly confined to the Central Valley and other interior areas of the State, is also practiced along the coast and therefore susceptible to tsunami inundation. Smaller coastal farms and enterprises could be disproportionately affected by a tsunami. The losses could be direct and immediate (destroyed crops, drowned/displaced livestock, obliterated farming equipment, and damaged/destroyed buildings). Longer-term losses could pertain to restoring the land from the effects of debris, salinization, and topsoil removal. Indirect impacts from contamination of the soils and food supply could result from tsunami damages to infrastructure housing hazardous waste (for example, chemical spills, manure, and pesticides stored on farms) or reworked marine sediments (Plumlee and others, 2013). Historically, events like the 2004 Indian Ocean and 2011 Tohoku, Japan, tsunamis caused enormous amounts of agricultural losses (for example, stock, revenue, and life) in many regions located closest to the tsunami's origin.

Types of Agricultural Damages from Tsunamis

Inundation causes various types of damages to agricultural enterprises. Low-lying terrain like deltas can be particularly susceptible to tsunami inundation due to wide expanses of flat land barely above sea level. Though tsunami waves are relatively slow-moving when they inundate the land compared to their speed in open water—wave speeds in open water can be as high as 500 miles per hour (mph), whereas wave speeds near the coast reduce to less than 40 mph

(International Tsunami Information Center, 2013)—the speed is still fast enough to tear up crops and pastures, displace or drown livestock, and damage infrastructure.

The rapid movement of tsunami inundation waters across croplands can remove topsoil from the land along with any crops. Topsoil tends to be the more organic (and therefore nutrient rich) component of arable land, so scouring reduces the overall viability of the soil for crops. Replacing the topsoil is time-consuming and expensive, though it can sometimes be accomplished using biomass-rich crops. In addition, scoured topsoil can be deposited in other areas, modifying local topography and changing soil properties (Subagyono and others, 2005). Furthermore, debris carried by tsunami waves can also damage or destroy crops by cluttering up cropland or depositing silts and clays that form a more impermeable barrier and make water infiltration into soil more difficult (Subagyono and others, 2005).

Salinization of crop soils is another destructive agricultural hazard caused by tsunamis. Tsunami inundation infiltrates crops and saturates soil, potentially rendering cropland useless. When too much salt is present in the soil, osmosis leads to water being leached out of instead of taken in by crops through their roots. In addition, sediment deposits can sometimes inhibit leaching—the removal of salt from soil by flushing it with freshwater. Generally unless heavy, consistent rainfall or persistent irrigation occurs to wash salt out of the soil, only deep-rooted or salt-tolerant crops can be grown on inundated land until the salt content is reduced sufficiently to permit more salt-sensitive crops to be grown again United Nations Food and Agriculture Organization (FAO)(2005a).

Contamination of soil, food, and water supplies is a concern both economically and ecologically. For example, following the 2011 Tohoku earthquake, Japanese agricultural products (such as rice and fish) from Fukushima Prefecture had their distribution restricted for fear that radiation from the damaged Fukushima Daiichi nuclear power plant had contaminated the products (Kajitani and others, 2013); radiation from damage to nuclear power plants is not a concern in our tsunami scenario because coastal power plants are outside the modeled inundation zone. Livestock can also be adversely impacted by contamination—poor water supplies or radiation poisoning can kill livestock and cause defects in livestock products (for example, eggs, milk, and meat).

All types of tsunami damages impact various aspects of agriculture. Crops can be damaged or destroyed. Infrastructure (for example, barns) can be flooded, damaged by debris, or simply broken by tsunami inundation. Other equipment like tractors can be washed away or damaged by water and debris. Lifeline and crucial services damages (such as transportation and electricity) can cause agricultural losses to farms (dairy farms, in particular) both in and outside the tsunami inundation zone. Farmers and their staff may suffer injuries, be displaced, or even lose their lives as a result of tsunami inundation; livestock may experience these same problems. Damages to crops may be affected by the amount of time the land remains inundated (Porter and others, 2010). Finally, the time of year the event occurs affects the severity of damages to crops and livestock. For example, seedlings and calves are more vulnerable than more established crops and livestock.

Historic Tsunamis and Agricultural Losses

A number of tsunamis have resulted in varying levels of damage to agriculture (for example, crops, infrastructure, and livestock). In the past 10 years, the 2004 Indian Ocean tsunami and the 2011 Tohoku tsunami have recorded information about crop and livestock

damages in various countries. Other tsunamis, such as the 2010 Chile, 2010 Sumatra, and 2009 Samoa tsunamis, also had some impact on agriculture in their countries of origin.

The 2004 Indian Ocean tsunami, one of the most destructive tsunamis in recorded history, damaged or destroyed agricultural land in many Southeast Asia countries. India and Indonesia were some of the hardest-hit countries, with nearly 40,000 hectares (ha; 99,000 acres) of Indonesia's field area destroyed and over 50,000 ha damaged and nearly 12,000 ha (30,000 acres) of India's crop lands damaged (International Fund for Agricultural Development, 2005). In Thailand, where damages were less severe, approximately 100 ha (250 acres) of cropland and 1,600ha (4,000 acres) of plantation land were affected, resulting in an estimated 376 million Baht ($12.3 million U.S.) in damages and losses. Uprooted oil palms and coconut trees required replacement. More than 10,000 animals drowned, leading to an estimated 17.6 million Baht ($570,000 U.S.) of livestock losses across six provinces (Asian Disaster Preparedness Center, 2005). Nearly 40 percent of the arable land on the island of Sumatra in Indonesia was estimated to be unusable for at least a few years (FAO, 2005b). The Maldives and Sri Lanka also had relatively significant agricultural damages: around 50 percent of agricultural land in the Maldives was completely destroyed, and approximately 1/3 of Sri Lanka's production in the peak cropping season was lost in the main paddy growing areas (International Fund for Agricultural Development, 2005).

In Japan after the 2011 Tohoku earthquake, agricultural damage was estimated at about 950 billion Yen (¥) ($9.32 billion U.S.). About 23,500 ha (58,000 acres) of land including about 20,000 ha [49,000 acres] of rice paddies and 3,500 ha [8,600 acres] of upland fields were washed away or flooded by tsunami inundation. After one year, less than half of fields damaged by salinization had been restored; over half of the damaged farms in the disaster zone were still inoperable (Japan Ministry of Agriculture, Forestry and Fisheries, 2012). After 2 years, 80 percent of the rice fields in Sendai have been desalinated and some farmers are cultivating rice for the first time in three years (Hirama, 2013).

The failure at the Fukushima Daiichi nuclear power plant following the tsunami introduced major concerns about radiation contaminating remaining crops in multiple prefectures surrounding the plant. Restrictions on export and consumption of leafy (lettuce, cabbage) and flowerhead (broccoli, cauliflower) vegetables from these prefectures was restricted for a short time pending more comprehensive testing. Dairy products like milk and eggs, as well as meat products, like pork, were also restricted pending further testing in Fukushima prefecture (Johnson, 2011).

Although tsunamis can cause serious damage to agricultural land, reports on agricultural damages in California following tsunamis of record are non-existent. The 2010 Chile and 2011 Tohoku tsunamis damaged marinas along much of the coast of Northern California without inundating land (CGS, 2012). Although no evidence of agricultural damages from the 1964 Alaska tsunami could be found, similar to the SAFRR tsunami scenario, land and communities in California were inundated.

Potential Agricultural Damages in the SAFRR Tsunami Scenario

Agricultural damages in the SAFRR tsunami scenario are summarized in terms of land exposure and crop income losses, soil and crop contamination sources; exposed livestock value, and damages to agricultural buildings and contents. We were not able to address field remediation costs and restoration times.

Methods

To establish how much agricultural land is potentially exposed in the SAFRR tsunami scenario inundation zone, agricultural land cover data were intersected with the scenario inundation zone and wave velocity/flow depth data and summarized by county using geographic information systems software. “Cropland” and “agricultural land” are defined as follows: cropland refers to land that was cropped (for example, for wheat or strawberries) and agricultural land includes both cropland and land that was not (but could have been) used for crops or was used for livestock (such as fallow/idle cropland or pasture).

Two different land use datasets were considered for the agricultural land exposure analysis. Vector land survey data from the California Department of Water Resources (DWR) and raster remotely sensed cropland data from NASS were both processed to provide a range of agricultural exposure values. DWR data collected through a series of land surveys and extensively ground-truthed are potentially more accurate. However, the surveys were completed between 1993 and 2006 and do not cover every coastal county (DWR, 2013). NASS Cropland Data Layer (CDL) data have complete coverage at 30-m resolution and are more current—CDL data are updated yearly—but are far more reliant on automated processes to complete the classification (NASS, 2013).

An examination of the 2007 Census of Agriculture for California revealed that every county in the State has at least a nominal amount of farmland in use (NASS, 2009). Therefore, the decision was made to use the CDL for this analysis to capture exposed agriculture in counties not surveyed by DWR. The currency of the CDL data was also preferable because crops can change from year to year—the entire study area was included in the 2012 CDL, unlike the DWR data where different counties were surveyed in different years. The 2012 crop distribution is not intended to predict what the crop distribution will be in 2014; this analysis uses these data as a proxy to provide a general idea of what agricultural impacts could be possible for the SAFRR tsunami scenario.

Other sources were used to address the other types of agricultural damages. DWR data was consulted for indications of livestock (poultry, feedlots, and dairy) in the inundation zone and confirmed using satellite imagery. Crude estimates of crop income loss and exposed livestock value relied on agricultural damage analyses conducted for the ARkStorm scenario (Porter and others, 2010). Sources of soil and crop contamination were extracted from the environmental and environmental-health implications in the SAFRR tsunami scenario (Plumlee and others, 2013). Finally, more detailed information about how building and content losses were calculated is provided in the Building Damage section of this report.

Agricultural Land Exposure

Approximately 90,600 acres of land lie in the scenario inundation zone; around 9,600 acres (11 percent) is agricultural land (based on the 2012 CDL). Alfalfa is the most common crop in the inundation zone, making up 42 percent of inundated agricultural land. Truck-transported crops (such as carrots and strawberries) and field crops are a distant second and third, only representing 0.5 and 0.4 percent of inundated agricultural land. Non-crop uses such as pastureland and fallow/idle land waiting to be rotated in the next growing season make up the majority of inundated agriculture at 57 percent of the total.

At the county level, Humboldt County is by far the most exposed agriculturally to the SAFRR tsunami scenario: 23 percent of the 22,064 inundated acres in the county is agricultural. San Luis Obispo, Mendocino, and Sonoma Counties also have a relatively high percentage of

inundated agricultural land relative to total inundated land (22, 18, and 15 percent, respectively), however the overall amount of inundated land in these counties is relatively small (1,972 acres, 2,397 acres, and 758 acres respectively). The vast majority of potentially affected cropland lies in Humboldt County (94 percent of total inundated cropland), and 99 percent of the affected cropland in the county contains alfalfa-type crops (such as alfalfa and hay). Monterey County ranks a distant third for exposed cropland at only 59 acres (1 percent of total inundated cropland), but the county has the most non-alfalfa cropland in the inundation zone. Truck-transported crops and field crops are prominent in Monterey County. Table 32 presents the distribution of agricultural land in the inundation zone by county, figure 78 illustrates the dominance of grass- and pasturelands in the inundation zone in Humboldt County, and figure 79 shows the wider variety of croplands in the inundation zone in Monterey County.

Borrowing from the ARkStorm agricultural analysis (Porter and others, 2010) and assuming that production on inundated agricultural lands is lost for one year for annual crops and alfalfa and multiple years for vineyards, rough estimates of crop income losses amount to approximately $3.5 million in 2010 dollars. This calculation includes no revenue losses from non-crop lands. More than 90 percent of the income losses accrue from inundation of alfalfa croplands. Vineyards are potentially the next greatest source of losses if the crop has to be reestablished, a costly process that occurs over multiple years. Truck-transported crops register as the third highest category of crop income losses.

Wave velocities and flow depths were modeled along with inundation for the SAFRR tsunami scenario. The maximum wave velocity on alfalfa croplands is 12 m/sec (27 mph) in Humboldt County and the maximum flow depth (the maximum height of the tsunami wave relative to the topography) is 5 m in Mendocino County. The overall maximum wave velocity on cropland is about 24 m/sec (54 mph) on grain cropland in Los Angeles County, whereas the greatest flow depth on cropland of around 6 m occurs on vineyards in Marin County. For the most part, however, wave velocities average around 2 m/sec (4 mph) and flow depths average around 1 m on cropland.

Table 32. County-level distribution of agricultural land in the SAFRR tsunami scenario inundation zone.

	Total (acres)			Agricultural Breakdown by Crop Class (acres)							
County Name	Inundated	Agricultural	County Total	Alfalfa[1]	Grains[2]	Field Crops[3]	Rice	Truck[5]	Tomatoes	Vineyards	Non-Crop[6]
Del Norte County	7,943	711	787,271	0	0	0	0	0	0	0	711
Humboldt County	22,064	5,151	2,552,467	3,861	0	14	1	1	0	0	1,274
Mendocino County	2,397	441	2,447,320	118	2	0	0	0	0	1	320
Sonoma County	758	116	1,016,190	0	0	0	0	0	0	0	116
Marin County	7,264	627	513,906	0	1	0	0	0	0	4	622
Contra Costa County	1,692	3	325,809	0	0	0	0	0	0	0	3
Alameda County	9,737	48	210,717	8	2	0	0	2	0	0	36
San Francisco County	1,617	59	148,323	0	0	0	0	0	0	0	59
San Mateo County	7,452	338	438,460	0	0	0	0	13	0	0	325
Santa Cruz County	795	67	313,973	0	0	5	0	0	0	0	63
Monterey County	4,741	442	2,366,171	12	0	14	0	24	8	1	383
San Luis Obispo County	1,972	428	2,239,106	32	0	2	0	4	0	1	389
Santa Barbara County	1,081	36	2,368,170	0	0	0	0	0	0	0	36
Ventura County	1,587	68	1,304,811	0	0	0	0	0	0	0	68
Los Angeles County	6,274	331	2,336,717	0	3	0	0	0	0	0	328
Orange County	6,420	368	336,942	0	0	0	0	0	0	0	368
San Diego County	6,828	334	2,553,199	0	5	0	0	0	0	0	329
Study Area Total	90,621	9,570	22,259,552	4,031	13	34	1	45	8	8	5,429

[1]Alfalfa crops include alfalfa, hay, and other pasture grasses.

[2]Grains includes wheat, rye, oats, and triticale.

[3]Field crops include corn, cotton, barley, safflower, beans, peas, and other non-staple grains/legumes.

[4]Orchard crops include fruit and nut trees (such as apple, orange, almond, and walnut).

[5] Truck crops include strawberries, carrots, cantaloupe, pumpkins, and other bush/bulb/vine (except grape)/tuber crops.

[6] Non-crop land includes fallow/idle cropland, shrubland, barren land identified as agricultural land by the National Agricultural Statistics Service (NASS), and

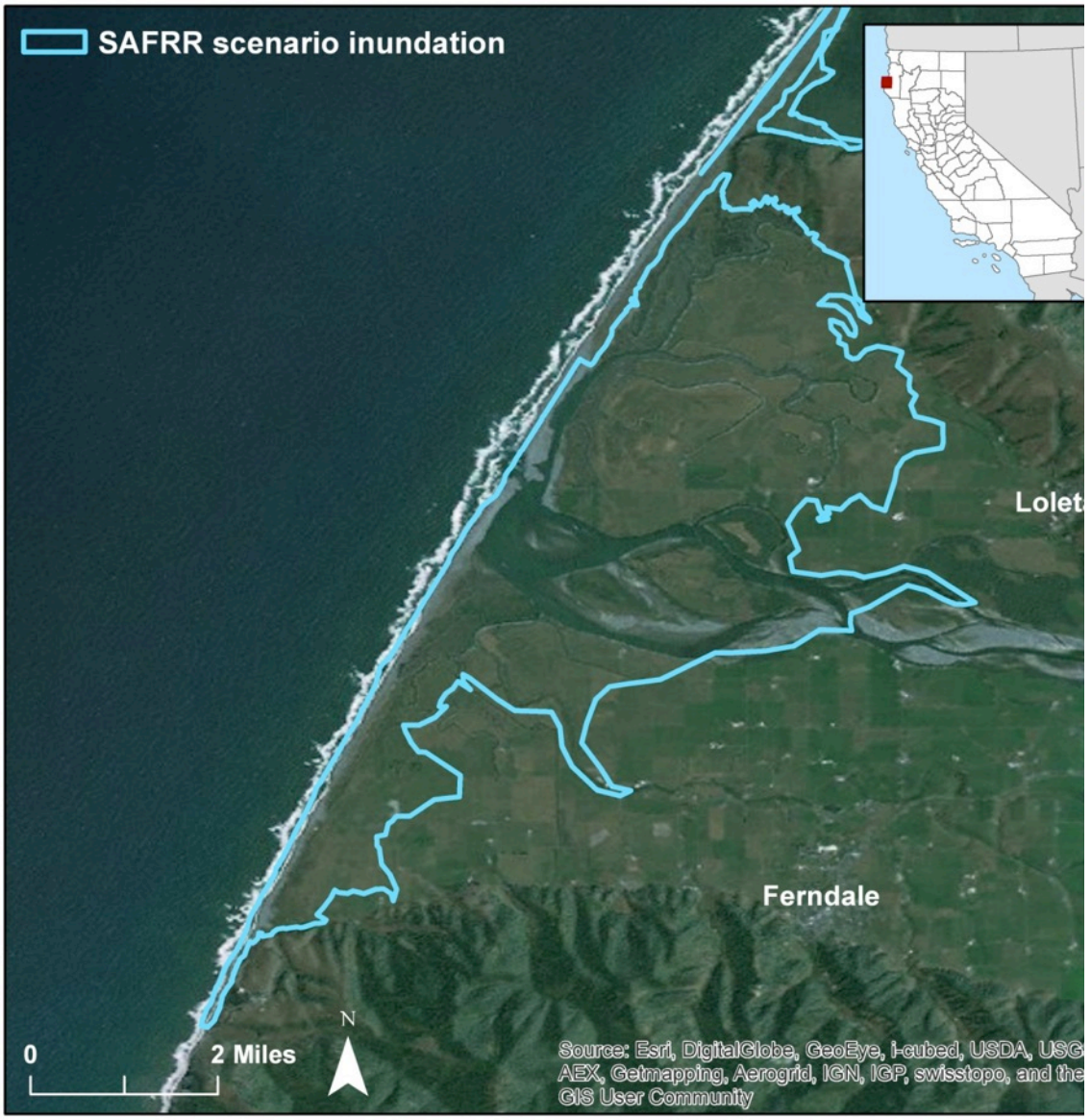

Figure 78. Satellite image showing Eel River Delta, Humboldt County, land inundated in the SAFRR tsunami scenario (blue outline). Much of the inundated area in Humboldt County is pastureland (l used for livestock) and land used for alfalfa-type crops.

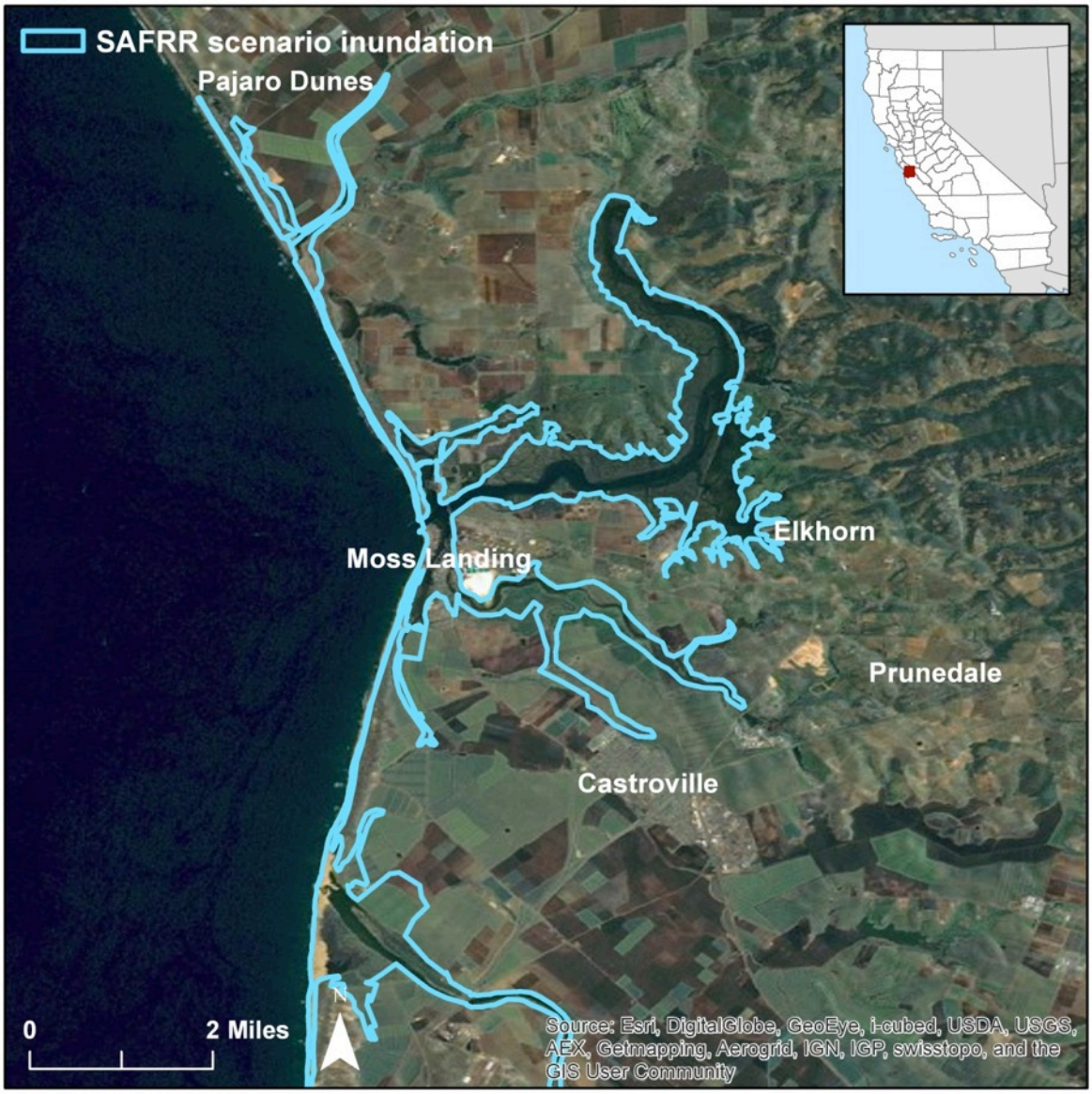

Figure 79. Satellite image showing land inundated in the SAFRR tsunami scenario (blue outline) around Moss Landing in Monterey County. Although far less of Monterey County's inundated land is agricultural relative to other affected counties, more of it is field crops and truck-transported crops.

Soil and Crop Contamination

Although no hazardous waste facilities are located in the tsunami scenario inundation zone (for example, Diablo Canyon Nuclear Power Plant in San Luis Obispo County is on the coast but not found to be in danger of inundation in this scenario), several urban and industrial contamination sources are close enough to the coast to pose a threat to agriculture. The Eel River Delta in Humboldt County, the largest agricultural extent in the inundation zone, is also at risk of contamination due to reworked marine sediments from cities upriver. The agricultural land

around Humboldt Bay north of the Eel River Delta is situated near a potential source of industrial contamination as well as reworked sediment contamination. In northern Monterey County, Moss Landing State Wildlife Area and Elkhorn Slough National Estuarine Sanctuary are at risk of being exposed to potential industrial contamination from the north (Plumlee and others, 2013). Some industrial facilities and processing plants (such as warehouses and chemical plants) can be found beyond but still close to the inundation zone (an example of this is the wastewater treatment facility just south of the airport in Oceano in San Luis Obispo County)—these facilities could pose contamination threats if the tsunami damage impacts operations or if inundation actually extends farther than modeled. For further detail and discussion regarding potential contamination and environmental hazards in general, refer to Plumlee and others (2013).

Livestock Exposure

Agricultural land includes land used to support livestock. Data from the California Department of Food and Agriculture (CDFA) (John Rowden, April 23, 2013, written commun.) suggested that some dairies were potentially located along the coast. DWR data indicated dairy land use in the inundation zone; the presence of two dairies in the inundation zone was confirmed by visually inspecting satellite imagery. The CDFA data also provided dairy herd numbers and sizes by county. Using the average herd size in Humboldt County and a value of $1,300/head (Porter and others, 2010) the exposed livestock value is approximately $250,000.

Summary of Agricultural Building and Content Damages

Agricultural land is not the only asset that would be damaged by the scenario tsunami. Agricultural buildings (defined by NIBS and FEMA [2009] as agricultural facilities and offices, which may include, for example, barns and silos) are also of concern for tsunami damages. Selected census-block-level data falling in the scenario inundation zone were used to calculate building and content losses by HAZUS-MH building occupancy type. Given tsunami inundation and velocity and depth, HAZUS building loss estimates are derived from damage state probabilities for building types, repair and replacement costs per square footage, and building square footage. For a more detailed explanation of how building losses were estimated and what criteria were used to select areas for analysis, please refer to the Building Damage section of this report. Slightly more than $190,000 in building losses and $1.04 million in content losses are estimated to be incurred in the almost 200,000 ft^2 of building area classified in HAZUS-MH as agricultural (code AGR1) in the tsunami inundation zone statewide. A maximum of 117 days is estimated to complete repairs to agricultural infrastructure statewide.

At the county level, San Diego County has the highest estimated agricultural building and content losses in the analyzed census blocks even though the county has little agricultural land in the inundation zone. Around 39,000 ft^2 of San Diego County building area classified as agricultural in the HAZUS-MH building inventory are in analyzed census blocks in the inundation zone (20 percent of the agricultural building stock that is inundated statewide). Building losses in San Diego County are estimated at around $76,000 (40 percent of the total State AGR1 building losses), whereas content losses are estimated to be approximately $210,000 (20 percent of the State total). The estimated building repair time in San Diego County of 117 days is the State maximum. In contrast, Humboldt County, which has the most agricultural land in the tsunami inundation zone, is a distant second for building and content losses ($31,000 [16 percent] and $180,000 [17 percent], respectively), while requiring an estimated maximum of 107 days to complete building repairs. San Mateo County has truck-transported crops in the scenario

inundation zone and agricultural building and content damages comparable to Humboldt County. A complete list of building damages by county is presented in table 33. Overall, crop income losses likely dominate agricultural building and content losses. Furthermore, if field remediation costs for a flood event (Porter and others, 2010) are an indication of tsunami inundation field remediation costs, these could be on a par with the crop income losses.

Table 33. Selected agricultural (HAZUS-MH AGR1) building loss statistics in the SAFRR tsunami inundation zone by county.

[ft^2, square feet; $, 2010 U.S. dollars]

County Name	Building Area (ft^2)	Building Value ($)	Building Loss ($)	Content Loss ($)	Maximum Repair Time (Days)
Del Norte County	591	46,728	260	3,110	0
Humboldt County	38,918	3,121,972	31,659	181,452	104
Mendocino County	8,715	714,759	3,796	43,850	0
Sonoma County	0	0	0	0	0
Marin County	22,342	1,969,329	13,525	135,200	11
Contra Costa County	277	23,733	132	1,580	0
Alameda County	27,881	2,408,096	9,982	129,177	5
San Francisco County	1,318	122,373	681	8,145	0
San Mateo County	20,213	1,816,089	41,028	157,314	26
Santa Cruz County	5,635	503,887	3,525	34,532	0
Monterey County	944	77,568	567	6,071	0
San Luis Obispo County	20,499	1,655,665	7,333	88,021	5
Santa Barbara County	0	0	0	0	0
Ventura County	4,208	338,718	1,539	19,581	0
Los Angeles County	2,574	205,313	1,784	16,895	0
Orange County	2,790	221,864	1,234	14,766	0
San Diego County	39,213	3,101,084	75,877	209,591	117
Study Area Total	196,119	16,327,178	192,923	1,049,284	117

Note: Values are based on percentages of building stocks by census block identified as inundated by the tsunami scenario. Only areas where inundation was modeled were considered for the analysis, and only census blocks in the inundation zone meeting the criteria specified in Building Damage section of this chapter were used.

Data and Research Needs

Although this preliminary analysis covers the entire California coast, it is reliant on data that are processed remotely and only field-verified in some locations. The CDL data are intended to provide detailed information about cropland in the United States, but the data are less accurate than survey data like the DWR data. When classification or validation processes change for remotely-sensed data like CDL, the results can vary significantly from one year to the next: for example, the total cropland acreage in the inundation zone in 2010 is approximately 2,600 acres whereas around 4,100 acres are identified from the 2012 data. This may be a result of variations in training data for data classification because the major land cover class that changed between the two years according to the analysis was grassland. USGS National Land Cover Dataset (NLCD) land cover data are used to classify anything not identified as agricultural, so one possibility is that portions of grass-based classes in 2010 were reclassified as NLCD grassland in 2012. Classifying cropland and pasture is extremely difficult because it tends to get confused with grassland when using automated classification methods (for an example, showing how grassland was the most inconsistently classified class between NLCD and the USGS Gap Analysis Program land-cover dataset, please refer to Wardlow and Egbert, 2003). The training data used from agricultural surveys and ground-truthing changed in 2011, which would have also

had an impact on how data were classified and might partially explain the difference in cropland between 2010 and 2012 CDL data (NASS, 2013). The DWR data, on the surface, seem like a better data source because those data were extensively verified in the field, but the lack of complete coverage and the number of years spent to complete such surveys make the available DWR data less reliable.

The available data for analyzing livestock impacts in the inundation zone was very limited. The resolution of agricultural census data is too coarse for strips of land along the coast. The CDL data only provides one class that is livestock-related and that is pasture grasses which neglects to identify herd sizes and feedlots. We were able to identify two dairies in the inundation zone using multiple sources from CDFA, DWR, and satellite imagery. Spatial livestock data is needed to better assess potential livestock exposure in the SAFRR tsunami scenario.

Finally, although research has been conducted on economic losses in agriculture due to flooding (for example, Porter and others, 2010) this particular analysis did not have the requisite information to establish field rehabilitation costs and times (and related crop income losses) for tsunami inundated agricultural land. Costs for leaching salt out of soil, cleaning up debris, and reestablishing damaged crops after a tsunami are largely unavailable. Some additional proxy data for calculating tsunamigenic agricultural losses could be obtainable from rising climate change research concerned with salinity management on agricultural lands. Although it might be possible to coarsely approximate losses based on observations of the 2011 Tohoku, Japan, earthquake, uncertainty about the type and extent of damage to agriculture in each county remains a barrier.

Opportunities for Agricultural Resilience

This analysis summarizes the types of agricultural damages possible in California from the SAFRR tsunami scenario. The 9,600 acres of inundated agricultural land may make up a very small portion of the approximately 25 million acres of agricultural land in the State. Consequently, the estimated crop, livestock, and building/content losses are not factored into the analysis of economic impacts in California. However, locally those acres support the livelihood of a number of farmers and employees. Salinization, debris deposition, soil scour, and contamination all present long-term issues that would need to be carefully and quickly dealt with in order to minimize productivity losses for affected farms. Given that most of these exposed agricultural acres are found in the poorer northern counties (California Department of Finance, 2009) the distribution of agricultural damages raises concern about financing the recovery of the affected enterprises. Impediments to recovery may further impact farmers in these counties.

The analysis assumes farmers do not mitigate any losses; warning of a far-field tsunami allows time for evacuation or protection of equipment, and livestock. Information specifically geared to dealing with livestock (for example, transportation and shelter) in California is posted (Division of Agriculture and Natural Resources, 1999). Although tsunami preparedness information directed specifically at farmers does not appear to be available, flood preparedness information can provide some basic guidelines. Taking precautions such as having disaster kits with food, water, and medical supplies readily available and tagging and recording livestock information will reduce losses. Web sites like *http://www.prep4agthreats.org and http://awic.nal.usda.gov* provide farmers with information regarding various aspects of disaster preparedness. However, less can be done to prevent field damages, putting the onus back on recovery to prevent further losses.

Fire Following Tsunami

By Charles Scawthorn

This section assesses the potential for fires following the scenario tsunami. We begin with a brief review of fires following historic tsunamis and the related literature to gain insight into ignition and fire spread mechanisms under post-tsunami conditions. The review reveals that tsunamigenic fires are typically fueled by spreading waterborne liquid fuels released from petrochemical facilities damaged by the tsunami. On the basis of this finding, we then examine the scenario affected area for petrochemical facilities, identifying 47 major tank farms and other facilities that might be impacted by the tsunami. This examination reveals two areas, the port of Richmond (in San Francisco Bay) and the port complex of Los Angeles/Long Beach, that contain petrochemical facilities that may be impacted by the tsunami, leading to spreading oil fires borne on the tsunami waters. Given the concentration of oil tank farms in the Ports of Richmond, and especially in the Port of Los Angeles/Port of Long Beach (POLA/POLB) complex, we feel it is possible but not very likely that a spreading fire will result from tsunami damage in at least one of these facilities. If such a fire were to occur, in the context of a tsunami and its attendant other damage, it is likely it would spread over water to other facilities, resulting in a common cause fire and possibly destruction of several of these facilities. Lastly, there are typically several tankers at berths in POLA/POLB—given the perhaps two to four hour warning for the scenario tsunami, it is quite possible that one or more oil tankers may be caught in the harbor and contribute to the size and severity of any spreading fire.

Review of Fires Following Historic Tsunamis and the Related Literature

Tsunamis are sometimes followed by fires. The literature on tsunamigenic fires is sparse—Shuto (1987) was perhaps the first to systematically examine the phenomenon, concluding after a review of historical events and an examination of the physics of oil spread on water that the final burned area due to spreading oil on water correlates with the boundary between the gravity-viscous and surface tension-viscous regimes of empirical formulas. Shuto compares numerical methods such as Goto (1985), which include the effects of inertia, gravity and viscosity empirical formulas that only give the size of the spread of oil, finding the former more informative. Subsequently, (Shuto, 2006) provides an equation for estimation of the final size of a burning oil spill on water:

$$A_B = 324 \cdot V \tag{25}$$

where A_B = Area burnt (square meters, m^2) and V = volume of spilled oil (kiloliters, kL). Shuto's equation is tabulated in table 34 for sizes of typical petroleum product tank sizes (small to very large)—for example, if the contents of a filled very large (50,000 kL) tank are completely released, the burn area is about 16 square kilometers (km^2), or equivalent a square about 4 km on a side.

Table 34. Burnt area given various size tanks, calculated using equation 25.
[H/D, height divided by diameter; m, meters; A_B, area burnt; m^2, square meters]

Volume (kilo liters)	Equivalent tank diameter (m) [H/D = 0.5]	Typical tank size	A_B (m^2)	Dimension of equivalent square (m)
1,000	14	small	320,000	566
3,000	20	medium	960,000	980
10,000	29	large	3,200,000	1,789
50,000	50	very large	16,000,000	4,000

To gain insight into ignition and fire spread mechanisms under post-tsunami conditions, we next review selected tsunamis, and the fires they caused.

1755 Lisbon Earthquake and Tsunami

The earthquake occurred on November 1, 1755, and was centered in the Atlantic Ocean, about 200 km west-southwest of Cape St. Vincent. Lisbon was heavily damaged. A very strong tsunami caused heavy destruction along the coasts of Portugal, southwestern Spain, and western Morocco. About 30 min after the quake, a large wave swamped the area near Bugie Tower on the mouth of the Tagus. The area between Junqueria and Alcantara in the western part of the city was the most heavily damaged by a total of three waves with maximum height estimated at 6 m, each dragging people and debris out to sea and leaving exposed large stretches of the river bottom. A devastating fire following the earthquake raged for five days and destroyed a large part of Lisbon. No information is available on the causes of the fires, but in central Lisbon they destroyed areas that had been damaged by the tsunami, so that some of the fires were likely caused by the tsunami.

1964 Alaska Earthquake and Tsunami

The most complete treatment of fires associated with the March 27, 1964, magnitude 9.2 Alaska earthquake and tsunami is the report by the National Board of Fire Underwriters (National Board of Fire Underwriters and Pacific Fire Rating Bureau, 1964). A number of communities were affected, in which almost all fires occurred in the waterfront areas and were associated with tsunami inundation. Specifically:

- Anchorage was by far the largest affected community but was not affected by tsunami, and “fires were few and of a minor nature.”
- Seward: tsunami waves “swept up into the town for a distance of l to 2 blocks in most areas and as far as 5 blocks in an area of small homes and trailer courts…An oil tanker had been loading gasoline and was in the process of loading diesel oil when the earthquake struck. Hose connections broke, oil and some residual gasoline from hose and pipe lines ignited, possibly from electrical sources or by friction, and a sea wave which quickly followed swept burning liquids along the waterfront and inland for several hundred feet. The fire involved 2 flammable liquid bulk plants and warehouses some 8 blocks apart, 2 dwellings, and the city's standby electric power plant.”
- Valdez: “Fires erupted at 2 waterfront tank farms from gasoline and oil leaking from tanks damaged by the earthquake and waves. The source of ignition at one plant was apparently power wires that dropped on a metal pump house roof. Burning liquids were carried along the waterfront, and the resulting fires involved parts of the 2 tank farms and

destroyed 4 business buildings. Fires were left to burn themselves out as fire-fighters either could not reach the fires due to high water and debris or, when flooding subsided, could get no water from fire hydrants. Fortunately there was no strong wind to spread fires further."

- Whittier: "The earthquake, followed by seismic sea waves, destroyed pier facilities and an oil tank, spread flammable liquids along the waterfront, and a fire that followed destroyed several tanks and waterfront structures in 2 different locations."
- Crescent City, California: "There were 2 fires, both in areas outside the city, during the emergency. One, believed to have occurred when a tank truck was thrown by a wave into an automobile sales and service garage, was in an area without mains or hydrants . . . . The second fire was about 300 feet away in a bulk oil plant. It reportedly occurred by arcing from fallen electrical wires igniting leaking gasoline and oil after undiked tanks were knocked over by a large stump or log. Fifty-five-gallon drums stored nearby exploded and burned, contributing to the spread of the fire. Fire-fighters and apparatus were described as being virtually surrounded by burning liquids floating on the water and these factors together with another threatened sea wave, made fire-fighting extremely difficult. Although this plant was destroyed, a seriously exposed bulk oil plant nearby was saved with only slight damage, water being obtained from a hydrant nearby."

In summary, significant fires only occurred in tsunami inundated areas, even at great distance in Crescent City, and were generally associated with liquid fuel facilities which, once ruptured, resulted in spreading fires on water that caused sympathetic fires at other liquid fuel facilities. Of particular interest is the oil tanker-related fire at Seward, which might have been mitigated with some warning.

1964 Niigata Earthquake and Tsunami

The June 16, 1964, magnitude 7.5 Niigata (Japan) earthquake is well known for two effects—the widespread occurrence of liquefaction and a large fire at the Showa oil refinery that burned for several days. As summarized by a recent report (Cruz and others, 2009):

"The oil refinery fires triggered by the 1964 Niigata earthquake and tsunami in Japan serve as an example of the potentially catastrophic effects of a tsunami when it affects a highly industrialized and urbanized area. During this event, a 4 m tsunami was triggered by the 7.5 magnitude earthquake which initially caused fires in five storage tanks and oil spills in hundreds more at two oil refineries in Niigata (Iwabuchi et al., 2006). The tsunami hit the already earthquake stricken facility resulting in:

- Additional damage to storage tanks and plant processing equipment by collision with tsunami-driven objects and by the hydrodynamic forces of the tsunami (Iwabuchi and others, 2006).
- The spread of leaked oil by the tsunami current into the harbor and on inundated land (Iwabuchi and others, 2006).
- The spread of burning crude oil carried by the flood waters causing the fires to extend to other parts of the plant including the heating furnace, the heat recovery boiler, the reactor of the catalytic conversion process, the hydrolysis treatment equipment, and the bottom of the hydrolysis reactor for the desulphurization process (Akatsuka and Kobayashi, 2008)

- The spread of ignited crude oil carried by the flood waters into residential areas and the destruction of 286 houses by the fire, 2006)."

1993 Hokkaido Nansei-oki Earthquake and Tsunami

The July 12, 1993, Hokkaido Nansei-oki, Japan, magnitude 7.7 earthquake and tsunami caused major damage on Okushiri Island, to the west of Hokkaido (figures 80, 81). As summarized in (Yanev and others, 1993):

> "The only known fire ignitions during the earthquake occurred in Aonae on the southern tip of Okushiri Island. Most of the town is oriented north-south and sited on or almost on the beach, only a few meters above sea level. The rest of the town is located on a central bluff about 20 m high where a lighthouse, the town offices, and the fire station are sited, as shown in (figure 80). The lower part of Aonae is densely built-up with narrow streets and typical building spacing of about 3 m. The buildings are generally one and two story, typically with Japanese wood post and beam construction, although some steel and concrete structures were also present. Exterior coverings are often noncombustible stucco or cement board over wood, with corrugated metal roofing. Large amounts of exposed wood trim, however, compromise the fire protection. Occupancies are generally commercial closer to the wharf area and residential behind (at the base of the bluff), although many buildings are mixed occupancies.

Figure 80. Photograph of fire ignitions in the town of Aonae on the southern tip of Okushiri Island, Japan, following the 1993 Hokkaido Nansei-oki earthquake and tsunami (photograph from Yanev and others, 1993).

The town is protected against fire by a 38-member trained volunteer fire department headed by a full-time professional. The apparatus consists of two engines of typical Japanese size and configuration-each pumper has a 2,000-liter booster tank and carries 10 lengths of 20-m-long 65-mm-diameter hose. The capacity of the pumps is approximately 2,600 liters per minute. Each engine also carries two 4-m lengths of hard suction hose equipped with bamboo strainer baskets. Relative to U.S. equipment, these fire engines are smaller in dimensions and capacity. This smaller size expedites passage through narrower Japanese streets, such as those in Aonae. A third fire engine was present in Aonae at the time of the earthquake; this engine was in poor condition, however, and was parked at the south end of town where it was destroyed by the tsunami.

Fire hydrants are located around the town but are not used because the water mains are insufficiently sized and pressured to provide adequate water for fire control. Small fires are fought from engine booster tanks, while the main fire emergency water is stored in underground cisterns sited throughout the town. Individual cistern capacity is 40,000 liters, which is accessed through a concrete manhole cover. Shortly after the earthquake, the fire department made a circuit of the town looking for fires. Seeing none and concerned about a possible tsunami, they returned to the fire station. Within a few minutes following the earthquake, the tsunami swept through the lower area wrecking many buildings and scattering debris over a wide area. The tsunami also destroyed the main water line at its attachment point near a bridge. At approximately 10:40 P.M. the fire department received a citizen alarm of a fire in the lower area. A brigade of 10 men immediately responded and attempted to reach the fire by driving down the main street but found the street blocked by debris. They then returned to the top of the bluff and took a second route down the southern part of the bluff.

Figure 81. Photograph of tsunami and fire damage on southeast Okushiri Island in the community of Aonae, Japan, following the 1993 Hokkaido Nansei-oki earthquake and tsunami. Orientation is looking northeast. Numerous fires broke out following the tsunami, adding to the property loss and misery. More than 120 people were killed in Japan (Okushiri and Hokkaido Islands) by the tsunami. (Photograph by Dennis Sigrist.)

The probable causes and the effects of the fire are illustrated in (figure 82). The fire began in a structure above the area directly affected by the tsunami, so it likely began as a result of the earthquake. The precise site of initial ignition is unknown, although the approximate location is shown in (figure 82). The initial source of the ignition is also unknown (at this time); however, villagers told of earthquake shaking turning over all of their furniture, so numerous ignition sources were available (e.g., cooking and heating appliances, and fuel storage tanks). At the time of ignition, wind was from the east at about 1.5 meters per second with gusts up to about 5 meters per second.

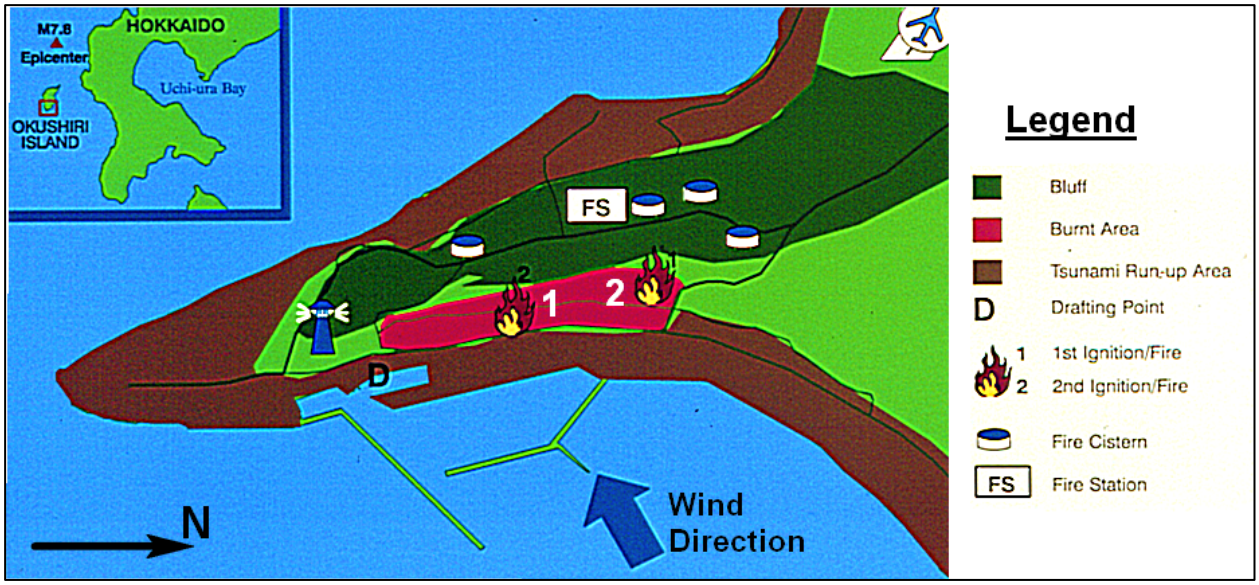

Figure 82. Diagram of tsunami effects in the town of Aonae on the southern tip of Okushiri Island, Japan, following the 1993 Hokkaido Nansei-oki earthquake and tsunami (from Yanev and others, 1993).

Firefighting was from hand lines supplied from the pumpers on top of the bluff, drafting from the cisterns. Fire progress was southward (cross-wind) and relatively slow; suppression efforts significantly impeded fire progress, but the firefighters were unable to stop the fire. Fire progress was aided by flammables normally stored in each home, as well as the fact that almost all houses had outdoor 490-liter elevated kerosene tanks for heating [e.g., propane tanks (20 kg) for cooking]. The kerosene tanks were quite likely a principal factor in the fire spread. All such tanks were found empty after the fire, most having vented safely through the top vent pipe. The venting was most likely caused by radiant heat causing the kerosene to boil. Eight exploded propane tanks and two ruptured kerosene tanks were documented. Reportedly, every time the fire department seemed to be gaining headway, the fire would flare up again, probably due to successive involvement of these tanks. Additional materials fueling the spread of the fire were considerable scrap wood in and among the buildings, and numerous vehicles, which added gasoline, tires, and flammable interiors to the conflagration.

Fire spread was southward at about 35 meters per hour, with firefighting on the downwind edge. Two hours into the fire, a second fire ignited behind the fire line. At about 4 A.M. (6 hours after the earthquake), available water from the cisterns was exhausted. Citizen volunteers assisted in moving the hose over debris from the bluff top to the port, where the two pumpers drafted from the harbor. At this point, the advancing fire front was about 90 m wide. The fire department used equipment to move debris and two buildings, creating a firebreak. Leading four hand lines from the drafting pumpers, the fire was successfully stopped at about 9 A.M., saving several dozen houses that were in the path of the advancing fire."

2004 Indian Ocean Earthquake and Tsunami

The December 26, 2004, Indian Ocean magnitude 9.1 earthquake and tsunami caused major damage and loss of life in Sumatra, Indonesia and in Thailand, Sri Lanka and India. Only

one minor fire is known to have been caused by the earthquake and tsunami (Scawthorn and others, 2006). Of more interest is the damage to the deep-water port at Kreung Raya, Aceh, Indonesia, (oil and dry cargo), which was inundated by the tsunami and lost half its piping and 3 of 9 oil tanks (fig. 83). A ship was offloading at the port at the time of the earthquake—it immediately slipped its moorings, headed out to sea, and was undamaged by the tsunami. No fire was reported at the oil terminal.

Figure 83. Photograph of Krueng Raya, Aceh, Indonesia, deep water port after the 2004 Indian Ocean tsunami. Three tanks (reported to have been empty or near empty) of nine tanks floated about 500 meters. (Photograph from Aceh Province Office.)

2011 Tohoku Earthquake and Tsunami

The March 11, 2011, magnitude 9.0 Tohoku, Japan, earthquake and tsunami caused extensive loss of life and damage in eastern Japan, and spawned 284 fires (Japan Fire and Disaster Management Agency, 2012) including two at major oil refineries. The tsunami was higher than expected and, despite warnings, was responsible for most of the life loss and damage, and about half of all the fires in the event. Analysis of all the significant tsunami-related fires is still underway and a full review is beyond the scope of this report so that only summary findings are provided:

> "Nearly half of the . . . fires that occurred . . . resulted from the tsunami. Typical fires that occurred in the Sanriku coastal region arose from a lot of combustible materials, such as houses and vehicles, which were destroyed and swept away by the tsunami waves toward a

mountain, caught fire from a source of fire (domestic and other various fuels) drifted there, and spread into town areas and forests. On the other hand, in plain areas where the population and industries were concentrated, a small number of fuels, such as household gas cylinders and vehicles scattered about the town, joined together into a mass of combustible materials, which are estimated to have made a great contribution to potential outbreak or spread of fires. In any region, it is estimated that tsunami fires were caused by a combination of various potential factors such as an electric leakage, a short circuit, and sparks from a crash, but most of them are accidental factors and it would remain difficult to investigate the true causes . . . . Finally, one of the similar characteristics in the regions where tsunami fires expanded is that the fires expanded as the local fire-fighting force was severely diminished due to the tsunami. The fires were left uncontrolled for about two days until emergency fire response teams arrived at the sites and started fire extinguishing activities . . . .” (Yamada and others, 2012)

Regarding causes of tsunamigenic fires, (Sekizawa and Sasaki, 2012) concluded:

1. Spillage, ignition, and flow of oil or LPG from upturned or collapsed storage tanks in industrial areas, and subsequent ignition of urban areas and buildings.
2. Spillage from upturned kerosene tanks and LPG cylinders in residential buildings, or spillage from broken distribution pipes.
3. Ignition of buildings by burning buildings or debris carried by the tsunami.
4. Ignition of buildings by burning ships or cars carried by the tsunami.
5. Acceleration of the oxidation of iron by salt contained in seawater, resulting in spontaneous ignition from heat trapped in mounds of debris containing iron.

Two basic mechanisms for tsunamigenic fire spread were identified based on this event—in the first phase, the fires are typically burning liquid fuels borne on the water surface, until the tsunami reaches its maximum runup. At that location, large amounts of building and other flammable debris are deposited by the tsunami, are ignited by the water borne fires, and burn for extended periods (Hokugo and others, 2012).

Another aspect of note is the damage in this event to ocean-going vessels. The tsunami did not arrive until 20 to 30 minutes following the shaking, so that vessels in port had some warning and might have been expected to leave shallow waters and ride out the tsunami. However, a number of large vessels totaling about 500,000 dead-weight ton (DWT) were damage in ports, such as the 91,000 DWT MV *Shiramizu*, which was grounded in the port of Shinchi (fig. 84).

Figure 84. Photograph of MV *Shiramizu* aground in Shinchi following the 2011 Tohoku, Japan, earthquake and tsunami (photograph by Charles Scawthorn).

Summary

On the basis of the foregoing, it may be observed:

1. Fires often, but not always, occur within the inundation zone of a tsunami. Notable tsunamis that are not recorded as causing numerous or large fires include the 1960 and 2010 Chilean events. As a rule of thumb, it is conservative to assume that tsunamis will cause fires.
2. Tsunamigenic fires are typically fueled by spreading water borne liquid fuels released from port or petrochemical facility piping or tanks damaged or floated by the tsunami. Sources of ignition are numerous and varied—investigating them in detail is probably less fruitful than conceding that, in the presence of such water borne fuels, that ignitions are very likely given the large extent of liquid fuels mingling with debris jostling and likely to generate sparks.
3. Large ships such as oil tankers, even with tsunami warning, may not be able to evacuate a port. Strong currents and congestion of vessels all attempting to evacuate simultaneously are challenges that should be investigated.

Fire in the SAFRR Tsunami Scenario

This section assesses the study area based on the findings from the previous section, focusing on coastal petrochemical facilities storing significant amounts of flammable product.

Method

To identify these facilities, an Environmental Protection Agency (EPA) database (*ftp://ftp.epa.gov/EmisInventory/emiss_shp2003/us/*, accessed March 1, 2013) was employed that identified 111 such facilities in California (fig. 85). The database dates from 2003 and therefore may be expected to have some errors. Facilities significantly inland were eliminated from this initial list, resulting in 46 facilities requiring review (fig. 86 and table 35). Each of these facilities, almost all of which are tank farms, are reviewed next.

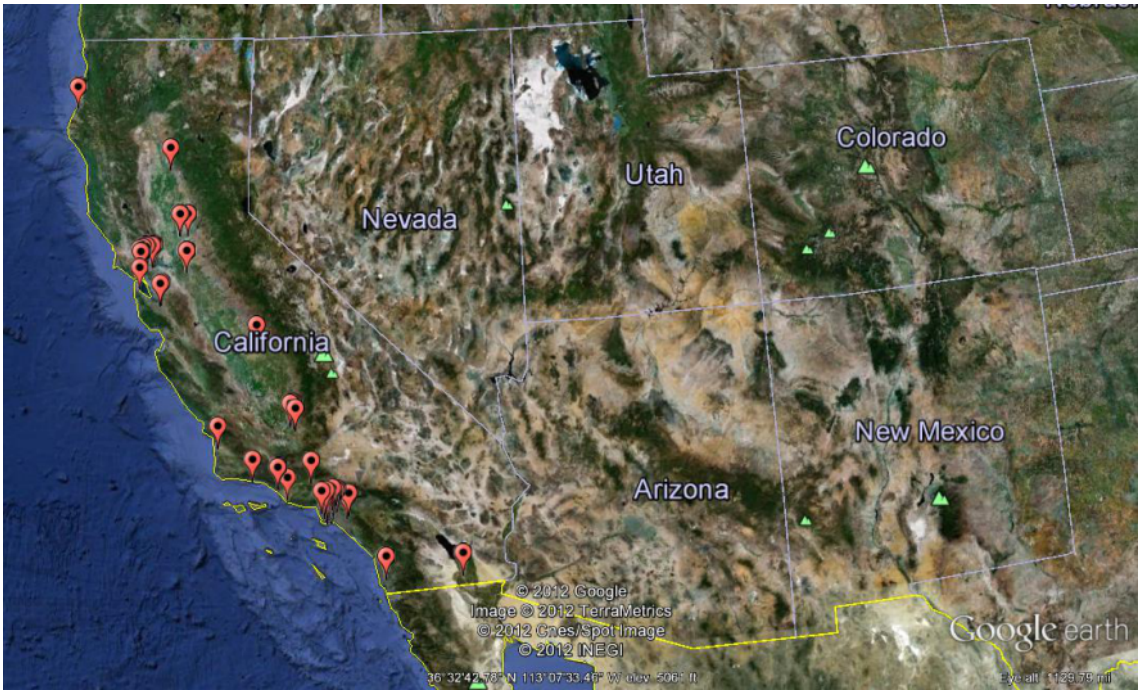

Figure 85. Map showing 111 California coastal petroleum facilities (data from Environmental Protection Agency database: *ftp://ftp.epa.gov/EmisInventory/emiss_shp2003/us/* accessed March 1, 2013) (base image from Google Earth).

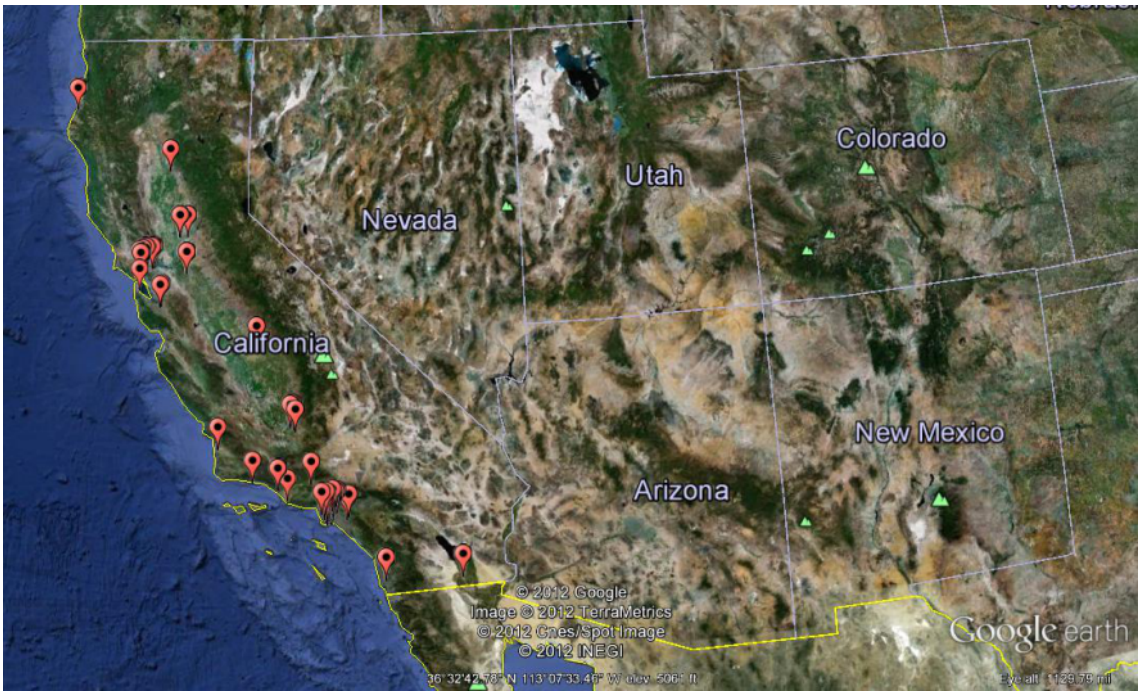

Figure 86. Map showing 46 California petroleum facilities sited in proximity to possible tsunami effects (data from Environmental Protection Agency database: *ftp://ftp.epa.gov/EmisInventory/emiss_shp2003/us/*, accessed March 1, 2013) (base image from Google Earth).

The methodology employed is a close visual examination of aerial imagery (that is, Google Earth imagery) of the facilities vis-à-vis the anticipated tsunami inundation depth, to determine whether the tanks are likely to be subjected to flooding. If flooded, floating and possible rupture of connections is considered possible, leading to release of flammable product. Almost all tanks examined are protected by a secondary containment berm or wall, as required by regulations, and the presence and approximate height of this protection (as could be judged from the Google Earth imagery) was considered. Regarding the aforementioned regulations, 40CFR112 requires " . . . secondary means of containment for the entire capacity of the largest *single container* and sufficient freeboard to contain precipitation . . . ." [emphasis added]. Data on the largest tank in each facility is also listed in table 35, and this is used to calculate a burnt area based on Shuto's equation (that is, equation 25).

Table 35. Summary findings for California petroleum facilities for fire following tsunami in the SAFRR tsunami scenario.

[Function (Fct): T=Tank Farm, R=Refinery. A_B, area burnt; m, meters; km^2, square kilometers]

No.	Name	City	Fct.	Latitude	Longitude	No. tanks	Largest tank diameter (m)	Largest tank height (m)	Tsunami height (m)	Protected?	Within flood zone	Flooded?	A_B (km^2)
1	Unocal	Eureka	T	40.796	-124.183	no tanks found							
2	Chevron	Eureka	T	40.778	-124.193	10	30	10	1.5	somewhat	yes	possible	2.3
3	Oil Term Co.	Eureka	T	40.770	-124.194	no tanks found							
4	Paktank	Richmond	T	37.958	-122.421	no tanks found							
5	Richmond	Richmond	R	37.923	-122.368	outside tsunami zone					no	marine terminal	
6	Texaco	Richmond	T	37.923	-122.368	many	40	20	2	yes	partial	possible	8.0
7	Unitank	Richmond	T	37.920	-122.369	many	13	13	3+	somewhat	partial	possible	0.6
8	Time Oil	Richmond	T	37.920	-122.363	many	20	20	3+	somewhat	partial	possible	2.0
9	Unocal	Richmond	T	37.918	-122.365	many	26	20	3+	somewhat	partial	possible	3.4
10	Petromark	Richmond	T	37.912	-122.386	no tanks found							
11	Arco	Richmond	T	37.913	-122.366	many	25	20	3+	somewhat	partial	possible	3.1
12	Shell	South San Francisco	T	37.640	-122.398	3	30	20	1	yes	no	unlikely	
13	Shell	San Jose	T	37.395	-121.876	no tanks found							
14	Southern Pacific P/L	Milpitas	T	37.374	-121.910	no tanks found							
15	Arco	Goleta	T	34.423	-119.832	no tanks found (Goleta Sanitary District, but next to airport)							
16	Shell	Ventura	T	34.308	-119.286	no tanks found							
17	USA-Oil	Ventura	T	34.298	-119.301	no tanks found							
18	Oxnard	Oxnard	R	34.125	-119.100	no tanks found							
19	El Segundo	El Segundo	R	33.903	-118.395	many				yes	no	no	
20	Wilmington	Wilmington	R	33.785	-118.263	outside tsunami zone							
21	Texaco	Wilmington	T	33.788	-118.239	outside tsunami zone							
22	Wilmington	Wilmington	T	33.789	-118.227	outside tsunami zone							

No.	Name	City	Fct.	Latitude	Longitude	No. tanks	Largest tank diameter (m)	Largest tank height (m)	Tsunami height (m)	Protected?	Within flood zone	Flooded?	A_B (km^2)
24	Wilmington	Wilmington	R	33.772	-118.288	outside tsunami zone							
25	Bray Oil Co.	Torrance	T	33.765	-118.294	outside tsunami zone							
26	Texaco	Long Beach	T	33.776	-118.221	9	45	10	1	yes	yes	possible	5.1
27	Petro-Diamond	Long Beach	T	33.776	-118.219	no tanks found							
28	Arco	Long Beach	T	33.777	-118.213	many	45	10	1~3m	yes	partial	possible	5.1
29	Time Oil	San Pedro	T	33.761	-118.292	outside tsunami zone							
30	Wilmington	Wilmington	T	33.765	-118.258	many	31	10	3	yes	partial	possible	2.4
31	Golden Eagle	Wilmington	T	33.761	-118.265	similar to no. 37 Shell						possible	5.1
32	Chevron Chem.	Wilmington	T	33.759	-118.266	similar to no. 37 Shell						possible	5.1
33	Union Pacific	Wilmington	T	33.759	-118.266	similar to no. 37 Shell						possible	5.1
34	Unocal	Wilmington	T	33.756	-118.271	many	45	17	2	yes	partial	unlikely	
35	Golden West	San Pedro	T	33.758	-118.258	no tanks found							
36	Gatx	Wilmington	T	33.756	-118.265	no tanks found							
37	Shell	Wilmington	T	33.755	-118.266	many	45	10	2+	yes	yes	possible	5.1
38	Chevron	Wilmington	T	33.752	-118.275	no tanks found							
39	Indies Terminals	Terminal Island	T	33.754	-118.260	no tanks found							
40	Refiners Marketing Co.	Terminal Island	T	33.747	-118.265	no tanks found							
41	Mobil	San Pedro	T	33.745	-118.264	7				yes	no	no	
42	C. Brewer	Long Beach	T	33.753	-118.205	no tanks found							
43	Exxon	Long Beach	T	33.751	-118.207	6	45	12	3	yes	yes	possible	6.1
44	Mobil	Terminal Island	T	33.736	-118.272	19	40	13	2	yes	no	unlikely	
45	C. Brewer	Long Beach	T	33.746	-118.189	1				yes	no	no	
46	Unocal	San Pedro	T	33.726	-118.282	many	24	17	2	yes	partial	possible	2.5
47	Oakland Airport	Oakland				3	24	24	1	yes	yes	unlikely	
48	Kinder Morgan	Port of Los Angeles	T			18	45	16	3	yes	yes	possible	8.1
49	UNK Port of Long Beach	Port of Long Beach	T			6	16	13	1	yes	yes	possible	0.8
50	Freeman, Chaffee, White Grissom Islands	Port of Long Beach	T	33.741	-118.154	many	13	8	1	no	yes	possible	0.3

Not examined are facilities not in the database, except a few identified during this investigation (for example, a few tanks at Oakland airport). Power plants, military installations and small fueling docks at local marinas are not examined. Small fueling docks exist at almost all marinas (for example, fig. 87), and undoubtedly some of these will rupture and release modest amounts of flammable liquids, leading to localized fires.

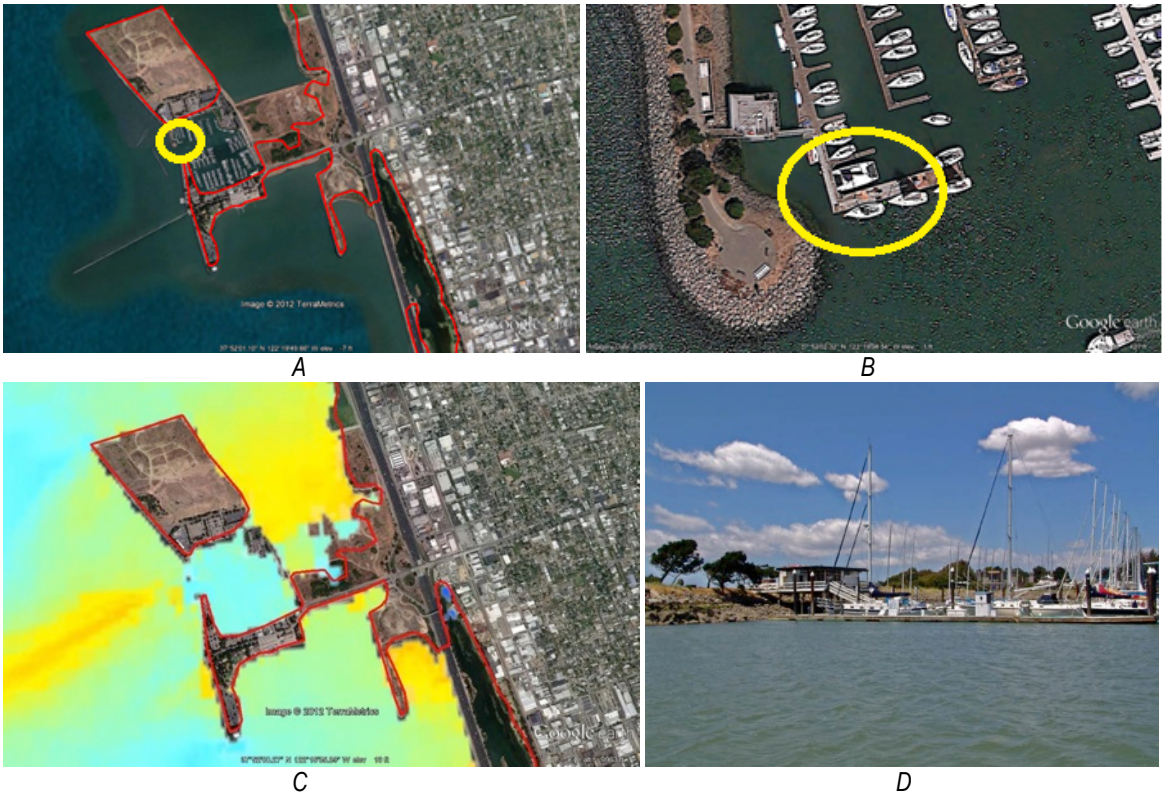

Figure 87. Images of example of small marina fueling dock not considered in this study of fire in the SAFRR tsunami scenario. Example is Berkeley Marina, California: *A*, marina and inundation boundaries; *B*, closeup of fueling dock; *C*, flood depths; and *D*, view of fueling dock from water level. (*A*–*C* base images from Google Earth; photograph by Charles Scawthorn.)

This methodology is necessarily limited in accuracy, and it is possible that large facilities have been overlooked, tanks misidentified, and other errors introduced. Nevertheless, the method are overall reasonable and the findings probably overall robust.

Humboldt Bay

Three facilities are listed in the EPA database for Humboldt Bay, as shown figures 88 and 89 (the latter showing flood depths, determined by others in this report). Examination of aerial imagery indicated in fact only one facility in existence at the time of the Google Earth imagery (fig. 90), the tanks of which are protected by a wall that would appear to be overtopped given the 2 to 3 m inundation expected at this site. The facility is therefore considered "possible" for flooding. Given the size of the largest tank, the resulting burnt area would be over 2 km^2.

Figure 88. Satellite image of Humboldt Bay, California, showing the three oil facilities in the area (base image from Google Earth).

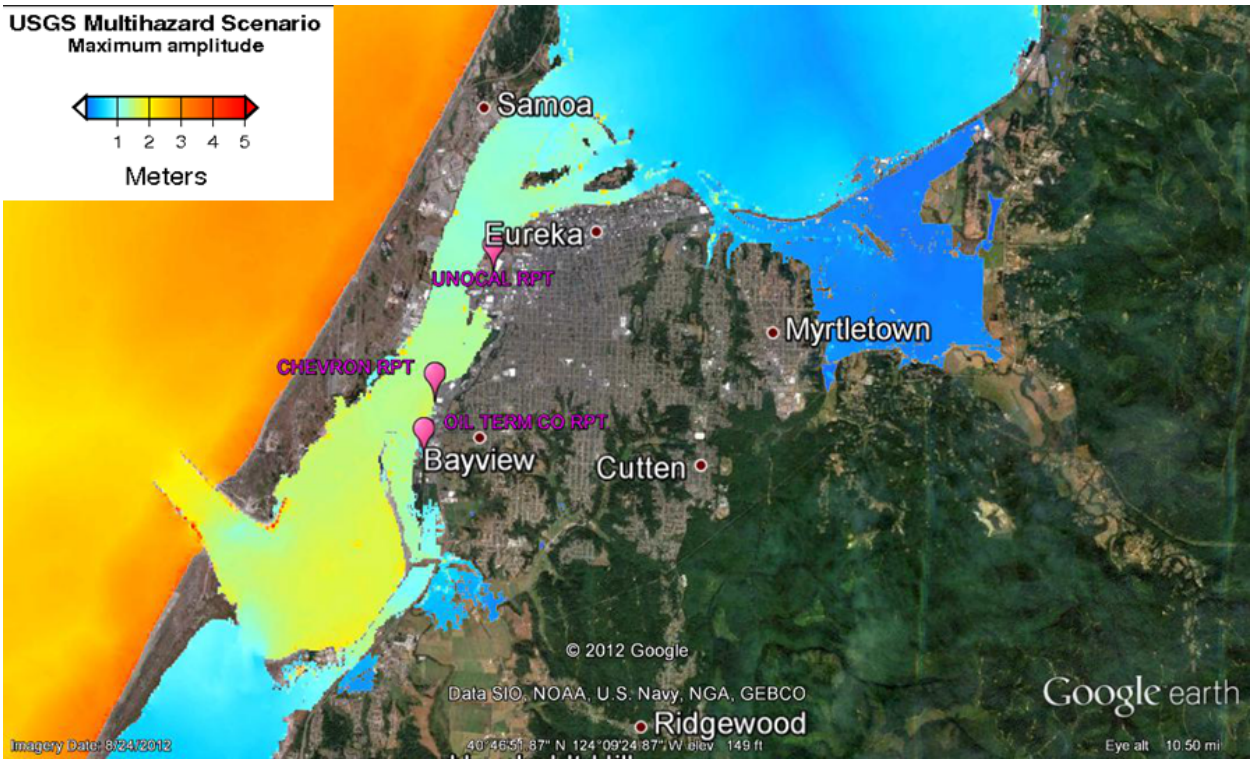

Figure 89. Satellite image of Humboldt Bay, California, showing the three oil facilities in the area and annotated with tsunami flood depths for the SAFRR tsunami scenario. The approximate depth of inundation as determined by others in this report is shown in the explanation at upper left (base image from Google Earth).

Figure 90. Satellite image of a Humboldt Bay, California, oil facility. In this image the approximate extent of inundation as determined by others in this report is shown by the red line (base image from Google Earth).

San Francisco, Los Angeles, and Other Regions

The same methodology was employed for remaining facilities, as listed in table 35. The interested reader can find images for these remaining facilities in figures 19–62 of Scawthorn (2013), at *http://www.sparisk.com/publications.html* (accessed March 1, 2013). In general, Scawthorn (2013) provides two figures for most facilities—the first figure showing the facility and inland extent of flooding (denoted by the red line) and the second figure showing the same view but with shading indicating the depth of inundation. Table 35 summarizes the findings for each facility.

Survey and Findings

As shown in table 35, 17 facilities are deemed as "possible" for release of flammable liquids, and a spreading fire. Five of the 17 facilities are in Port of Richmond, and in close proximity, and 11 are within the interconnected Ports of Los Angeles and Long Beach (POLA/POLB).

To better understand the potential vulnerability of marine oil terminals to tsunami, a survey of several tank farms and oil terminals was conducted in the POLA/POLB on January 22, 2013 (see figs. 91 through 93). In summary, observations and findings of the survey were:

- A typical POLA/POLB marine oil terminal cross-section is shown in figure 94. Product flow is from the ship via flexible hosing to an on-wharf manifold, then via steel piping to an on-shore manifold. The steel piping may run on or under the wharf. Onshore, the

product piping may (not always) be partially buried, and will often have a second onshore manifold prior to the piping entering the tank secondary containment. Interior to the secondary containment, each tank will typically have a valve just prior to the tank shell. Fire lines and monitors run outside the secondary containment, often supported on the exterior wall of the secondary containment, and are therefore vulnerable to damage if tsunami run-up reaches the height of the fire line.

- Tanks are typically thin-walled steel tanks. In our observation, some tanks were bolted to their foundation but more often (especially larger tanks) were not fixed to their foundation, and thus susceptible to flotation.
- Tanks invariably will have secondary containment—typically in POLA/POLB this is a concrete wall, typically cantilevered and sometimes buttressed. Some walls were cast-in-place reinforced concrete, whereas others were built of concrete masonry units. The wall height is calculated so as to contain the contents of the largest single tank, plus rainwater, and varied in our observations from about 6 to 20 ft.
- In California, minimum engineering, inspection and maintenance criteria for marine oil terminals (MOTs) are established by Chapter 31F, Marine Oil Terminals, of the California Building Code. Chapter 31F establishes environment loading, including seismic, wind and tsunami, and specifies tsunami run-up at POLA/POLB as 8 ft (and 7.5~7.9 ft at Port of Richmond).
- Secondary containment walls are presumably designed so as to withstand lateral fluid pressure from the tank side. Chapter 31F does not specifically address secondary containment but, because tsunami run-up is specified, lateral fluid pressure appropriate to the specified tsunami run-up height should be a design condition for the secondary containment walls. Discussions with operators and POLA engineering staff could not confirm that this design condition was actually employed.
- Several of the oil terminal wharves in POLA are of flammable older wood construction, and could be structurally damaged in a significant tsunami. Other fuel-related wharves in POLA/POLB are of concrete construction, less flammable but still susceptible to significant damage when subjected to a spreading-oil-on-water fire.
- Displacements of wharf structures would likely break on-wharf product piping that in some cases run beneath the wharf decking (and therefore is more susceptible to tsunami damage). Most on-wharf and wharf-shore piping does not appear designed for tsunami currents (for example, lacked lateral support).
- Industry practice appears to be to generally valve off wharf piping from onshore storage tanks when not transferring product, so that relatively little product (for example, tens to hundreds of barrels) would be spilled given wharf piping breakage under most circumstances. The only exception to this would be during product transfer (that is, offloading a ship) but, given even a few minutes warning, valves (which are manually operated) can be readily closed.

Figure 91. Photographs of Port of Los Angeles Berth 163 wood wharf and manifold and piping to storage tanks (photographs by Charles Scawthorn).

A (b)

C

Figure 92. Photographs of Port of Los Angeles Berth 163: *A*, roadway leading between secondary containment leading to Berth 163, with fire lines external to containment (susceptible to tsunami damage); *B*, interior of secondary containment showing buttresses; and *C*, electrical equipment between wharf and secondary containment (photographs by Charles Scawthorn).

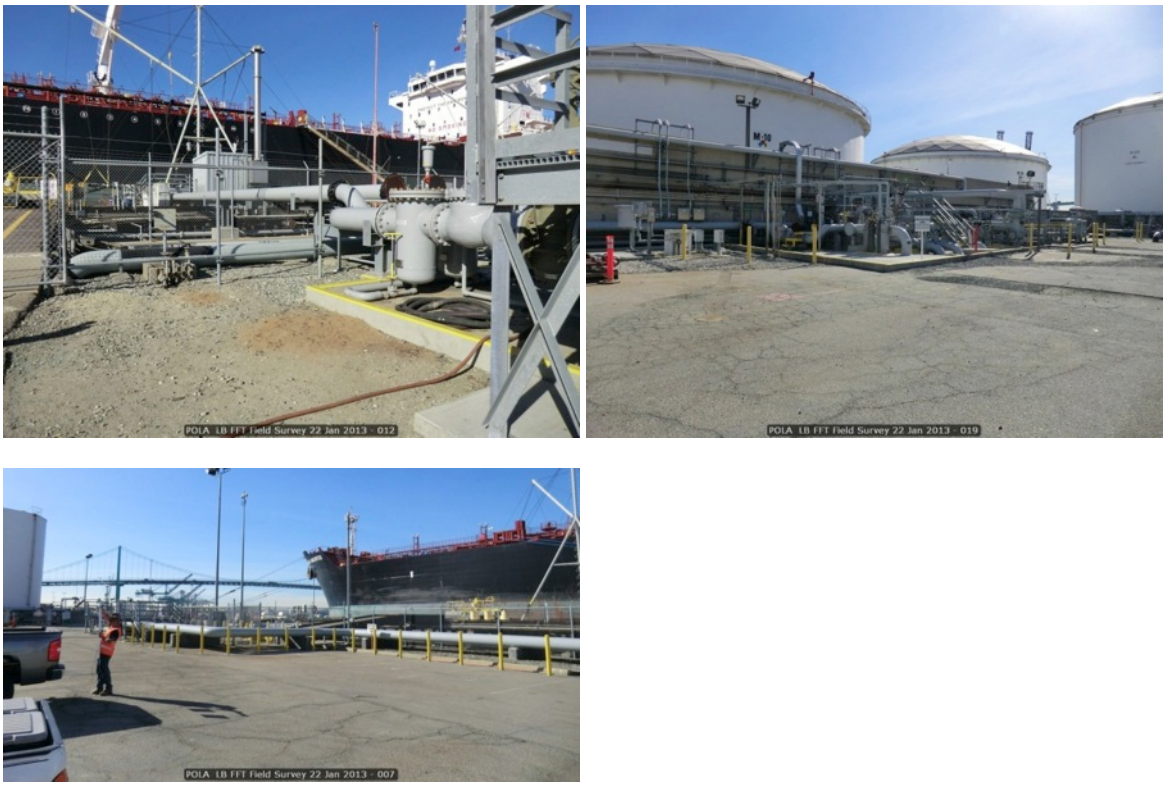

Figure 93. Photographs of Port of Los Angeles Berth 167-9 manifolding, piping, and secondary containment. Long runs of pipe not laterally restrained. (Photographs by Charles Scawthorn.)

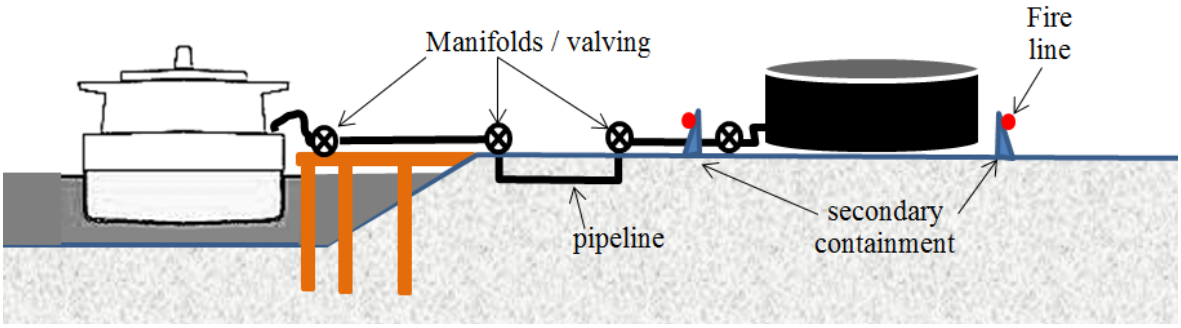

Figure 94. Cross-section diagram of a typical marine oil terminal (image from Charles Scawthorn).

Overall, given the tsunami heights predicated for the SAFRR tsunami scenario, on-wharf and onshore product piping exterior to the secondary containment would appear to be somewhat vulnerable to tsunami forces, such that the possibility of pipe breakage would appear likely in at least a few locations. A limited amount of flammable product would be released, and ignition sources are present (for example, electrical equipment). Combined with large lengths of flammable wood piers at several marine oil terminals, even a limited amount of flammable

product release could lead to a major pier fire. However, the great majority of flammable product is held in tanks behind secondary containment. Structural integrity of the secondary containment under tsunami loading is unclear. On the basis of limited observation at POLA/POLB, we did not observe a containment or tank that appeared very likely to fail under the SAFRR tsunami scenario. However, we recommend that design for secondary containment integrity under tsunami loading should be verified, or the integrity confirmed by engineering analysis.

Given the concentration of oil tank farms in the Ports of Richmond, and especially in the POLA/POLB complex, we feel it is possible but not very likely that a spreading fire will result from tsunami damage in at least one of these facilities. If such a fire were to occur, in the context of a tsunami and its attendant other damage, it is likely it would spread over water to other facilities, resulting in a common cause fire and possibly destruction of several of these facilities.

As contrasted with Richmond, the POLA/POLB scenario is mitigated by the presence in the port of several Los Angeles City Fire Department fireboats (including one of the world's largest and most modern fireboats, fig. 95). However, strong currents from the tsunami would greatly complicate fighting a spreading fire.

Figure 95. Photograph of Los Angeles Fire department fireboat 2, the *Warner L. Lawrence*. One of the largest and most technologically advanced fireboats in the world, it has the capability to pump as much as 38,000 U.S. gallons per minute (2.397 cubic meters per second) as far as 400 feet (121.9 meters). (Photograph courtesy Los Angeles Fire Department.)

Lastly, as was noted above, half a million tons of sea-going vessels were destroyed in the 2011 Tohoku tsunami (including 17,000 fishing vessels, as well as two nuclear submarines damaged). Others in this project have emphasized the strong currents that will be generated in ports as a result of the SAFRR scenario tsunami, which will make ship handling unmanageable. Figure 96 is a random "snapshot" of the traffic in POLA/POLB, showing 32 major vessels inside the breakwater (major 50,000 or more DWT—the largest vessel in the snapshot is 160,000 DWT), as well as many other vessels (and perhaps a thousand untracked pleasure craft). Given the perhaps 2 to 4 hour warning for the scenario tsunami, and possible difficulty in having sufficient pilots for all the large vessels, we feel that it is quite possible that one or more oil

tankers may be caught in the harbor, and subjected to strong currents such as to break the ship loose (if moored) and send it careening about the channels and harbor. This situation could contribute to the size and severity of any spreading fire.

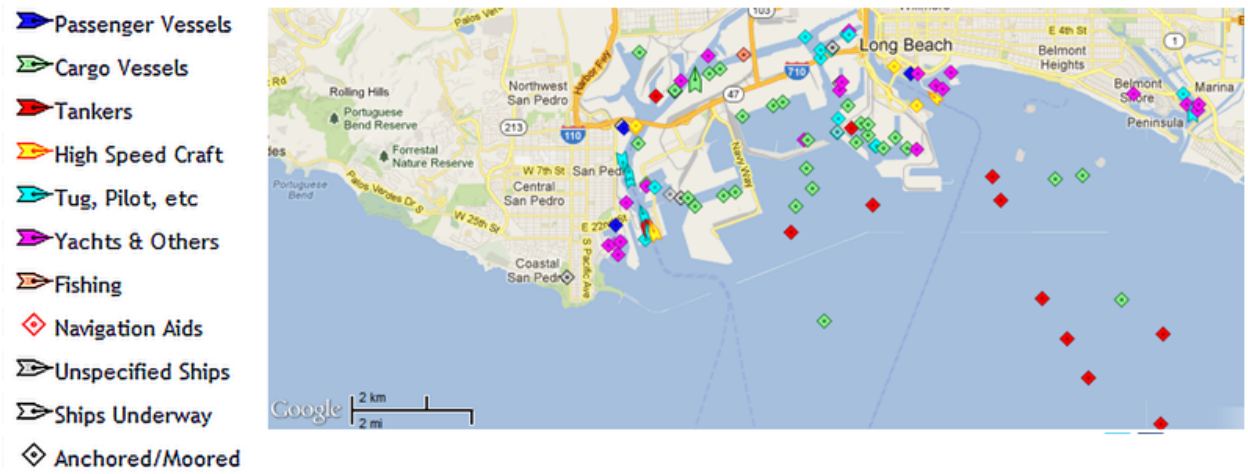

Figure 96. Map image showing a random "snapshot" of Ports of Los Angeles and Long Beach ship traffic—six tankers and 26 cargo vessels are inside the breakwater (base image from Google).

Fire Study Limitations and Acknowledgments

Regarding the methodology employed in this study, it is possible that large facilities have been overlooked, tanks misidentified, and other errors committed. It is emphasized that these findings are based only on observation and qualitative methods and that greater accuracy would be achieved with more detailed, quantitative methods. Lastly, the assistance of personnel at several POLA/POLB berths and of POLA/POLB staff is gratefully acknowledged.

Acknowledgments

The authors thank chapter reviewers: Frank Blackburn (San Francisco Fire Department, Ret.), Michael Burke (Port of Seattle), Mehmet Celebi (USGS), Laurene Eisele (Port of San Francisco), Martin Eskijian (University of Southern California), Stuart Fricke (Port of Los Angeles), Bill Graf (Imagecat, Inc.), John Headland (Moffatt and Nichol), Uday Prasad (Port of San Francisco), Steve Ng (Caltrans), Joe Roger (Port of San Francisco), Bethann Rooney (Port Authority of New York and New Jersey), Tom Shantz (Caltrans), Aaron Sherburne (Port Authority of New York and New Jersey), Bruce Smith (San Diego Association of Governments), Doug Thiessen (Port of Long Beach), Mara Tongue (USGS), Ted Trenkwalder (Ben C. Gerwick, Inc.), Zachary Whitman (University of Canterbury, Christchurch, New Zealand), and Mark Yashinsky (Caltrans). SAFRR coordinators also provided some peer review of the damages chapter: Lucy Jones (USGS), Kevin Miller (California Governor's Office of Emergency Services, Cal OES), Carl Mortensen (USGS), Geoff Plumlee (USGS), and Stephanie Ross (USGS).

Thanks also to panelists, correspondents, and other participants: Robel Afewerki (Port of Los Angeles Engineering), Rich Baratta (Port of Long Beach), Richard Berman (Port of San Francisco), Roy Bibbens (Caltrans), Chris Brown (Port of Los Angeles), Sonia Brown (Cal OES), Damon Burgett (Port of San Francisco), Ed Byrne (Port of San Francisco), Eric Caris

(Port of Los Angeles Business Development), Tom Carter (Port of San Francisco), Mo Chang (U.S. Army Corps of Engineers), Mike Christensen (Port of Los Angeles), Bent Christiansen (Port of Los Angeles), Ken Chu (Port of San Francisco), Tim Clark (Port of Los Angeles), Brandon Cowan (Port of San Francisco), George Cummings (Los Angeles Port Police), John Davey (Port of San Francisco), Sherban Duncan (Port of San Francisco), Lauren Eisele (Port of San Francisco), Eric Endersby (Morro Bay Harbor Director), Andrienne Fedrick (Port of Los Angeles), Desiree Fox (Caltrans), Stuart Fricke (Port of Los Angeles), Keith Garcia (Los Angeles Port Police), Rene Garcia (Caltrans), Tony Gioiello (Port of Los Angeles), Aaron Golbus (Port of San Francisco), Mike Graychik (Los Angeles Port Police), Ed Green (Port of Long Beach), Anne Hardinger (City of Berkeley), Anita Hayden (Los Angeles Port Police), Jack Hedge (Port of Los Angeles Real Estate), Suzie Howser (Port of Humboldt Bay and Woodley Island Marina), Radiah Jones (U.S. Coast Guard), Jill Lemon (U.S. Coast Guard), Dan Kane (Port of Long Beach), Kevin Keady (Caltrans), Michael Keenan (Port of Los Angeles Planning), Caryn Margita (U.S. Coast Guard), Joe Maldonado (Port of Los Angeles CBM Division), Kathy Merkovsky (Port of Los Angeles), Linda McIntyre (Moss Landing Harbor District), Steve Ng (Caltrans), Leon Nixon III (Los Angeles Port Police), Diane Oshima (Port of San Francisco), Tom Ostrom (Caltrans), Karl Pan (Port of Los Angeles), Scott Phemister (Port of Long Beach), Abbas Pourheidari (Caltrans), Uday Prasad (Port of San Francisco), Steven Reel (Port of San Francisco), Jeffrey Robinson (Area G Disaster Management), Joe Roger (Port of San Francisco), Petty Santos (Los Angeles Port Police), Shaun Shahrestani (Port of Los Angeles), Daryoush Tavatli (Caltrans), Karen Taylor (Port of San Francisco), Doug Thiessen (Port of Long Beach), Curtis Thompson (Los Angeles Port Police), Martin Villa (U.S. Coast Guard), Ronnie Villanueva (City of Los Angeles), David Walsh (Port of Los Angeles), and Jennifer Williams (U.S. Coast Guard).

References Cited

Akatsuka, H., and Kobayashi, H., 2008, Fire of petroleum tank, etc. by Niigata earthquake: Japan Science and Technology Agency, Failure Knowledge Database, accessed December 18, 2012, at *http://www.sozogaku.com/fkd/en/cfen/CB1012035.html.*

Akiyama, M., Frangopol, D.M., Arai, M., and Koshimura, S., 2012, Probabilistic assessment of structural performance of bridges under tsunami hazard: Proceedings of the American Society of Civil Engineers Structures Congress, March 29–31, 2012, Chicago, p. 1919–1928.

American Railway Engineering and Maintenance-of-Way Association (AREMA), 2012, Chapter 9 seismic design for railway structures: Manual for Railway Engineering, vol. 2—Structures: Lanham, Md., American Railway Engineering and Maintenance-of-Way Association, p. 9–1–7.

American Society of Civil Engineers [ASCE], Coasts, Oceans, Ports, and Rivers Institute [COPRI], 2005, Report of damage assessment from December 26, 2004, Indian Ocean tsunami: American Society of Civil Engineers, Coasts, Oceans, Ports, and Rivers Institute

American Society of Civil Engineers [ASCE], Coasts, Oceans, Ports, and Rivers Institute [COPRI], 2010, Earthquake and tsunami damage of Chile earthquake of February 27, 2010: American Society of Civil Engineers, Coasts, Oceans, Ports, and Rivers Institute

American Society of Civil Engineers [ASCE], Technical Council on Lifeline Earthquake Engineering [TCLEE], 2011, Report of the 11 March 2011 M_w 9.0 Tohoku, Japan earthquake and tsunami: American Society of Civil Engineers, Technical Council on Lifeline Earthquake Engineering

Applied Technology Council [ATC], 2012, ATC-58—Guidelines for seismic performance assessment of buildings, 100% Draft: Redwood City, Calif., Applied Technology Council

Asian Disaster Preparedness Center, 2005, The economic impact of the 26 December 2005 earthquake and Indian Ocean tsunami in Thailand: Bangkok, Thailand: Asian Disaster Preparedness Center, accessed May 30, 2013, at *http://www.adpc.net/maininforesource/dms/thailand_assessmentreport.pdf*.

Berkman, S.C., and Symons, J.M., 1964, The tsunami of May 22, 1960 as recorded at tide stations: U.S. Department of Commerce, Coast, and Geodetic Survey.

Byers, W.G., 2011, Railroad damage from two hurricanes: Natural Hazards Review, v. 12, no. 1, p. 6–8.

California Department of Finance, 2009, 2008 California statistical abstract: Sacramento, California, Department of Finance, accessed August 27, 2013, at *http://www.dof.ca.gov/HTML/FS_DATA/STAT-ABS/documents/CaliforniaStatisticalAbstract2008.pdf.*

California Department of Water Resources [DWR], 2013, California land and water use: California Department of Water Resources Web site, accessed May 22, 2013, at *http://www.water.ca.gov/landwateruse/lusrvymain.cfm*.

California Geological Survey [CGS], 2012, California Geological Survey—Anniversary of the March 11, 2011 Tohoku-oki earthquake and tsunami: California Department of Conservation Web site, accessed May 20, 2013, at *http://www.conservation.ca.gov/cgs/geologic_hazards/Tsunami/Inundation_Maps/Pages/2011_tohoku.aspx.*

California State Lands Commission, 2010, Marine Oil Terminal Engineering and Maintenance Standards (MOTEMS), 2010 title 24, CCR, part 2, California Building Code, chapter 31F—Marine Oil Terminals: California State Lands Commission, Marine Facilities Division, accessed August 27, 2013, at *http://www.slc.ca.gov/division_pages/mfd/motems/CHAPTER%2031F%20MOTEMS%20EFFECTIVE%2001-01-2011.pdf.*

Caltrans, 2010, Memo to designers 20-13: Tsunami hazard guidelines: Sacramento, California Department of Transportation, 3 p.

Center for Deep Earth Exploration [CDEX], 2012, Deep bonds from shared adversity: Japan Agency for Marine-Earth Science and Technology, CDEX Web Magazine accessed August 27, 2013, at *http://www.jamstec.go.jp/chikyu/magazine/e/future/no12/page02.html.*

Chile Railways, 2010, March 3, 2010, memo from General Manager to Accounting Department of Empresa de los Ferrocarriles del Estado (Chile): Chile Railways memo.

Cruz, A.M., Franchello, G., and Krausmann, E., 2009, Assessment of tsunami risk to an oil refinery in southern Italy: European Commission, Joint Research Centre, Institute for the Protection and Security of the Citizen, Ispra, p. 68.

Davison, C., 1936, Great earthquakes: London, Thomas Murby and Company, p. 209.

Division of Agriculture and Natural Resources [DANR], Veterinary Medicine Extension, 1999, DANR guide to disaster preparedness: Davis, Calif., University of California–Davis, accessed May 31, 2013, at *http://www.vetmed.ucdavis.edu/iawti/local-assets/pdfs/DANRGuide2.pdf*.

Federal Highway Administration, 2011, Bridge scour and stream instability countermeasures; Experience, selection, and design guidance, 3rd ed.—Design guideline 14 rock riprap at bridge abutments: Federal Highway Administration Website, accessed August 27, 2013, at *http://www.fhwa.dot.gov/engineering/hydraulics/pubs/09112/page14.cfm*.

General Accounting Office, [GAO], 2003, Comparison of States' highway construction costs—Letter to Peter G. Fitzgerald—Subcommittee on financial management, the budget, and International Security Committee on Governmental Affairs, United States Senate, November 3, 2003: General Accounting Office, accessed August 27, 2013, at *http://www.gao.gov/assets/100/92297.html*.

Goto, C., 1985, A simulation method of oil spread due to tsunamis: Proceedings of the Japan Society of Civil Engineers, no. 357–2, p. 217–223 [in Japanese].

Goto, Y., 2008, Tsunami damage to oil storage tanks: The 14th World Conference On Earthquake Engineering, October 12–17, 2008, Beijing, accessed August 27, 2013, at *http://www.iitk.ac.in/nicee/wcee/article/14_15-0005.PDF*.

Headland, J., Smith, E., Dykstra, D., and Ribakovs, T., 2006, Effects of tsunamis on moored/maneuvering ships: Proceedings of the 30th International Coastal Engineering Conference, American Society of Civil Engineers, p. 1603–1624.

Hirama, S., 2013, Farmers again cultivating rice fields hit by 2011 tsunami: The Asahi Shimbun, accessed June 18, 2013, at *http://ajw.asahi.com/article/0311disaster/recovery/AJ201306110061*.

Hokugo, A., Nishino, T., and Inada, T., 2012, Damage and effects caused by tsunami fires—Fire Spread, Fire Fighting and Evacuation: Proceedings of the International Symposium on Engineering Lessons Learned from the 2011 Great East Japan Earthquake, March 1–4, 2012, Tokyo, Japan, p. 43–62, accessed August 27, 2013, at *http://www.jaee.gr.jp/event/seminar2012/eqsympo/pdf/papers/113.pdf*.

International Fund for Agricultural Development, 2005, Tsunami Response: United Nations, International Fund for Agricultural Development Web site, accessed May 17, 2013, at *http://www.ifad.org/tsunami/index.htm*.

International Tsunami Information Center, 2013, About tsunamis—Are tsunamis dangerous?: United Nations Educational, Scientific, and Cultural Organization Web site, accessed May 17, 2013, at *http://itic.ioc-unesco.org/index.php?option=com_content&view=category&layout=blog&id=1139&Itemid=1139&lang=en*.

Iwabuchi, Y., Koshimura, S., and Imamura, F., 2006, Study on oil spread caused by the 1964 Niigata earthquake tsunami: Journal of Disaster Research, v. 1, p. 157–168.

Japan Fire and Disaster Management Agency, 2012, 2011 Great East Japan earthquake: Tokyo, Japan Fire Department Disaster Management Agency, status report, part 145 [13 March], 36 p. [in Japanese], accessed August 27, 2013, at *http://www.fdma.go.jp/*.

Japan Ministry of Agriculture, Forestry and Fisheries, 2012, FY2011 annual report on food, agriculture and rural areas in Japan: Japan Ministry of Agriculture, Forestry and Fisheries, accessed May 23, 2013, at *http://www.maff.go.jp/j/wpaper/w_maff/h23/pdf/e_all.pdf*.

Japan National Institute of Land and Infrastructure Management [NILIM] and Public Works Research Institute [PWRI], 2011, Quick survey report on bridge damage for the northeast Japan earthquake and tsunami: Japan National Institute of Land and Infrastructure Management and Public Works Research Institute, accessed August 27, 2013, at *http://www.pwri.go.jp/caesar/event/pdf/110312kyouryou.pdf*.

Johnson, R., 2011, Japan's 2011 earthquake and tsunami—Food and agriculture implications: Washington, D.C., Library of Congress, Congressional Research Service, accessed August 27, 2013, at *http://www.fas.org/sgp/crs/row/R41766.pdf*.

Kajitani, Y., Chang, S.E., and Tatano, H., 2013, Economic impacts of the 2011 Tohoku-Oki earthquake and tsunami: Earthquake Spectra, v. 29, n. S1, p. S457–S478.
Kawasumi, H., 1968, General report on the Niigata earthquake of 1964: Tokyo, Tokyo Electrical Engineering College Press, 550 p.
Kelley Blue Book, 2013, Ten steps to buying a new car: Kelley Blue Book Web site, accessed June 23, 2013, at *http://www.kbb.com/car-advice/car-buying/step-5-know-when-the-price-is-right/*.
Krausmann, E., and Cruz, A.M., 2013, Impact of the 11 March 2011, Great East Japan earthquake and tsunami on the chemical industry: Natural Hazards, v. 67, p. 811–828.
Laferrierre, R.R., Capt., 2011, Merchant vessel dispersal plan for Los Angeles—Long Beach harbors: San Pedro, U.S. Coast Guard, accessed August 27, 2013, at *http://www.mxsocal.org/pdffiles/Coast%20Guard%20Dispersal%20Plan.pdf*.
Lander, J., Lockridge, P.A., and Kozuch, J., 1993, Tsunamis affecting the west coast of the United States 1806–1992: Boulder, Colo., National Oceanic and Atmospheric Administration, National Geophysical Data Center Key to Geophysical Research Documentation No. 29, 242 p., available at *ftp://ftp.ngdc.noaa.gov/hazards/publications/Kgrd-29.pdf*.
Moffatt and Nichol, 2007, Tsunami hazard assessment for the ports of Long Beach and Los Angeles: Moffatt and Nichol Engineers report prepared for the Ports of Long Beach and Los Angeles, Long Beach, Calif.
Morris, C., 1909, Morris's story of the Great Earthquake of 1908, and other historic disasters: Philadelphia?, p. 82.
National Agricultural Statistics Service [NASS], 2009, California—State and county data: United States Department of Agriculture, National Agricultural Statistics Service, 2007 Census of Agriculture, v. 1, Geographic Area Series, part 5
National Agricultural Statistics Service [NASS], 2013, United States Department of Agriculture, National Agricultural Statistics Service, accessed May 22, 2013, at *http://www.nass.usda.gov/research/Cropland/sarsfaqs2.html#Section3_9.0*.
National Board of Fire Underwriters and Pacific Fire Rating Bureau, 1964, The Alaska earthquake—March 27, 1964: New York, N.Y., The National Board of Fire Underwriters
National Institute of Building Sciences and Federal Emergency Management Agency [NIBS and and FEMA], 2009, Multi-hazard loss estimation methodology hurricane model HAZUS®MH MR4 technical manual—Appendices: Washington, D.C., Federal Emergency Management Agency, 446 p.
Okal, E.A., Fritz, H.M., Raad, P.E., Synolakis, C.E., Al-Shijbi, Y., and Al-Saifi, M., 2006a, Oman field survey after the December 2004 Indian Ocean tsunami: Earthquake Spectra, v. 22, sec. 3, p. S203–S218.
Okal, E.A., Fritz, H.M., Raveloson, R., Joelson, G., Pancoskova, P., and Rambolamanana, G., 2006b, Madagascar field survey after the December 2004 Indian Ocean tsunami: Earthquake Spectra, v. 22, sec. 3, p. S263–S283.
Okal, E.A., Sladen, A., and Fritz, H.M., 2006c, Mauritius and Réunion Islands—Field survey after the December 2004 Indian Ocean tsunami: Earthquake Spectra, v. 22, sec. 3, p. S241-S261.
Okamoto, S., 1984, Introduction to Earthquake Engineering: Tokyo, University of Tokyo Press, p. 78 and 80.
Ono, K., 1968, Railroads—general report on the Niigata earthquake, *in* Kawasumi, H., and others, eds.: Tokyo, Tokyo Electrical Engineering College Press, p. 463–482.

PIANC [World Association for Waterborne Transport Infrastructure] 2009, Mitigation of tsunami disasters in ports—Draft version III: PIANC Working Group 53.
Port of Oakland, 2013, Port of Oakland maritime facilities: Oakland, Calif., Port of Oakland, accessed June 29, 2013, at *http://www.portofoakland.com/pdf/mari_map.pdf*.
Porter, K., Wein, A., Alpers, C., Baez, A., Barnard, P., Carter, J., Corsi, A., Costner, J., Cox, D., Das, T., Dettinger, M., Done, J., Eadie, C., Eymann, M., Ferris, J., Gunturi, P., Hughes, M., Jarrett, R., Johnson, L., Le-Griffin, H.D., Mitchell, D., Morman, S., Neiman, P., Olsen, A., Perry, S., Plumlee, G., Ralph, M., Reynolds, D., Rose, A., Schaefer, K., Serakos, J., Siembieda, W., Stock, J., Strong, D., Sue Wing, I., Tang, A., Thomas, P., Topping, K., and Wills, C., 2010. Overview of the Arkstorm scenario: U.S. Geological Survey Open-File Report 2010–1312, p. 201, available at *http://pubs.usgs.gov/of/2010/1312/*.
Plumlee, G.S., Morman, S.A., and San Juan, C., 2013, Potential environmental and environmental-health implications of the SAFRR California tsunami scenario**:** U.S. Geological Survey Open-File Report 2013–1170–F*http://pubs.usgs.gov/of/2013/1170/F/*.
Porter, K.A., Kennedy, R.P., and Bachman, R.E., 2007, Creating fragility functions for performance-based earthquake engineering: Earthquake Spectra. v. 23, sec. 2, p. 471–489, accessed January 3, 2013, at *http://www.sparisk.com/pubs/Porter-2007-deriving-fragility.pdf*.
Raichlen, F., 1972, Discussion of—Tsunami-responses of San Pedro Bay and Shelf, California: Journal of Waterways, Harbors and Coastal Engineering, v. 98.
Saint-Amand, P., 1961, Los terremotos de Mayo—Chile 1960: China Lake, Calif., U.S. Naval Ordnance Test Station, 39 p.
Scawthorn, C., 2013, Fire following tsunami—A contribution to the Next Wave tsunami scenario: SPA Risk LLC, accessed March 20, 2013, at *http://www.sparisk.com/pubs/Scawthorn-2013-SAFRR-FFT.pdf*.
Scawthorn, C., Ono, Y., Iemura, H., Ridha, M., and Purwanto, B., 2006, Performance of lifelines in Banda Aceh, Indonesia during the December 2004 great Sumatra earthquake and tsunami: Earthquake Spectra*,* v. 22, p. S511–S544.
Sekizawa, A., and Sasaki, K., 2012, Overview of fires following the great East-Japan earthquake: Proceedings of the International Symposium on Engineering Lessons Learned from the 2011 Great East Japan Earthquake, March 1–4, 2012, Tokyo, Japan, p. 43–62, accessed August 27, 2013, at *http://www.jaee.gr.jp/event/seminar2012/eqsympo/pdf/papers/127.pdf*.
Shuto, N., 1987, Spread of oil and fires due to tsunamis: International Tsunami Symposium, National Oceanic and Atmospheric Administration, Pacific Marine Environmental Laboratory, Seattle, Vancouver, B.C.
Shuto, N., 2006, Tsunamis, disasters and countermeasures: The International Workshop on Fundamentals of Coastal Effects of Tsunamis, December 26–28, 2006, Hilo, Pre-meeting materials, accessed December 2, 2012, at *http://www.tsunami.oregonstate.edu/workshop/2006/doc/premeeting/Shuto.pdf*.
Spaeth, M.G., and Berkman, S.C., 1967, The tsunami of March 28, 1964—As recorded at tide stations: U.S. Department of Commerce, Coast and Geodetic Survey, Technical Bulletin No. 33
Sturman, G.G., 1973, The Alaska railroad, the great Alaska earthquake of 1964—Engineering: National Academy of Sciences, p. 958–986.
Subagyono, K., Sugiharto, B., and Jaya, B., 2005, Rehabilitation strategies of the tsunami affected agricultural areas in Nangroe Aceh Darussalam, Indonesia—*in* Salt-affected soils from sea water intrusion: Strategies for Rehabilitation and Management Regional Workshop,

Bangkok, Thailand, 23 p., accessed May 22, 2013, at *http://www.cgiar.org/www-archive/www.cgiar.org/tsunami/publications/files/rehabilitationstrategies.pdf*.
Suppasri, A., Mas, E., Charvet, I., Gunasekera, R., Imai, K., Fukutani, Y., Abe, Y., and Imamura, F., 2013, Building damage characteristics based on surveyed data and fragility curves of the 2011 Great East Japan tsunami: Natural Hazards, v. 66, p. 319–341.
TrueCar, Inc., 2013, TrueCar, Inc., Web site, accessed June 23, 2013, at *http://www.truecar.com*.
U.S. Census Bureau, 2012a, Table 1060—New motor vehicle sales and car production—1990–2010: U.S. Census Bureau, accessed June 23, 2013, at *http://www.census.gov/compendia/statab/2012/tables/12s1060.pdf*.
U.S. Census Bureau, 2012b, 2010 U.S. export and import data for Port of Los Angeles and Port of Long Beach: U.S. Census Bureau, USA Trade Online Web site, accessed October 25, 2012, at *https://usatrade.census.gov/*.
U.S. Census Bureau, 2013, FT920; U.S. merchandise trade—Selected highlights: U.S. Census Bureau Web site, accessed May 1, 2013, at *http://www.census.gov/foreign-trade/Press-Release/ft920_index.html*.
United Nations Food and Agriculture Organization [FAO], 2005a, FAO Field Guide—20 things to know about the impact of salt water on agricultural land in Aceh Province: United Nations Food and Agriculture Organization, accessed May 13, 2013, at *http://www.fao.org/ag/tsunami/docs/saltwater-guide.pdf*.
United Nations Food and Agriculture Organization [FAO], 2005b, Spotlight—After the tsunami: United Nations Food and Agriculture Organization, Agriculture and Consumer Protection Department Web site, accessed May 17, 2013, at *http://www.fao.org/ag/magazine/0502sp2.htm*.
Wardlow, B.D. and Egbert, S.L., 2003, A state-level comparative analysis of the GAP and NLCD land-cover data sets: Photogrammetric Engineering & Remote Sensing. v. 69, no. 12, p. 1387-1397
Willis, B., 1929, Earthquake Conditions in Chile: Washington, D.C., Carnegie Institution of Washington
Wilson, B.W., 1971, Tsunami-responses of San Pedro Bay and Shelf, California: Journal of Waterways Harbors and Coastal Engineering, v. 97.
Wilson, R.I., Admire, A.R., Borrero, J.C., Dengler, L.A., Legg, M.R., Lynett, P., Mccrink, T.P., Miller, K.M., Ritchie, A., Sterling, K., and Whitmore, P.M., 2012, Observations and impacts from the 2010 Chilean and 2011 Japanese tsunamis in California (USA): Pure and Applied Geophysics. v. 169, sec. 7, p. 1–21.
Yamada, T., Hiroi, U., and Sakamoto, N., 2012, Aspects of fire occurrences caused by tsunami: Proceedings of the International Symposium on Engineering Lessons Learned from the 2011 Great East Japan Earthquake, March 1–4, 2012, Tokyo, Japan, p. 43–62, accessed August 27, 2013, at *http://www.jaee.gr.jp/event/seminar2012/eqsympo/pdf/papers/71.pdf.*
Yanev, P.I., Scawthorn, C., and National Center for Earthquake Engineering Research (U.S.) and EQE International, 1993, Hokkaido Nansei-Oki, Japan earthquake of July 12, 1993: Buffalo, N.Y., National Center for Earthquake Engineering Research
Yashinsky, M., 2012, Lessons for Caltrans from the 2011 great east Japan earthquake and tsunami: Proceedings of the International Symposium on Engineering Lessons Learned from the 2011 Great East Japan Earthquake, March 1–4, 2012, Tokyo, Japan, p. 43–62, accessed August 27, 2013, at *http://www.jaee.gr.jp/event/seminar2012/eqsympo/pdf/papers/192.pdf.*